UNIVERSITY OF CALGARY

Elucidating the role of prolactin receptor during β cell adaptation to metabolic stressors

by

Daniel Lee

A THESIS

SUBMITTED TO THE FACULTY OF GRADUATE STUDIES

IN PARTIAL FULFILMENT OF THE REQUIREMENTS FOR THE

DEGREE OF MASTER OF SCIENCE

GRADUATE PROGRAM IN BIOCHEMISTRY AND MOLECULAR BIOLOGY

CALGARY, ALBERTA

MAY, 2024

Abstract

The role of prolactin receptor (PRLR) during β cell adaptation to pregnancy has been extensively studied. Human epidemiological studies have revealed a potential role of prolactin outside pregnancy in maintaining glucose homeostasis. In this study, we discovered that the absence of PRLR in pancreatic β cells leads to impaired glucose tolerance in multiparous mice challenged with a high-fat diet (HFD). Unlike during pregnancy, where PRLR regulates β cell mass expansion, we observed that PRLR had a smaller role in regulating β cell mass in this model. Pancreatic islets from our knockout mice had a similar insulin secretory capacity as the wild-type mice *in vitro*, suggesting that an *in vivo* factor was responsible for the difference in glucose homeostasis. Interestingly, a difference in in vivo insulin secretion was observed when mice were challenged with oral but not intraperitoneal glucose, suggesting a defect in the incretin effect. The incretin effect, where oral glucose administration elicits a greater insulin secretory response compared to intravenous administration, is mediated by incretin hormones glucose-dependent insulinotropic polypeptide (GIP) and glucagon-like peptide-1 (GLP-1). We found a reduction in mRNA expressions of both incretin hormone receptors, GIP receptor (*Gipr*) and GLP-1 receptor (*Glp-1r*), in the pancreatic islets of our islet-specific PRLR knockout mice in comparison to wild-type controls after 12 weeks of HFD. Additionally, the mRNA expression of transcription factors, E2F transcription factor 1 (*E2f1*) and peroxisome proliferator-activated receptor-γ (*Pparg*), which have been shown to regulate the expressions of *Gipr* and *Glp-1r* and are downstream of PRLR, were downregulated. Together, these results suggest PRLR may have a role in the maintaining incretin effect during metabolic stress outside of pregnancy. Our findings contribute to our understanding of the complexity of PRLR in maintaining glucose homeostasis outside of pregnancy.

Preface

Some of the data from this thesis has been published in Lee D., Kahlon R., Kola-Ilesanmi D., Rahman M., Huang C. Beta-cell adaptation to metabolic stresses requires prolactin receptor signaling. bioRxiv 2024.01.20.575603; doi: https://doi.org/10.1101/2024.01.20.575603. This thesis is original and independent work by Daniel Lee. When appropriate, works by other students from the Huang lab are included to support rationale of experiments performed by Daniel Lee, and are clearly indicated in figure legend. Carol Huang, Carrie Simone Shemanko, Mark Ungrin, and Myriam Hemberger contributed to manuscript edits. Carol Huang was the supervisory author on this project and was involved throughout the entire project in concept formation.

Chapter 2: Table 2.1 is modified from Table 6 in Sweeting et al. (2022). Table 2.1 is modified from Table 6 in Sweeting et al. (2022). Table 2.2 is modified from the manuscript of Pinhas-Hamiel et al. (2007). Table 2.3 is modified from manuscripts of Sievenpiper et al. (2018) and Stumvoll et al. (2005). Table 2.4 is modified from Figures 3 and 5 of Campbell et al. (2013). Figures 2.1, 2.2, 2.3, and 2.4 were generated with manuscripts of Figure 2.1: Thorens et al. (1988) and Ashcroft (2005), Figure 2.2: Mayendraraj et al. (2022) and Ämmälä et al. (1993), Figure 2.3: is modified from Figure 1 in Kim et al. (2012) and Figure 2.4: is from Brooks et al. (2012), Galsgaard et al. (1999), Camaya et al. (2022), Freeman et al. (2000), and Chamberlain et al. (2014).

Chapter 3: Transgenic mice were generated by Vipul Shrivastava as described in Shrivastava et al. (2021). All experimental procedures were approved by the Animal Use Review Committee at

the University of Calgary in accordance with standards of the Canadian Council on Animal Care: AC18-0184 Regulation of β cell proliferation by prolactin and AC22-0174 Regulation of β cell proliferation by prolactin. Carol Huang organized breeding schemes and administered tamoxifen to all mice in this project. All genotyping was performed by Kenichi Ito, Centre for Genome Engineering, University of Calgary. Raneet Khalon performed immunofluorescence, imaging, and quantification of phosphorylated STAT5 (Figures 3.5 and 3.6). Carol Huang contributed to data collected in physiological testing (Figures 3.8-3.14 and Supplemental Figures 3-8). Carol Huang assisted with the isolation of pancreatic islets and the whole pancreas.

Chapter 4: Raneet Khalon, Sristi Dey, and Valerie Ho assisted with immunofluorescence, imaging, and quantification of β cell morphometrics (Figures 4.7-4.12 and Supplemental Figures 11 and 12). Carol Huang assisted with experimental procedures and data collected during physiological testing (Figures 4.15-4.17). Raneet Khalon performed immunofluorescence, imaging, and quantification of PDX1 (Figures 4.19 and 4.20)

Chapter 5: Figure 5.1 was used from Shrivastava et al. (2021) of which I am an author.

Acknowledgements

First, I am grateful to Dr. Carol Huang for their mentorship that not only enriched my academic experience but also played a pivotal role in the successful completion of this research project. Without her invaluable insights, thoughtful discussions, and continuous encouragement, this would not be possible. I am grateful to have learned so much personally, academically, and professionally under her supervision.

I wish to express my sincere gratitude to my supervisory committee members Dr. Carrie Shemanko and Dr. Myriam Hemberger for the advice and support I needed during my thesis. I would also like to acknowledge previous members of the Huang lab, Raneet Khalon, Sristi Dey, and Valerie Ho, who helped contribute to this project. As well as friends and mentors, past and present, in the Childs, Guo, Hemberger, and Shutt labs, who were always willing to provide support when difficulties arose.

I would like to thank my friends in both B.C. (shout out to TSF) and Saskatchewan (Abdul Salama), who provided emotional and social support during the pandemic. I dedicate this thesis to my parents, Lisa and Steve Lee, for their unconditional love and support in all the decisions I have made.

Table of Contents

List of Tables and Figures

List of Abbreviations

Abbreviation	Definition
AC	Adenylate cyclase
ADP	Adenosine diphosphate
Akt	Protein kinase B
ANOVA	Analysis of variance
ATF-6	Activating transcription factor 6
ATP	Adenosine Triphosphate
AUC	Area Under Curve
BIP	Binding immunoglobulin protein
BMI	Body mass index
cAMP	Cyclic adenosine monophosphate
CD	Control diet
cDNA	Complementary DNA
cKO	Conditional knockout
CREB	cAMP response element-binding protein
CreER	Cre recombinase-estrogen receptor
Ct	Cycle threshold
DAG	Diacylglycerol
DEGs	Differentially expressed genes
DEPC	Diethyl pyrocarbonate
E2F1	E2F transcription factor 1

ELISA	Enzyme-linked immunosorbent assay
EPAC	Exchange protein directly activated by cAMP
ER	Endoplasmic reticulum
FBG	Fasting blood glucose
FBS	Fetal bovine serum
FFAs	Free fatty acids
FFAR1	Free fatty acid receptor 1
FOXM1	Forkhead box M1
G15	Gestational day 15
GCK	Glucokinase
GH	Growth hormone
GIP	Glucose-dependent insulinotropic polypeptide
GIPR	Glucose-dependent insulinotropic polypeptide receptor
GLP-1	Glucagon-like peptide-1
GLP-1R	Glucagon-like peptide 1 receptor
GLUT2	Glucose transporter 2
GPCR	G protein-coupled receptor
GSIS	Glucose-stimulated insulin secretion
GTT	Glucose tolerance test
HFD	High-fat Diet
HSP90	Heat shock protein 90
IGI	Insulinogenic index
Ins1	Insulin 1

Ins2	Insulin 2
IP_3	Inositol-1,4,5-triphosphate
IPGTT	Intraperitoneal Glucose Tolerance Test
ITT	Insulin tolerance test
IR	Immediately releasable
IRE1α	Inositol-Requiring Enzyme-1 alpha
IRS2	Insulin receptor substrate 2
JAK/STAT	Janus kinase/signal transducer and activator of transcription
JAK2/STAT5	Janus kinase 2/signal transducer and activator of transcription 5
K_{ATP}	ATP-dependent K^+
KI67	Kiel 67
K_m	Michaelis constant
KRB	Krebs-Ringer buffer
LRRC55	Leucine-rich repeat containing 55
MAFA	MAF BZIP transcription factor A
mM	mmol/L
NEUROD1	Neurogenic differentiation 1
NKX6.1	Nk6 homeobox 1
OCT	Optimal cutting compound
OGTT	Oral glucose tolerance test
PAX6	Paired box 6
PBS	Phosphate buffered saline
PC	Pyruvate carboxylase

PC1/3	Prohormone convertase 1/3
PC2	Prohormone convertase 2
PDH	Pyruvate dehydrogenase
PDX1	Pancreatic and duodenal homeobox-1
PERK	Protein kinase RNA-like ER kinase
PFA	Paraformaldehyde
PIP_2	Phosphatidylinositol-4,5-bisphosphate
PKA	Protein kinase A
PL	Placental lactogen
PPA1	Inorganic pyrophosphatase 1
PPARA	Peroxisome proliferator-activated receptor α
PPARB	Peroxisome proliferator-activated receptor β
PPARG	Peroxisome proliferator-activated receptor γ
PPARs	Peroxisome proliferator-activated receptors
PPREs	Peroxisome proliferator response elements
PRL	Prolactin
PRLR	Prolactin receptor
PRLR-L	Prolactin receptor long
PRLR-S	Prolactin receptor short
pSTAT5	Phosphorylated signal transducer and activator of transcription 5
RIP	Rat insulin promoter
RR	Readily releasable
RTqPCR	Real-Time quantitative Polymerase Chain Reaction

SEM	Standard error of the mean
STAT5	Signal transducer and activator of transcription 5
TCA	Tricarboxylic acid
TCF1	T cell-specific transcription factor-1
TCF7L2	Transcription factor 7-like 2
TZD	Thiazolidinediones
UPR	Unfolded protein response
WT	Wild type
Xbp1	X-box Binding Protein 1
Xbp1-S	X-box binding protein 1 spliced
Xbp1-U	X-box binding protein 1 unspliced

Chapter 1: Introduction

1.1 Outline

This thesis contains five chapters investigating the role of prolactin receptor (PRLR) in maintaining glucose homeostasis outside of pregnancy. Chapter 1 includes a brief introduction to the background of this project, its significance, a synopsis of the hypothesis, its objective, and three specific aims. Chapter 2 contains a detailed literature review of relevant research areas important to understanding this study. These areas include our current knowledge of diabetes, pancreatic β cells, the incretin effect, β cell compensation, and dysfunction, and the involvement of PRLR in β cell mass and function.

Chapter 3 delves into the first experimental aim of this study: does prolactin signaling in β cells affect β cell physiology during times of metabolic stress? Chapter 4 describes the second aim of this study: how do β cells compensate when PRLR is lost? Additionally, it discusses the third aim: what are the molecular mechanisms governing differences in β cell function and compensation?

Finally, Chapter 5 concludes this thesis with a general discussion of strengths and limitations, an overall summary and interpretation of results, and suggestions for future directions.

1.2 Background

1.2.1 Overview of diabetes

The incidence of diabetes has risen considerably and is expected to continue rising globally.[1] Diabetes is a metabolic disorder where pancreatic β cells are unable to meet the body's insulin requirements. Current treatments aim to manage the disease through dietary, lifestyle, and therapeutic approaches.[2,3] For the most severe form of diabetes, type 1 diabetes (T1D), islet transplantation is potentially curative but is limited by cadaveric donor islet availability and side effects from anti-rejection medications.[4] Type 2 diabetes (T2D), which accounts for more than 90% of diabetes cases, is characterized by β cell dysfunction and insulin resistance, with medication and exogenous insulin as the only treatment options and no cure.[3] Finally, up to 20% of pregnant women with no prior history of diabetes develop gestational diabetes mellitus (GDM).[5] A promising approach to cure the various forms of diabetes is to use stem cell-derived β cells but currently, they lack the mature insulin secretory responses found in mature islets.[6,7] Therefore, any strategies that can help us understand how to increase the mass and function of pre-existing or stem cell-derived β cells could improve current therapeutic options.

1.2.2 The pancreatic β cell

Islets of Langerhans in the pancreas consist of endocrine cells, encompassing α-, β-, δ-, ε- and pancreatic polypeptide cells, responsible for producing the hormones glucagon, insulin, somatostatin, ghrelin, and pancreatic polypeptide, respectively. Among these, pancreatic β cells play a pivotal role in synthesizing, storing, and secreting insulin, which prompts peripheral tissues (such as the liver, muscle, and fat) to uptake glucose and reduce blood glucose levels.[8] The primary trigger for insulin secretion is glucose, which, upon entering β cells, undergoes

oxidative phosphorylation, resulting in an influx of Ca^{2+} and subsequently exocytosis of insulin granules.[9,10] Moreover, various nutrients, hormones, and neuronal signals can either stimulate or inhibit insulin secretion.[11]

1.2.3 The incretin effect

The incretin effect describes a physiological phenomenon where oral glucose elicits a greater insulin secretory response in comparison to intravenous glucose administration.[12] The incretin hormones, GIP and GLP-1, are primarily released from the enteroendocrine cells in the small and large intestines in response to nutrient detection. They then bind to their respective receptors, GIPR and GLP-1R, on β cells, enhancing insulin secretion.[13] The incretin effect contributes up to 50-80% of insulin secretion postprandially and plays a crucial role in regulating blood glucose after a meal.[13–15]

1.2.4 β Cell compensation

During periods of metabolic stress such as pregnancy and obesity, there is a decrease in the ability to respond to insulin (insulin resistance), leading to an increase in insulin demand. Compensatory mechanisms observed during pregnancy and obesity in rodents have shown an increase in β cell mass, in part driven by β cell proliferation.[16,17] During pregnancy, pregnancy-associated hormones such as prolactin, estrogen, progesterone, cortisol, and placental hormones are responsible for maternal adaptations in response to insulin resistance.[18–20] During obesity, the effects of long-term HFD have shown that glucose, insulin, and incretin hormones GIP and GLP-1 stimulate β cell proliferation to meet the increased insulin resistance observed.[21–24]

1.2.5 β cell dysfunction

During periods of high demand for insulin, such as pregnancy and obesity, there is increased insulin biosynthesis, which can lead to the accumulation of unfolded proteins in the endoplasmic reticulum (ER). The accumulation of unfolded proteins can trigger a signaling cascade known as the unfolded protein response (UPR). In an attempt to resolve UPR, insulin biosynthesis may slow down, resulting in lower insulin content within β cells, and consequently, less insulin available for secretion.[25] If UPR is not resolved, it can lead to ER stress and β cell dysfunction and/or apoptosis.[26] In both rodents and humans, β cell apoptosis is a factor in the pathogenesis of insulin deficiency and consequently T2D.[17] The chronic elevation of glucose and free fatty acids (FFAs) has been shown to impair insulin biosynthesis and secretion and is known as glucolipotoxicity.[27–31] Aging has been shown to induce β cell function as senescence is associated with a decreased ability to increase β cell mass and function.[32,33]

1.2.6 Prolactin signaling

The hormone prolactin (PRL) and its receptor PRLR were initially discovered for their role in stimulating lactation in mammary glands. However, they are now known to have more than 300 other biological functions in many other tissues.[34–39] The role of PRLR in pancreatic β cell compensation during pregnancy has been reported by many studies.[40–45] Previous work from the Huang lab demonstrated that both whole-body (constitutive) and β cell-specific heterozygous deletion of PRLR are deleterious to glucose homeostasis during pregnancy.[38,46] The role of PRLR outside of pregnancy has not been extensively studied, but epidemiological studies in humans have found that within a metabolically fit range, higher serum prolactin levels are associated with lower risk and prevalence of T2D in both adults and obese children. [47–50]

1.3 Significance

Current treatments for T2D consists of dietary and lifestyle changes, as well as medication, including insulin. Commonly prescribed drugs such as sulfonylureas stimulate insulin secretion but are often associated with weight gain and lose efficacy over time, leading to dependence on exogenous insulin. Islet transplantation is available for a very small population of patients with T1D, but its clinical utility is limited by cadaveric donor islet availability and side effects from anti-rejection medication.[4] A new avenue of study, utilizing stem cell-derived β cells, shows promise but they lack the insulin secretory responses found in mature islets and may encounter issues related to immunogenicity.[6,7] A larger question remains: how can we protect pre-existing and potentially, newly implanted/transplanted β cells in humans? This project will delineate the effects of PRLR in glucose homeostasis through its actions in β cells and identify the molecular mechanisms responsible, using an *in vivo* model of impaired glucose metabolism.

1.4 Objective and Hypothesis

The Huang lab has previously demonstrated the role of PRLR in β cells during pregnancy. Epidemiological studies suggest a role of PRLR outside of pregnancy. This project aimed to determine the role of PRLR in pancreatic β cells *in vivo* after repeated exposure to metabolic stressors. We hypothesize that PRLR is required to maintain normal β-cell function and to protect pancreatic β cells against repeated exposure to metabolic stressors, namely pregnancies followed by a Western diet, i.e. a high fat diet (HFD).

1.5 Specific Aims

Aim 1. Does prolactin receptor in β cells affect β cell physiology during times of metabolic stress

This study used a transgenic mouse with an inducible deletion of PRLR, achieved through the Cre-LoxP method using Cre recombinase fused with estrogen receptor (CreER) driven by pancreatic and duodenal homeobox-1 (PDX1) (*Pdx1*CreER: $Prlr^{fl/fl}$). The experimental group consisted of mice expressing CreER and homozygous floxed PRLR (*Pdx1*Cre^{ER}: $Prlr^{fl/fl}$), where upon tamoxifen administration, CreER would be activated, leading to the removal of LoxP floxed exon 5 of *Prlr* (*Pdx1*CreER: $Prlr^{-/-}$), herein denoted as conditional knockout (cKO). The control group consists of mice with *Pdx1*CreER: $Prlr^{+/+}$ and those without *Pdx1*CreER (i.e. $Prlr^{fl/fl}$), as they both show no reduction in PRLR expression.[46] For the purpose of this thesis, the control group will be denoted as "wild type" (WT).

Tamoxifen are given to both WT and cKO female mice at age 8 weeks, at the time of sexual maturation. After administering tamoxifen, both WT and cKO mice underwent 2-3 pregnancies and were then placed on a HFD or control diet (CD) for 12 weeks, mimicking the human experience, as most people consume a Western Diet. Gene knockout was assessed by measuring mRNA expression of both long and short isoforms of *PRLR* (*PRLR-L* and *PRLR-S*) in islets. Phosphorylated signal transducer and activator of transcription 5 (pSTAT5) served as a surrogate marker for PRLR activation, determined using immunofluorescence.

Glucose homeostasis in mice was evaluated through physiological tests at the following time points: Virgin, Postpartum, after 6- and 12- Weeks of HFD or CD. These tests include an oral

glucose tolerance test (OGTT) and intraperitoneal glucose tolerance test (IPGTT) to assess glucose homeostasis, insulin sensitivity was measured via an insulin tolerance test (ITT), and fasting blood glucose (FBG). Additionally, other metabolic parameters, such as changes in weight in response to diet and fed blood glucose, were monitored weekly and bi-weekly, respectively. To evaluate both *in vivo* and *in vitro* insulin secretion, blood samples were collected during OGTT and IPGTT to measure serum insulin, and in vitro insulin secretion was measured from isolated pancreatic islets cultured under stimulatory conditions to assess insulin secretion capacity independent of in vivo secretagogues, including nutrients, hormones, and neuronal signals.

Aim 2. How do β-cells compensate when prolactin receptor is lost?

To assess potential compensation mechanisms in response to metabolic stresses, such as up regulation of β cell mass, insulin content, and the expression of β cell pro-function genes, the following methods were employed. Immunofluorescence was utilized to detect differences in β cell proliferation using Kiel 67 (Ki67), and β cell apoptosis was measured using cleaved caspase 3 as a marker. Other morphometric analyses included measuring β cell mass, and the average number and size of both β cells and pancreatic islets. β-cell mass was determined by β-cell area (insulin-positive pancreatic area) multiplied by pancreatic weight. Insulin content was measured from isolated islets used for *in vitro* insulin secretion, and mRNA expressions of both insulin genes, Insulin 1 (*Ins1*) and Insulin 2 (*Ins2*) were measured using Real-Time quantitative Polymerase Chain Reaction (RTqPCR). Additionally, we measured the mRNA expression of genes involved in β cell dysfunction, particularly those associated with the unfolded protein response (UPR) and β pro-function by RTqPCR.

Aim 3. What are the molecular mechanisms governing differences in β cell function and compensation?

To investigate the molecular mechanisms underlying differences in glucose homeostasis and β cell function, we utilized a candidate gene approach to determine the expression of genes known to regulate β cell growth, survival, and function. Specifically, we examined the regulation *Ins1* and *Ins2* expressions by measuring mRNA expression of transcription factors known to control insulin gene expression. Furthermore, to assess differences in the incretin effect, we measured the mRNA expression of exchange protein directly activated by cAMP (*Epac*), which is downstream of the incretin signaling pathway, along with transcription factors known to regulate the expressions of *Gipr* and *Glp-1r* using RTqPCR.

Chapter 2: Literature Review

2.1 Diabetes

Types of diabetes

Diabetes mellitus comprises a group of metabolic disorders caused from the impaired production and/or secretion of the hormone insulin by pancreatic β cells.[51] In T1D, an autoimmune attack on β cells leads to the destruction of insulin-producing β cells, resulting in absolute insulin deficiency.[52] T2D occurs when the production and secretion of insulin (β cell function) cannot compensate for the decreased responsiveness of peripheral tissues to insulin (i.e. insulin resistance), leading to elevated blood glucose (hyperglycemia).[3] GDM is observed in mothers with no pre-pregnancy history of hyperglycemia but who exhibit hyperglycemia during pregnancy.[53] The incidence of T2D accounts for more than 90% of the cases of diabetes, while T1D accounts for less than 10%, and GDM occurs in up to 20% of pregnant women.[3,5] In all forms of diabetes, pancreatic β cells are unable to secrete enough insulin to maintain normal blood sugar levels, resulting in hyperglycemia. This thesis will focus on GDM and T2D.

Gestational diabetes mellitus

Pregnancy induces changes in maternal metabolism. In early gestation, mothers increase insulin sensitivity to store nutrients for the fetus, compared to late gestation where increased insulin resistance is observed, allowing nutrient availability for fetal growth.[54] To compensate for insulin resistance in the later stages of gestation, maternal β cells need to increase in number and/or function. The β cell adaptations observed during the later stages of gestations include an increase in β cell mass through proliferation and a decreased threshold for glucose-stimulated insulin

secretion (GSIS), facilitated by pregnancy-associated hormones: placental lactogen (PL), prolactin (PRL), estrogens, and growth hormone (GH).[43,55,56]

GDM occurs when β cells fail to compensate for insulin resistance, and it is hypothesized that this failure is due to an inability to increase β cell mass.[40] Clinical studies have suggested that β cell dysfunction is observed first, as women who develop GDM appear to have abnormal insulin secretion before the onset of insulin resistance.[57,58] GDM is also associated with complications for both offspring and mothers, increasing the risk of GDM recurrence and development of T2D in both the offspring and mothers (Table 2.1).[53,59,60] The dynamic changes in maternal metabolism during pregnancy highlight the significant risks and complications for both offspring and mothers if hyperglycemia occurs, emphasizing the importance of intervention to mitigate adverse outcomes.

Complications	**Offspring**	**Maternal**
Short-term	Stillbirth Neonatal death Preterm birth Congenital malformations Macrosomia	Preeclampsia Gestation hypertension Postpartum hemorrhage Hydramnios Traumatic labor
Long-term	Metabolic syndrome Childhood obesity Hyperinsulinemia Excess abdominal adiposity High blood pressure	Recurrence of GDM Type 2 diabetes Hypertension Ischemic heart disease Chronic kidney disease

Table 2.1 Offspring and maternal complications associated with GDM

Short-term and long-term offspring and maternal complications associated gestational diabetes mellitus.[53]

Type 2 diabetes

The causes of T2D are multifactorial, and current research has identified genetic and lifestyle

risk factors linked to an increased risk. Genome-wide association studies have identified genes associated with T2D, such as transcription factors: transcription factor 7-like 2 (*TCF7L2*) and *PPARG*. However, no single gene variant has a causal relationship with the development of T2D.[61] Therefore, it is suggested that a combined effect of diabetes-associated genes and other factors related to β cell function may lead to disease progression.

Normal blood glucose levels are maintained by balancing insulin action and secretion. The most well-established risk factor for T2D is obesity, characterized by a constant state of hyperinsulinemia (increased secretion of insulin) due to insulin resistance.[62] Obesity leads to increased levels of free fatty acids, adipokines (i.e. hormones secreted by adipocytes), and cytokines that cause inflammation in insulin-responsive peripheral tissues, resulting in insulin resistance.[63] One of these adipokines, leptin, has been shown to directly inhibit insulin secretion in pancreatic β cells, whereas another adipokine, acylation stimulating protein, has been shown to increase insulin secretion.[64,65] This is an example of cross-talk between an insulin-responsive peripheral tissue and β cells, highlighting their influences on each other. β cells will continue to compensate for insulin resistance until a tipping point is reached. Once the demand for insulin cannot be met, a chronic state of hyperglycemia occurs.[66] The chronic state of hyperglycemia can lead to both acute and chronic complications (Table 2.2).[67]

Traditionally, it was believed that insulin resistance precedes β cell dysfunction, culminating in a tipping point where the inability to compensate for insulin resistance marks the pathogenesis of T2D. However, recent research suggests an emerging viewpoint: in some cases, β cell dysfunction may precede insulin resistance. Genome-wide associate studies on T2D have

highlighted that the most significant risk variants in healthy individuals are associated with β cell dysfunction.[61,68–71] During β cell dysfunction, insulin production and/or secretion are impaired. Conversely, during insulin resistance, insulin may still be secreted at high levels and can be managed by insulin-sensitizing medications.[66] Both β cell dysfunction and insulin resistance are key contributors to the pathogenesis of T2D, yet current understanding leans toward β cell dysfunction playing a more significant role. This is because β cells will continually adapt to insulin resistance until the amount of insulin secreted is insufficient.

Acute	Diabetic ketoacidosis Hyperglycemic hyperosmolar state Hyperglycemic diabetic coma
Chronic	Cardiovascular disease Dyslipidemia Hypertension Nephropathy Neuropathy Non-alcoholic fatty liver disease Psychiatric disorders Retinopathy

Table 2.2 Acute and chronic complications associated with type 2 diabetes (T2D)

Acute and chronic complications associated with type 2 diabetes.[67]

Management of diabetes

The criteria for diagnosing GDM and T2D are a fasted blood glucose level of ≥7.0 mmol/L (mM), a blood glucose level ≥11.1 mM two hours after a 75g OGTT, or a glycated hemoglobin A1C ≥6.5%.[3,72] To manage GDM and T2D, lifestyle changes such as diet and exercise can be beneficial.[3,53] If hyperglycemia persists, various therapeutics can be offered (Table 2.3). [2,3] Although the criteria for diagnosing GDM and T2D share similarities, management is crucial due to negative health outcomes for both the primarily affected mothers and their offspring.

Therapy	Mechanism of action	Condition
Nutrition	Alter diet to reduce blood glucose	GDM&T2D
Insulin	Exogenous insulin to supplement inadequate endogenous insulin	GDM&T2D
Sulfonylureas	Close K_{ATP} channels to cause membrane depolarization of β cells	GDM&T2D
Metformin	Decreases hepatic glucose output	GDM&T2D
Thiazolidinediones	Increase insulin sensitivity in peripheral tissues	T2D
Glucagon-like peptide 1 agonists	Enhance insulin secretion by increasing intracellular Ca^{2+}	T2D

Table 2.3 Common therapies for gestational diabetes mellitus (GDM) and type 2 diabetes (T2D)

Common therapeutic options for both gestational diabetes mellitus (GDM) and type 2 diabetes (T2D).[2,3]

Consequences of diabetes

According to the International Diabetes Federation, 9.3% of the world's population (463 million adults aged 20-79) is currently living with diabetes, and this number is predicted to increase to 578 million by 2030 and 700 million by 2045.[1] The progression of diabetes may lead to various life-altering complications, such as cardiovascular disease, amputation, kidney disease, and retinopathy and blindness.[73] The incidence of diabetes will escalate with rising cases of obesity in Canada; currently, 1 in 4 Canadian adults are obese and this prevalence is projected to increase over the next two decades.[74]

2.2 β cells of Pancreatic Islets

Pancreatic islets

β cells constitute the majority in a cluster of endocrine cells in the pancreas, known as the Islets of Langerhans. In human islets, the cell population distribution includes 60% insulin-secreting β cells, 30% glucagon-secreting α cells, and the remaining 10% is comprised of somatostatin-

secreting δ cells, pancreatic polypeptide-secreting γ cells, and ghrelin secreting- ε cells.[75] Interspecies similarities and differences between humans and rodents islets. Single-cell RNA-sequencing data has revealed transcriptomic-level similarities within each islet cell type.[76] Isolated human islets have been shown to secrete more insulin at baseline glucose levels (5.6 mM), but less at high glucose levels (16.7 mM) compared to mouse islets.[77] Rodent islets have a greater proportion of centrally clustered β cells compared to humans, where β cells are scattered within the islet and intermixed with other endocrine cells.[78] Additionally, human islets but not rodent islets elicit insulin secretion at a low glucose level (1 mM).[78] Despite interspecies differences in β cell function and islet architecture, rodent islets exhibit significant functional similarities with human islets such that information gain from rodents provide important and translatable insight in humans, therefore are commonly used in research settings.

The two most abundant endocrine cell types, α cells and β cells, play crucial roles in maintaining blood glucose homeostasis. Alpha cells synthesize, store, and secrete glucagon, a hormone that signals fat, liver, and muscle tissues to break down glycogen, thereby increasing blood glucose levels.[79] In contrast, β cells are responsible for the synthesis, storage, and secretion of insulin, a hormone that targets peripheral tissues such as the fat, liver, and muscle to take up glucose from the blood for energy production and storage.[8] Together, the antagonistic hormone pair of glucagon and insulin regulates blood glucose levels. Paracrine effects are also observed, where insulin from β cells inhibits glucagon release from α cells, while glucagon and small amounts of GLP-1 from α cells stimulate insulin secretion in β cells.[79] Finally, somatostatin from δ cells acts on nearby α and β cells to inhibit the release of both glucagon and insulin.[80] The interplay of

these hormones from different endocrine cells within Islets of Langerhans all work collectively to maintain blood glucose homeostasis.

Insulin biosynthesis

Insulin, a peptide hormone, is exclusively synthesized by pancreatic β cells. Insulin mRNA is translated into proinsulin and then converted to insulin by prohormone convertase 1/3 (PC1/3) followed by prohormone convertase 2 (PC2).[81,82] Proinsulin mRNA accounts for 20% of the total mRNA in β cells.[83] While humans have a single insulin gene, mice have two insulin genes: *Ins1* and *Ins2*.[84,85] Single or double knockout of *Ins1* and *Ins2* in the Non-Obese Diabetic strain of mice revealed that a single copy of *Ins2* (*Ins1*$^{-/-}$: *Ins2*$^{+/-}$) protects both male and female mice from diabetes. In contrast, a single copy of *Ins1* (*Ins1*$^{+/-}$: *Ins2*$^{-/-}$) in males but not females led to diabetes.[85] These findings suggest that *Ins1* and *Ins2* have differential contribution to β cell function in rodents, with sexual dimorphism showing that males are more susceptible to developing diabetes. Sexual dimorphism is also observed in humans, where sex steroid hormones such as estrogens protect premenopausal women from T2D by increasing insulin sensitivity, GSIS, and decreasing β cell apoptosis.[86,87]

Several transcription factors have been identified to regulate insulin gene expression. Among these, PDX1 is best characterized, binding to the promoter regions of both *Ins1* and *Ins2* and also plays a role in both prenatal pancreas development and postnatal maturation of β cells.[81,88] PDX1 is one of the earliest detectable transcription factors in the developing pancreas, with its expression restricted to mature pancreatic β cells, pancreatic duct, duodenum, and stomach postnatally.[89,90] Other important transcription factors during pancreas development include MAF

BZIP transcription factor A (MAFA), the helix-loop-helix protein Beta 2 (NEUROD1), Nk6 homeobox 1 (NKX6.1), and paired box 6 (PAX6). In rodents, PAX6 promotes *Ins1* expression, while MAFA promotes *Ins2* expression. NEUROD1 can promote both *Ins1* and *Ins2* expressions, whereas NKX6.1 shows post-transcriptional regulation of *Ins1* and *Ins2* expressions.[81,91] These transcription factors have all been shown to directly regulate insulin biosynthesis and be involved in the regulation of β cell development and maturation.[92]

Nutrients such as glucose and fatty acids, along with hormonal signals including insulin, PL, PRL, GH, estrogen, and incretins (GIP and GLP-1), have been demonstrated to regulate the activities of these transcription factors. Glucose is the major nutrient that regulates insulin gene transcription and biosynthesis, and mediates its effects through transcription factors PDX1, MAFA, and NEUROD1.[93] Fatty acids like palmitate have been shown to inhibit insulin gene expression by preventing nuclear translocation of PDX1 and blocking *MafA* mRNA expression.[94] Insulin can act in an autocrine manner where it binds to insulin receptors to increase PDX1 nuclear translocation.[95] Hormones of the lactogenic family: PRL, PL, and GH stimulate insulin gene expression by activating the Janus kinase/Signal transducer and activator of transcription (JAK/STAT) pathway, where STAT proteins promote insulin gene transcription.[96] Estrogens increase insulin transcription by binding to the transcription factor NEUROD1, amplifying NEUROD1 nuclear localization and binding to the insulin promoter.[97] Finally, the incretin hormones GIP and GLP-1, are secreted by the gut in response to nutrients, potentiate insulin secretion, and induce insulin gene expression.[13] These examples highlight the complex integration of nutrient and hormonal signals regulating insulin gene transcription and insulin biosynthesis.

Insulin secretion

Insulin secretion, like its biosynthesis, is controlled by various nutrient, neuronal, and hormonal signals. The classical insulin secretory pathway responds to glucose, a process known as glucose-stimulated insulin secretion (GSIS). During GSIS, glucose enters pancreatic β cells through glucose transporter 2 (GLUT2), undergoing glycolysis to produce pyruvate. Pyruvate then enters the tricarboxylic acid cycle (TCA) and undergoes mitochondrial oxidative phosphorylation, leading to an increase in the adenosine triphosphate: adenosine diphosphate ratio (ATP:ADP). This increase in ATP:ADP ratio causes ATP-dependent K^+ (K_{ATP}) channels to close, resulting in membrane depolarization and the opening of voltage-gated Ca^{2+} channels, allowing Ca^{2+} influx. This Ca^{2+} influx triggers the exocytotic release of insulin-containing granules (Figure 2.1).[9,10]

β cells have two pools of insulin granules: immediately releasable (IR), which make up ~5% of insulin granules, and the remaining 95% are readily releasable (RR) granules that require preparatory reactions and priming to undergo exocytosis.[98] A few minutes after blood glucose begins to rise, there is a sharp rise in serum insulin from the IR granule pool, followed by a slow and sustained secretion from the RR granule pool.[98] Therefore, insulin secretion is biphasic, involving a rapid first phase followed by a slow and sustained second phase. Clinically, it has been suggested that a reduction in first phase of insulin secretion is one of the earliest detectable abnormalitites in developing T2D.[99,100]

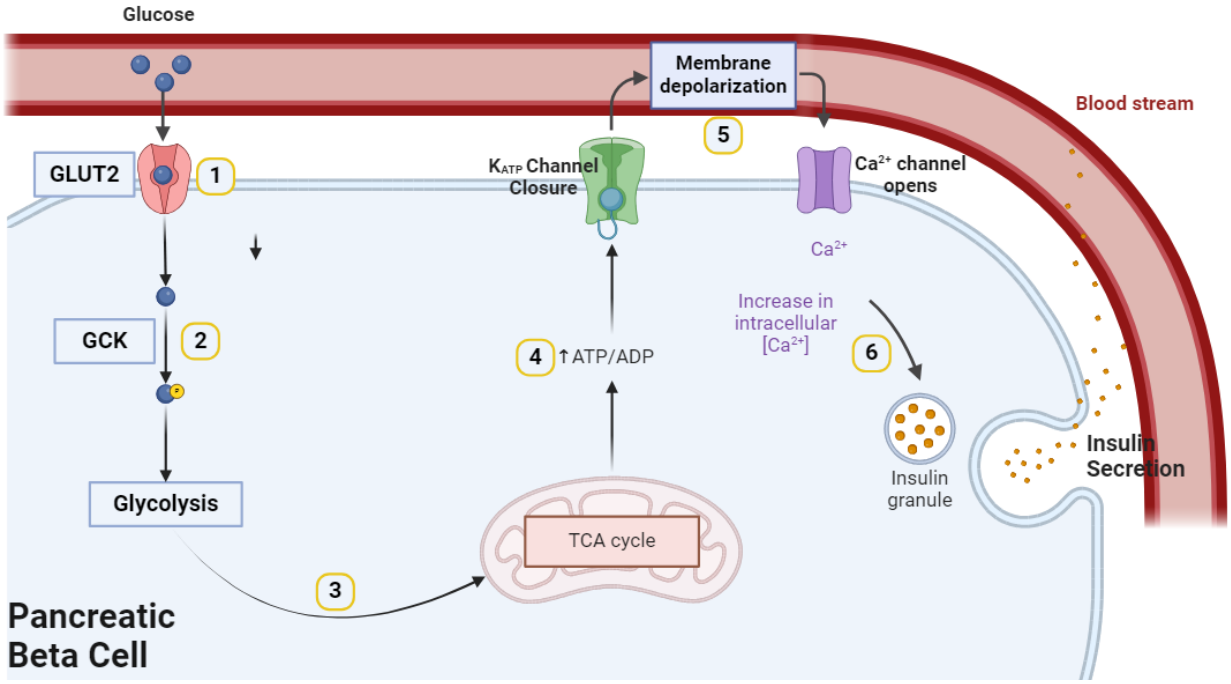

Figure 2.1 Glucose-stimulated insulin secretion in pancreatic β cells

Glucose-stimulated insulin secretion (GSIS) pathway in pancreatic β cells: 1) Glucose enters the β cell through glucose 2 transporters (GLUT2). 2) Glucose is phosphorylated by the rate-limiting enzyme glucokinase (GCK) to enter glycolysis. 3) The products of glycolysis enter the tricarboxylic acid (TCA) cycle in the mitochondria to increase the ratio of adenosine triphosphate (ATP) to adenosine diphosphate (ADP). 4) An increase in intracellular ATP closes ATP-dependent potassium (K_{ATP}) channels, resulting in membrane depolarization. 5) Membrane depolarization opens voltage-dependent Ca^{2+} channels and causes Ca^{2+} influx increasing intracellular Ca^{2+}. 6) An increase in intracellular Ca^{2+} leads to the exocytosis of insulin granules into the bloodstream. This figure was created with BioRender.

Regulation of insulin secretion

Pancreatic islets are highly vascularized structures, with the endocrine pancreas containing ten times more vasculature compared to the exocrine pancreas.[101] This increased vasculature facilitates unrestricted nutrient entry into β cells and the secretion of insulin into the bloodstream. Glucose entry into β cells is mediated by GLUT2, which has a high Michaelis constant (K_m) for glucose and transport capacity, allowing rapid entry of extracellular glucose into β cells.[102,103] Once inside, glucose is phosphorylated by GCK, the rate-limiting enzyme of glycolysis. GCK has two unique properties: a low K_m and GCK is not inhibited by its product, glucose-6-phosphate.[102] The product of glycolysis, pyruvate, enters the tricarbocylic acid (TCA) cycle to be oxidized by two pathways, catalyzed by pyruvate dehydrogenase (PDH) or pyruvate carboxylase (PC).[104] While PDH is more common in most cells, pancreatic β cells have very high levels of PC.[105] Knockdown experiments of PDH and PC showed that PC activity but not PDH activity influences insulin secretion both *in vitro* and *in vivo*.[104,106]

Apart from glucose, other nutrients can stimulate insulin release. Amino acids such as arginine, L-glutamine, L-alanine, and homocysteine regulate insulin secretion both *in vitro* and *in vivo,* due to overlapping pathways with glucose in the mitochondria.[107,108] Fatty acids within β cells can be converted into long-chain acyl-CoA, entering the mitochondria for oxidization via the β oxidation pathway, which also increases the ATP:ADP ratio akin to glucose and amino acid metabolism.[109] Elevated long-chain acyl-CoA in the cytoplasm raises intracellular Ca^{2+}, stimulating insulin granule exocytosis and directly interacting with exocytotic machinery in pancreatic β cells.[110,111] Free fatty acids (FFAs) in the bloodstream can amplify insulin secretion through free fatty acid receptor 1 (FFAR1), a G protein-coupled receptor (GPCR) where

activation of FFAR1 triggers phospholipase C cleavage of phosphatidylinositol-4,5-bisphosphate (PIP_2), producing inositol-1,4,5-triphosphate (IP_3) and diacylglycerol (DAG).[112,113] IP_3 stimulates Ca^{2+} efflux from the ER, whereas DAG enhances the second phase of GSIS.[113] FFAR1 agonists have shown efficacy in overcoming diabetic phenotypes by stimulating intracellular Ca^{2+} and cyclic adenosine monophosphate (cAMP), leading to insulin and GLP-1 secretion.[114]

Various hormones, both within and outside the endocrine pancreas, can augment insulin secretion. Insulin itself acts in an autocrine manner through insulin receptors to stimulate insulin secretion in β cells.[115] Proglucagon in pancreatic α cells can be cleaved into glucagon, which synergizes with insulin by binding to glucagon receptors on β cells to enhance GSIS. Conversely, somatostatin secreted from δ cells inhibits both insulin and glucagon secretion.[116,117] Estrogen and progesterone enhance insulin secretion *in vitro*, with estrogens closing K_{ATP} channels to cause membrane depolarization, while progesterone increases intracellular Ca^{2+}, leading to insulin granule exocytosis.[118,119] Glucocorticoids inhibit insulin release and β cell responsiveness to glucose.[118] PRL, PL, and GH have been shown to increase in in vitro GSIS in rat, mouse, and human islets.[120] Adipokines such as leptin inhibit insulin secretion, while acylation stimulating protein stimulates it.[64,65] Finally, incretin hormones GIP and GLP-1 have potent postprandial effects on insulin secretion, discussed in greater detail below.[12]

2.3 The incretin effect

Incretin effect

The incretin effect is a physiological phenomenon whereby oral glucose elicits greater insulin secretion compared to intravenous glucose administration.[12] The incretin hormones GIP and

GLP-1 bind to their respective receptors, GIPR and GLP-1R, on pancreatic β cells to exert the incretin effect.[13] Both GIP and GLP-1 exhibit glucose-dependent behaviour, enhancing insulin secretion when blood glucose levels are elevated, but showing no effect at low blood glucose levels.[12] GLP-1 is three to five fold more potent compared to GIP in T2D patients, as these patients are resistant to GIP-stimulated insulin secretion therefore, research and therapeutic alternatives have focused on GLP-1.[121] The incretins enhances first phase insulin secretion, accounting for up to 50-80% of postprandial insulin secretion, and plays a crucial role in regulating blood glucose levels after meals.[13–15,122]

Incretin synthesis and secretion

GIP is synthesized and secreted from enteroendocrine K cells in the duodenum and jejunum of the small intestines, while GLP-1 is produced and secreted from enteroendocrine L cells in both the small and large intestines.[13] ProGIP in K cells undergoes cleavage by PC1/3 to form GIP whereas proglucagon in L cells undergoes cleavage by PC1/3 to form GLP-1.[123,124] Similarly, proglucagon in L cells undergoes cleavage by PC1/3 to form GLP-1, whereas in pancreatic α cells, proglucagon is cleaved by PC2 to yield glucagon.[124]

Initially, it was believed that the production of GIP and GLP-1, as well as PC1/3 activity, were exclusive to enteroendocrine cells. Under normal conditions, pancreatic α cells cleave proglucagon with PC2 to yield glucagon but recent evidence suggests that during periods of increased insulin demand, pancreatic α cells can upregulate PC1/3 to generate intra-islet GIP and GLP-1.[124,125] In enteroendocrine K and L cells, GIP and GLP-1 respectively are released in response to nutrients (carbohydrates, proteins, lipids) in the intestinal lumen.[15] Differences in

nutrient sensing within the intestinal lumen have been observed between K and L cells, possibly due to the anatomical location of K cells being proximal to the distal location of L cells in the intestines.[15]

Incretin signaling in β cells

GIP and GLP-1 have pleiotropic effects on various metabolic tissues other than the pancreas (Table 2.4).[13] Both GIPR and GLP-1R are GPCRs, and their activation stimulates $G_{\alpha s}$, leading to cAMP production via adenylate cyclase (AC).[23] This increase in cAMP produces protein kinase A (PKA) and exchange protein directly activated by cAMP (EPAC), both of which result in the closure K_{ATP} channels, membrane depolarization, and the opening of voltage-gated Ca^{2+} channels, causing influx of Ca^{2+}. This increases intracellular Ca^{2+} triggers exocytosis of insulin granules (Figure 2.2). [23,126] GLP-1 has also been demonstrated to regulate the transcription factor PDX1, facilitating PDX1 translocation from the cytosol into the nucleus in a cAMP/PKA-dependent manner. Whether GIP also regulates PDX1 translocation is not as well documented, but given that both GIPR and GLP-1R lead to cAMP and PKA production, it is likely, also induce PDX1 nuclear translocation.[127] Besides increasing insulin transcription and secretion via PDX1, the activation of both GIPR and GLP-1R have mitogenic and anti-apoptotic effects in β cells.[23]

Regulation of incretin signaling

Activated GPCRs often internalize to amplify the biological effect or signal downstream pathways.[128] Internalized GLP-1R colocalizes with AC to further amplify insulin secretion by generating cAMP mediated by β arrestin.[129,130] The activation of GIPR and GLP-1R in β cells is

partly regulated by EPAC, which has two isoforms (EPAC1 and EPAC2).[131] As mentioned earlier, EPAC mediates cAMP-dependent mobilization of intracellular Ca^{2+} stores to increase insulin granule exocytosis and the downregulation of EPAC reduces the effects of incretins on insulin secretion.[131,132]

The regulation of both GIPR and GLP-1R is also under the control of various stimuli and transcription factors. Chronic elevation of both glucose and lipids has been shown to decrease receptor expression and negatively affect the actions of both GIPR and GLP-1R.[27,28,133,134] Few transcription factors have been found to regulate the expression of GIPR and GLP-1R. Notably, TCF7L2 is one of the strongest known genetic risk factor for T2D and has been shown to regulate the expression and function of both GIPR and GLP-1R.[135,136] Transcription factors such as E2F transcription factor 1 (E2F1), MAFA and NKX6.1 regulates insulin transcription as well as the expression of GLP-1R, while Pax6 has been shown to regulate both GIPR and GLP-1R expression.[91,137–139] Peroxisome proliferator-activated receptors (PPARs) are ligand-activated transcription factors consisting of three subtypes: PPAR α (PPARA), PPAR β (PPARB), and PPAR γ (PPARG), where PPARG has been shown to regulate GIPR expression.[140,141] PPARs play important roles in regulating glucose and lipid homeostasis as they control genes involved in adipogenesis, lipid metabolism, inflammation, and metabolism.[142] PPARG agonists such as thiazolidinediones (TZDs) increase insulin sensitivity in peripheral tissues (adipose, liver, and muscle) [143] and importantly, growing evidence suggests that PPARs also affect insulin secretion in pancreatic β cells.[144–146] Activation of PPARA has been shown to increase GLP-1R expression whereas PPARG has been shown to increase GIPR expression in insulin-secreting cell lines.[147,148]

Incretin	Target tissue	Physiological effect
GIP[#]	Adipocyte	Lipogenesis[#] Adipokine secretion[#]
GLP-1[*] GIP[#]	Blood vessel	Blood flow[*] Endothelial function[#]
GIP[#]	Bone	Formation[#] Resorption[#]
GLP-1[*] GIP[#]	Brain	Food intake[*] Neuroprotection[*#] Neurogeneration[#]
GLP-1[*] GIP[#]	Heart	Cardiac function[*] Triglyceride metabolism[#]
GLP-1[*]	Immune cells	Inflammation[*]
GLP-1[*]	Intestine	Lipoprotein secretion[*]
GLP-1[*]	Liver	Glucose output[*]
GLP-1[*] GIP[#]	Pancreas	Insulin secretion[*#] Glucagon secretion[*#] β cell proliferation[*#] β cell apoptosis[*#]
GLP-1[*]	Portal vein	Glucose sensing[*]

Table 2.4 Physiological effects of incretin hormones glucose-dependent insulinotropic polypeptide (GIP) and glucagon-like peptide-1 (GLP-1) on various tissues

Physiological effects of incretin hormones glucose dependent insulinotropic polypeptide (GIP) and glucagon-like peptide-1 (GLP-1) on target tissues, where "[#]" indicates the physiological effects of GIP only, "[*]" indicates the physiological effects of GLP-1 only, and "**[*#]**" represents the effects that both GIP and GLP-1.[13]

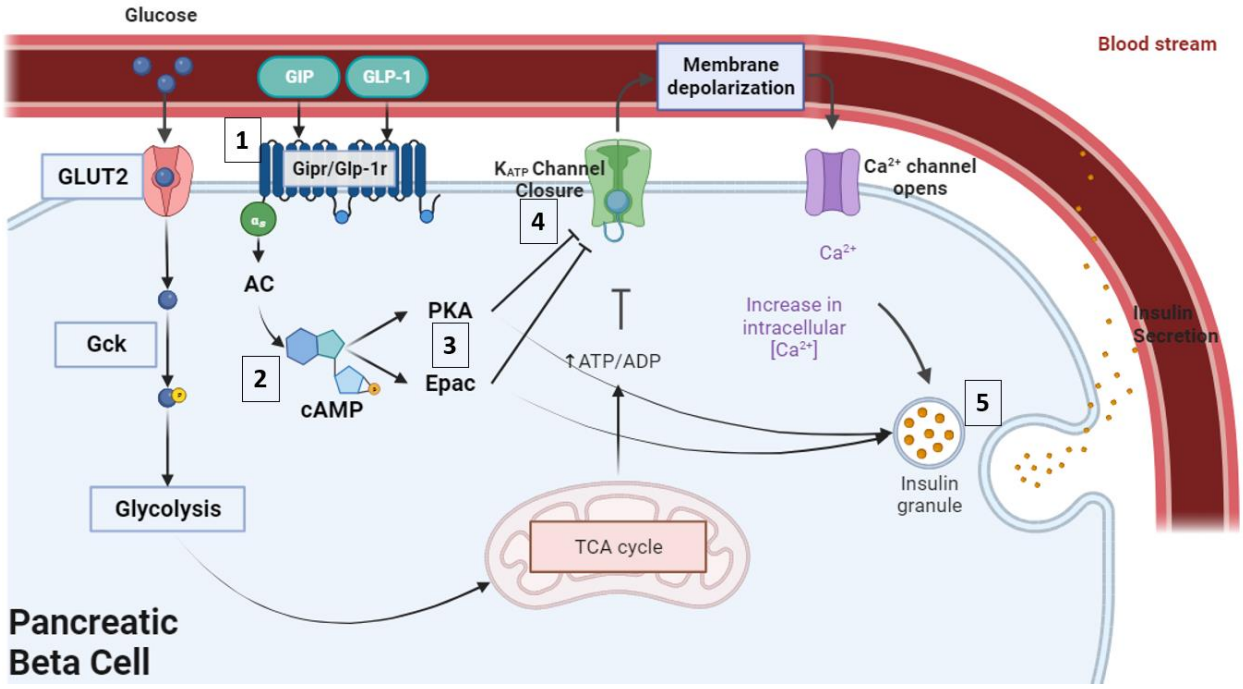

Figure 2.2 GIPR and GLP-1R signaling pathway in pancreatic β cells

Incretin hormones glucose-dependent insulinotropic polypeptide (GIP) and glucagon like peptide 1 (GLP-1) secreted from the gut exert their effects on pancreatic β cells by binding to G protein-coupled receptors (GPCRs): GIP receptor (GIPR) and GLP-1 receptor (GLP-1R). 2) Activation of both GIPR and GLP-1R results in $G_{\alpha s}$ activation and production of cyclic adenosine monophosphate (cAMP) by adenylate cyclase (AC). 3) cAMP production leads to the production of protein kinase A (PKA) and exchange protein directly activated by cAMP (EPAC). 4) Both PKA and EPAC close K_{ATP} channels, causing membrane depolarization and an increase in intracellular Ca^{2+} 5) The increase in intracellular Ca^{2+} results in insulin granule exocytosis in a glucose-dependent manner. This figure was created with BioRender.

2.4 β cell compensation

Periods of metabolic stress, such as obesity and pregnancy, lead to increased insulin demand primarily due to peripheral tissue insulin resistance. Obesity is characterized by excessive adipose tissue growth resulting from either excessive nutrient intake and/or reduced physical activity.[149] However, different forms of fat affect insulin resistance differently. In humans with the same body mass index (BMI), a higher proportion of visceral fat increases the risk of insulin resistance, whereas subcutaneous fat offers protection against it.[150] In aged rats, the elimination of visceral fat restored insulin sensitivity to levels comparable to those seen in young rats.[151]

β cell compensation during pregnancy

During pregnancy, there is a physiological adaptation to insulin resistance as the mother shifts to utilizing lipids instead of carbohydrates for energy, directing nutrients to the developing fetus.[152] Research has shown that a 200-250% increase in insulin secretion is necessary to maintain normal glycemic conditions during pregnancy; failure to meet this increase in insulin secretion will result in GDM.[16] This increase in insulin secretion is achieved by lowering the threshold for GSIS and by increasing overall β cell mass through β cell proliferation.[43,54]

The maternal β cell adaptations observed during pregnancy are mirrored by alterations in the production of maternal hormones such as prolactin, estrogen, progesterone, and cortisol in addition to placental hormones that can induce changes in the metabolic tissues of the mother.[18–20] Rodent studies have shown that pancreatic islets treated with lactogen hormones including, prolactin, growth hormone, and placental lactogen, both *in vivo* and *in vitro*, induced a decrease in the threshold for GSIS and increases in β cell mass as seen during pregnancy.[43] In addition to

circulating hormones, local signaling molecules such as hepatocyte growth factor and serotonin are important in the increased insulin secretory capacity and β cell mass.[40,41]

Human studies from pancreatic tissues obtained from women who passed during gestation have revealed similarities and differences compared to rodents in β cell adaptations during pregnancy. While rodent studies have reported a 3- to 4-fold increase, humans have a 1- to 2-fold increase.[38,40,153–155] It appears that the adaptive increase in β cell mass in human pregnancy is not as great as the changes observed in rodents, and this difference may be explained by differences in gestation periods, as human samples were from a gestation period that did not coincide with β cell proliferation. Functional *in vitro* studies on human islets during pregnancy have not been studied; therefore, further studies must be done to compare interspecies differences between rodents and humans.

B cell compensation during obesity

During obesity, there is an increased demand for insulin due to peripheral tissue insulin resistance. Long-term high fat diet (HFD) in rodents results in nearly a two-fold increase in β cell mass as a compensatory mechanism to combat increased insulin resistance.[17] This increase in β cell mass is stimulated by nutrients such as glucose as well as hormones including insulin, GIP, and GLP-1. Glucose metabolism has been shown to play a role in β cell replication. For instance, conditional deletion of glucokinase in β cells of adult mice revealed a drastic reduction in β cell proliferation, mediated by plasma membrane depolarization of K_{ATP} channels.[21] Insulin signaling in β cells activates the phosphoinositide 3-kinase (PI3K)/protein kinase B (Akt) pathway to increase β cell proliferation through cell cycle regulators such as cyclin D1, cyclin D2, p21, and

cyclin-dependent kinase-4 activity.[22] The incretins, GIP and GLP-1, can also stimulate β cell proliferation, where cAMP production activates PKA. This activation can further stimulate the transcription factor cAMP response element-binding (CREB) protein, which in turn activates cell cycle regulators cyclins A2 and D1.[23,24] A study by Mosser et al. has shown that β cell proliferation was significantly increased after only three days of HFD in 8 week old C57Bl/6J male mice, prior to significant changes in β cell mass and insulin resistance, mediated by the transcription factor Forkhead box M1 (FOXM1).[156] These studies highlight how various signals can stimulate β cell proliferation in rodent models.

A study by Gupta et al. highlights the progressive decline in glucose homeostasis after chronic exposure to HFD.[157] At the transcriptional level, young C57BL/6Ntac male mice given a HFD showed an increase in the expressions of β cell functional genes: *Glut2, Gck, Pc*, *Glp-1r*, and *Gipr* after 8 weeks of the HFD but as they continued on the HFD, all these genes are significantly downregulated after 16 weeks of HFD, in comparison to mice fed a control diet.[157] In the same study, these transcriptional changes were associated with significant increases in β cell mass from weeks 8 to 16 and β cell proliferation at week 10. Both glucose tolerance and insulin sensitivity progressively worsened in HFD-fed compared to control diet fed mice. Additionally, isolated islets from HFD-fed mice exhibited increased insulin responsiveness to glucose, GLP-1, and GIP at 2 weeks compared to chow-fed mice *in vitro*, but at 16 weeks insulin secretion in response to high glucose and GIP was drastically reduced from islets of HFD mice compared to control diet fed mice.[157]

Evidence for β cell proliferation in humans is inconclusive, as some studies have found no difference in β cell replication between diabetic versus nondiabetic subjects, while others have found a differences in diabetic versus nondiabetic subjects in obese individuals.[158,159] However, in both rodents and humans, evidence for β cell apoptosis exists, ultimately leading to insulin deficiency and consequently T2D.[17] Nevertheless, only a fraction of pregnant women and obese individuals develop GDM or T2D, as β cells compensate by increasing β cell mass and function.[160]

2.5 β cell dysfunction

As mentioned above, not all obese individuals and pregnant mothers develop T2D and/or GDM. Both T2D and GDM only manifest when β cells are unable to compensate for the increased demand for insulin due to insulin resistance. Peripheral tissues responsible for responding to insulin are primarily the liver, as well as muscle and fat, which undergo glucogenesis and lipogenesis to store glucose and fat.[161] During the development of T2D, there is often excessive caloric intake of glucose and lipids, both contribute to insulin resistance. As the disease progresses, there are transient and modest increases in blood glucose levels, which in turn increases the demand on β cells to produce more insulin.[162] Similarly, during the later stages of gestation, maternal insulin resistance is observed to divert nutrients to the developing fetus, failure to compensate for this insulin resistance results in GDM.[16] β cell dysfunction occurs when there is insufficient insulin production and/or secretion.[66] Individuals whose β cells cannot continue to hypersecrete insulin to meet the progressive increase in insulin requirement as insulin resistance worsens will develop T2D and/or GDM.[16,163]

Unfolded protein response

Chronic exposure to excess nutrients and hyperglycemia signals β cells to adapt to their physiological state by synthesizing more insulin. The ER is an important organelle for insulin biosynthesis, accounting for half of the total protein produced in β cells.[164] During times of high demand for insulin biosynthesis, the accumulation of unfolded/misfolded proinsulin triggers an intracellular signaling cascade called the UPR and if UPR is not resolved, it may lead to ER stress.

Three ER transmembrane proteins are involved in the UPR: protein kinase RNA-like ER kinase (PERK), activating transcription factor-6 (ATF6), and inositol-requiring enzyme-1 (IRE1α).[165] During the UPR, the presence of unfolded proteins, the ER chaperone immunoglobulin heavy chain binding protein (BIP), activates the three pathways of UPR: PERK, ATF6, and IRE1α.[165] Together, these pathways trigger the transcription of genes encoding ER chaperones, oxidoreductases, and ER-associated degradation proteins to remove unfolded proteins from the cytosol.[166] Downstream of the three pathways of UPR are: active ATF6 and spliced X box binding protein-1 (Xbp1-S) downstream of IRE1α have been shown to decrease insulin transcription, whereas ATF4, downstream of PERK, has been shown to affect insulin biosynthesis at translational level (Figure 2.3).[167]

β cells transition from periods of insulin biosynthesis to UPR-mediated recovery from ER stress, in hopes to restore ER protein homeostasis for β cell survival.[168] However, a constant state of hyperglycemia and insulin demand may prevent the UPR-mediated recovery period, and can lead to programmed cell death (apoptosis) in β cells. The extrinsic and intrinsic apoptosis pathways are two distinct mechanisms by which cells undergo programmed cell death. The extrinsic

pathway is initiated by external signals received from the cell, typically from other cells or the environment mediated by ligand binding to death receptors.[169] In the intrinsic apoptosis pathway, internal signals such as cytokines, oxidative stress, radiation, and toxins result in the release of pro-apoptotic proteins from the mitochondrial membrane.[170]

During the intrinsic apoptosis pathway, the release of pro-apoptotic proteins is in part, controlled by B-cell lymphoma 2 (BCL-2) family of proteins.[170] The BCL-2 family contain both anti-apoptotic proteins such as BCL-2 and pro-apoptotic proteins such as Bcl-2-assocated protein X (BAX), where the ratio of BAX to BCL-2 expression acts a cell death switch, determining life or death of cells in response to apoptotic stimuli. The activation of BAX increases outer membrane permeability of the mitochondria, inducing caspase activation, and ultimately apoptosis.[171] An increased ratio of BAX:BCL-2 increases susceptibility to apoptosis, whereas a decreased ratio protects against apotosis.[172]

The activation of PERK, ATF6, IRE1α pathways during the UPR can lead to the upregulation of the transcription factor C/EBP homologous protein (CHOP), where CHOP upregulates pro-apoptotic proteins, promoting apoptosis through activation of the intrinsic apoptosis pathway, where overexpression of CHOP decreases BCL-2 protein expression and $CHOP^{-/-}$ mice have increased *Bax* mRNA levels.[173] Prolonged exposure to a Western diet in male mice has shown that after 16 weeks of HFD, there are increased mRNA expressions of UPR-related genes: *Chop*, *BIP*, and *Xbp1*-S in pancreatic islets [157] Therefore, UPR-related ER stress can induce apoptosis, decreases β cell mass and contributes to the progression of T2D.[26]

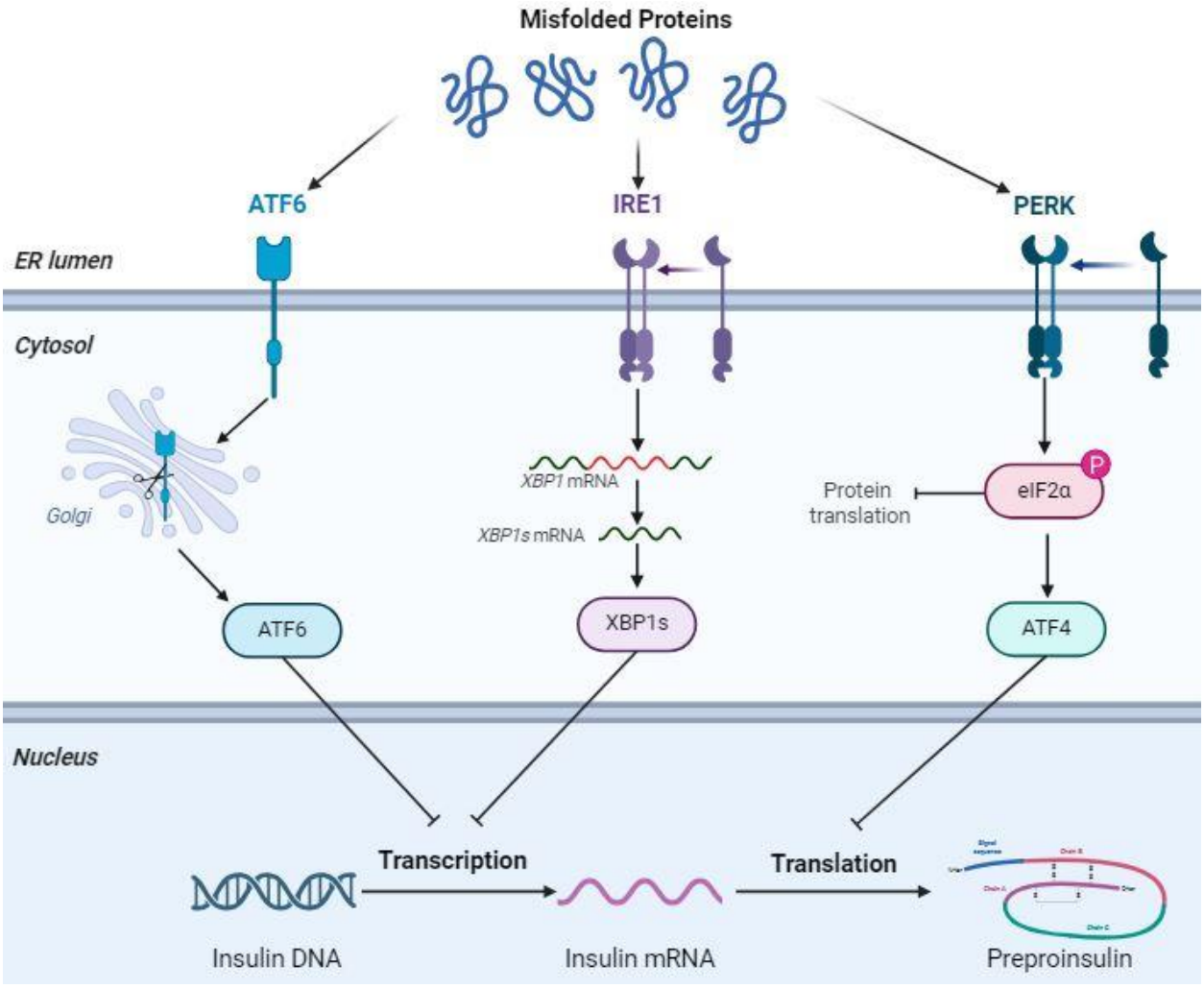

Figure 2.3 Unfolded protein response (UPR) and the effects on insulin biosynthesis

Unfolded protein response (UPR) and the effects on insulin biosynthesis. Misfolded/unfolded proteins can activate the activating transcription factor 6 (ATF6), inositol-requiring enzyme-1 (IRE1α), and protein kinase RNA-like ER kinase (PERK) pathways. ATF6 and spliced X box binding protein-1 (Xbp1-S), downstream of IRE1α suppress insulin mRNA expression. Activating transcription factor 4 (ATF4), downstream of PERK, inhibits proinsulin synthesis.[167] This figure was created in BioRender.

Glucolipotoxicity

Short-term exposure to nutrients, such as after a meal, evokes a physiological response from the β cells where insulin are released from IR and RR granules to lower blood sugar.[174] A study by Jetton et al. showed that in rats, glucose infusion ($1.8g \cdot kg^{-1} \cdot h^{-1}$) for 96 hours increased β cell mass by up to 2.5-fold with no evidence of β cell proliferation, suggesting β cell hyperplasia to be responsible for the increase in β cell mass.[175] In contrast, Pascoe et al. have shown that in mice, glucose infusion (50% dextrose, $100\mu l \cdot h^{-1}$) for 96 hours increased β cell proliferation but no statistically significant differences were observed in β cell mass.[176] These contradictory findings may be due to interspecies differences between rats and mice and caution must be taken into account when interpreting results. However, exposure of rodent and human islets to high glucose (15-30 mM) for several days *in vitro* can lead to β cell apoptosis and death.[29] Additionally, β cells exposed to high glucose leads to a reduction in the gene expression of key β cell transcription factors, such as *Pdx1* and *Mafa*, known as dedifferentiation.[30,31,177] Together, these deleterious effects of chronic hyperglycemia are called glucotoxicity.

In humans, as an individual becomes obese, lipid metabolism is altered and leads to elevated production and release of FFAs, ceramides, triglycerides, and cholesterol into the plasma and interstitial space.[178] Similar to the acute exposure to glucose being beneficial, short-term exposure of β cells to FFAs increases GSIS and is responsible for nearly 30% of insulin secreted in healthy and diabetic humans.[179,180] Chronic elevation of lipids can have either adaptive or maladaptive effects on the β cells exposed.[27] The adaptive effects of lipids are in part mediated by PPARs, which regulate genes involved in β cell mass and insulin secretion by FFAR1.[112,113,181,182] Conversely, exposure to lipids can also be toxic to β cells. Pascoe et al. also

observed that mice infused with both FFAs and glucose blunted β cell proliferation observed during only glucose infusion.[176] This blunted β cell proliferative capacity in addition to increased β cell apoptosis and decreased insulin secretion has been shown *in vitro* in human islets.[183] *In vitro* studies have shown that palmitic acid (0.5 mM) induced apoptosis in rat islet cells, while human islets exposed to palmitate (0.125 mM) inhibited insulin response to glucose.[184,185] 24 hour culture of rat islets in 125μM oleate with 5.6mM glucose resulted in a 50% reduction in insulin content compared to islets cultured in 5.6mM glucose only.[186] The concentrations of lipids in these *in vitro* studies would not be observed under physiological conditions and are much higher concentration than what is found under diabetic conditions in humans however, the harmful effects of chronic lipid exposure is called lipotoxicity.

In humans, lipid infusions in healthy young individuals potentiate GSIS whereas individuals with a history of diabetes that were infused with lipids displayed a reduction in both the first and second phases of insulin secretion.[187,188] These clinical studies suggest that some individuals may be predisposed to be more susceptible to lipotoxicity of β cells and develop T2D.
Interestingly, humans infused with lipids impaired the incretin effect in both non-diabetic and diabetic individuals.[189] The impairment of the incretin effect due to FFAs may be due to a reduction in GLP-1R as *in vitro* work with rat insulinoma INS-1E cells and the islets from db/db strain of mice showed that incubation with palmitate decreased *Glp-1r* expression as well as downstream cAMP production, CREB activation, and consequently insulin secretion.[190] Since the cryoarchitecture differs between species, how incretins augment insulin secretion in intact islets has been challenging.[78] Using in situ imaging, researchers have shown that in human islets, GLP-1 signals coordinated insulin release from pancreatic islets and lipotoxicity disrupted cell-

cell communication within islets to perterb both GLP-1 and GIP responses .[191] In the same study, to mimic lipotoxic conditions, C57/BL6 mice were feed HFD for 18 weeks but the coordinated response to GLP-1 and GIP were still intact in rodent islets, suggesting species-specific differences in the incretin response during lipotoxic conditions.[191]

The dysregulation of both lipid and glucose metabolism precedes the onset of T2D and is therefore implicated in the development of T2D. In summary, long-term exposure of glucose (glucotoxicity) and lipids (lipotoxicity) lead to β cell dysfunction and possibly apoptosis, reducing the functional β cell mass and together, is known as glucolipotoxicity.[27,28,187–189,191,29–31,176,177,184–186]

Aging

Within an islet, there is β cell heterogeneity, with subpopulations of different insulin secretory capacity. Through single-cell mass cytometry and transcriptome analyses, differences are observed between the islets of young and aged humans at the transcriptomic and proteomic levels, coinciding with differences in β cell survival, proliferation, and function.[192] In untreated male db/db mice, β cell proliferation is greatest at 10 weeks of age, and drops greatly by 24 weeks of age.[193] Young male mice (6-week-old) challenged with HFD exhibit over five-fold more proliferating β cells compared to normal diet controls but this increase in β cell proliferation was not observed in old (8-month-old) mice.[194] Studies in rodents have suggested that senescence is observed by 1-year of age whereas human β cell senescence is observed by 20 years of age.[195] It has been shown that during times of metabolic stress, β cells transition from a

more proliferative phenotype to a more senescent phenotype, and this decrease in capacity to proliferate may hinder β cell adaptation to further metabolic challenges.

Healthy mature β cells secrete low levels of insulin under basal condition and has a robust insulin secretory response to high glucose, whereas senescent β cells have high basal insulin secretion but blunted insulin secretory response to high glucose.[196] Aging has also been shown, in both rodents and humans, to decrease the proliferative capacity of β cells and increase susceptibility to apoptosis.[32,33]Aging also plays a role in determining β cell mass, as senescence decreases β cell proliferative capacity, it has been shown that the selective removal of senescent β cells in rodents improved glucose metabolism.[197]

2.6 Prolactin signaling

Prolactin

PRL was discovered as a hormone secreted by the anterior pituitary and named after its role in lactation.[34] PRL is part of a family of the lactogenic hormone family, which includes GH and PL, originating from the anterior pituitary and mammalian placenta respectively.[198] It is now known that prolactin has more than 300 other biological functions, and its receptor, PRLR, is expressed in many non-mammary gland tissues, including on pancreatic β cells.[35–39]

The human *PRLR* gene can be alternatively spliced to yield one long, one intermediate, and two short isoforms, all of which have identical extracellular domains but differing cytoplasmic domains.[199] In mice, two isoforms of PRLR exist, *Prlr*-L and *Prlr*-S isoforms. Both *Prlr* -L and *Prlr*-S are present in the pancreas but *Prlr*-L expression predominates.[200] PRLR-L has been

studied the most and has been shown to activate three signaling pathways: Janus kinase 2 (JAK2) and STAT (JAK2/STAT5) pathway, PI3K/Akt pathway, and the mitogen-activated protein kinase (MAPK) pathway summarized below (Figure 2.4).[34,201] It is of note that *in vivo* PRLR-L and PRLR-S may have different signaling pathways that may be tissue-specific.[202,203]

Prolactin signaling during pregnancy

The role of PRLR signaling in β cell compensation during pregnancy has been reported by many studies.[40–42] To adapt to maternal insulin resistance, rodents have shown β cell hypertrophy and proliferation to increase β cell mass, followed by atrophy, decreased proliferation, and apoptosis postpartum to return β cell mass to non-pregnant stages.[43,204] In humans, β cell hyperplasia is present with little to no evidence of alterations in proliferation and apoptosis.[154] The lack of similar findings between rodents and humans may be due to interspecies differences as well as limited human samples at various gestational stages.

PRLR signaling has been found to be integral for the β cell adaptations observed in rodents. During pregnancy, there is an increase in circulating lactogenic hormones: PRL, PL, and GH.[120] To mimic pregnancy-hormones during pregnancy, *in vitro* culture of islets with PRL have been shown to upregulate protein expressions of GLUT2 and GCK.[205] Additionally, *Prlr* mRNA levels increase 4-fold in the β cells of pregnant mice compared to non-pregnant mice and treating pancreatic islets with PRL *in vitro* has been shown to increase *Prlr* mRNA levels .[56] Mice overexpressing PL in β cells results in increased β cell mass through proliferation, consequent hyperinsulinemia, causing hypoglycemia [206] In contrast, the global homozygous deletion of PRLR results in decreased β cell mass, insulin transcription, and insulin content, with the

inability to sustain pregnancy beyond mid-gestation due to placental deficiency preventing the study of those of PRLR in glucose homeostasis throughout pregnancy.[207,208] Our lab showed that mice with heterozygous PRLR deletion have decreased β proliferation, β cell mass and developed glucose intolerance.[38] The islets of heterozygous PRLR-null mice were shown to have a reduction in the expression phosphorylation of Janus kinase 2 (JAK2), insulin receptor substrate 2 (IRS2), and Akt during pregnancy.[201] Furthermore, islets from male mice cultured with PL have been shown to induce pregnancy-related mRNA changes similar to those seen in female islets during gestation.[209]

PRLR is unique in that it is activated by multiple ligands: PRL, PL, and GH.[210] As previously mentioned, three signaling pathways: JAK2/STAT5, PI3K/Akt, and MAPK pathways, are activated by a ligand binding to PRLR.[34,201] The JAK2/STAT5 signaling cascade is the main pathway activated by PRLR in β cells, where JAK2 is recruited to phosphorylate signal transducer and activator of transcription 5 (STAT5). Phosphorylated STAT5 (p-STAT5) homodimers translocate to the nucleus and bind to promoters of target genes, including the expression of PRLR itself and stimulating proliferation by promoting retinoblastoma protein phosphorylation and E2F1 upregulation by STAT5-cyclin dependent kinases.[211,212]

During the PI3K/Akt pathway, PI3K can be activated directly by ligand binding to PRLR and indirectly by insulin receptor substrate (IRS) proteins. IRS2 proteins once active, converts PIP2 into PIP3. PIP3 then recruits phosphoinositide-dependent protein kinase 1 (PDK1) to activate Akt and can have stimulatory or inhibitory effects determined by Akt isoform and site of

phosphorylation.[213] The islets of heterozygous PRLR-null mice were shown to have a reduction in phosphorylation of JAK2, IRS2, and Akt during pregnancy.[201]

Finally, in the MAPK pathway, where ligand binding to PRLR, activates RAS proteins that stimulate RAF kinases, which in turn phosphorylates mitogen-activated protein kinase kinase (MEK), and subsequently MAPK.[34] Phosphorylated MAPK translocates to the nucleus and regulates the gene expression of β cell proliferation by removing the tumor suppression protein MENIN.[214] Rodent studies have also found that the MAPK signaling pathway is crucial in maintaining β cell mass and exocytosis of insulin granules.[215]

The role of prolactin during obesity

T2D is often associated with obesity, and it has been shown that FFAs negatively affect β cell function *in vitro*, yet no clear evidence has been found *in vivo*. PRLR-null mice challenged with a high-fat diet developed greater insulin resistance, glucose intolerance, and increased adipocyte hypertrophy. In these mice, exogenous treatment of PRL improved insulin sensitivity, prevented adipocyte hypertrophy, and reduced inflammation in visceral fat.[216] This coincides with both *in vivo* and *in vitro* evidence supporting that PRL suppresses lipid storage and adipokine release in lipid metabolism.[217]

Rodent studies have shown the importance of STAT5, downstream of the Jak2/STAT5 pathway, where dominant-negative mutant STAT5 mice had impaired glucose tolerance and a reduction in pancreatic insulin content and β cell area in response to a HFD.[218] Other studies have shown that targeted deletion of MEK1 and MEK2, downstream of the MAPK pathway, results in glucose

intolerance due to decreased insulin production, β cell proliferation, and β cell mass under HFD conditions.[215] Leucine-rich repeat containing 55 (LRRC55), one of the most highly upregulated genes increases 60-fold during pregnancy in a PRLR-dependent manner. Our lab has previously shown that overexpression of LRRC55 protected β cells from apoptosis after exposure to the FFA, palmitate, mimicking an obese state.[219] Finally, Pepin et al. utilized a β cell-specific PRLR rodent model to compare transcriptional changes during pregnancy versus a HFD and found a small amount of overlapping differentially expressed genes, suggesting that pregnancy-induced adaptive mechanisms may be different from those activated by nutritional stress.[220] Furthermore, when these mice were challenged with HFD, no difference in glucose tolerance was observed.[220]

The role of prolactin during type 2 diabetes

A long-standing view of PRL is that of having a diabetogenic role (i.e. elevates blood glucose), supported by studies in patient with severe hyperprolactinemia. For example, when 26 patients with prolactinomas (benign tumor of the pituitary gland that produce excess PRL) were treated with bromocriptine (suppresses PRL), it was found to improve glucose tolerance and insulin sensitivity.[221] Furthermore, patients with hyperprolactinemia have been associated with increased insulin resistance.[222–224] However, emerging clinical evidence has contradicted this idea of prolactin being diabetogenic.

Large cohort studies have found that within normal serum prolactin ranges, women with higher serum prolactin (>687.4 pmol/l) had a lower risk of T2D (*N*=8615).[47] In another study, an inverse relationship between serum PRL and T2D risk was shown in both men and women (*N*=3993).[48] In yet another study, an inverse relationship between insulin resistance and serum

prolactin levels was observed (*N*=1683).[49] Finally, obese children with lower serum prolactin levels were at greater risk of metabolic syndrome (a group of health problems consisting of obesity, high blood pressure, and hyperglycemia) (*N*=162).[50] Together, these studies indicate that serum prolactin may be a potential marker for risk of developing T2D.

Furthermore, there are sex differences in serum prolactin levels throughout life as well as a sharp increase in abnormal glucose homeostasis after menopause.[225,226] These observations led to our hypothesis that at extremely low and high levels, serum prolactin is deleterious to glucose metabolism, but within a normal range, higher serum prolactin is associated with metabolic fitness.

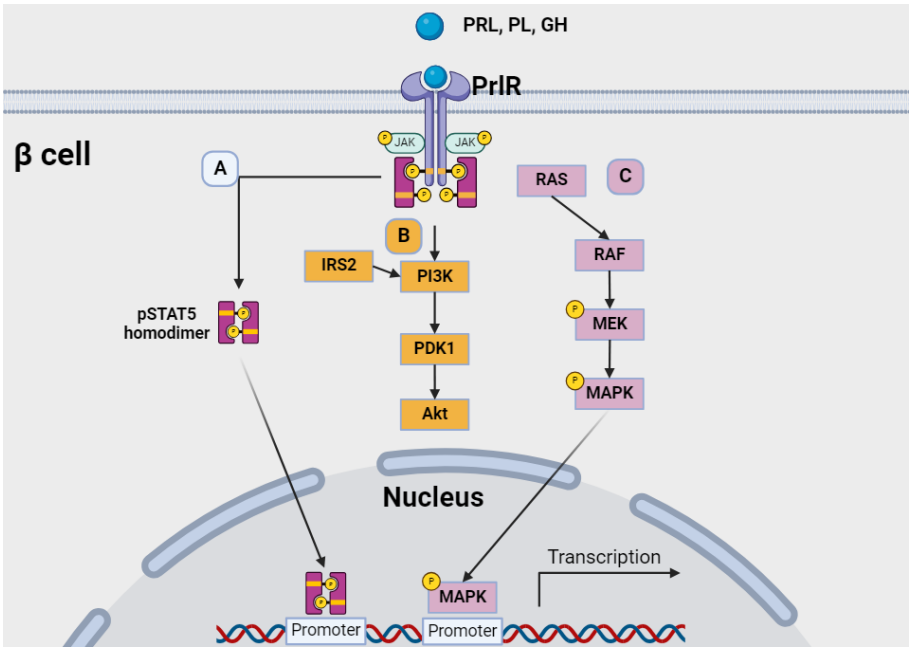

Figure 2.4 Activation of prolactin receptor (PrlR) and activation of A) JAK2/STAT5, B) PI3K/Akt, and C) MAPK pathways

Prolactin receptor (PrlR) is activated by ligands prolactin (PRL), placental lactogen (PL), and growth hormone (GH).[210] A) In the Janus kinase 2 (JAK2)/signal transducer and activator of transcription 5 (STAT5) (JAK2/STAT5) pathway, JAK2 phosphorylates STAT5. Phosphorylated STAT5 (pSTAT5) homodimers translocate to the nucleus and bind to promoters of target genes.[211] B) In the phosphoinositide 3-kinase (PI3K)/protein kinase B (Akt) pathway, PI3K can be activated by ligand binding to PrlR and indirectly by insulin receptor substrate 2 (IRS2). IRS2 converts phosphatidylinositol-4,5-bisphosphate (PIP2) into phosphatidyl inositol-3,4,5-triphosphate (PIP3), where PIP3 recruits phosphoinositide-dependent protein kinase 1 (PDK1)to activate Akt.[213] C) In the mitogen-activated protein kinase (MAPK) pathway, ligand binding to PrlR, activates RAS proteins to stimulate rapidly accelerated fibrosarcoma (RAF) kinases, which in turn phosphorylates mitogen-activated protein kinase kinase (MEK), subsequently activating MAPK.[34] Phosphorylated MAPK translocates to the nucleus and regulates gene expression.[214] This figure was created in BioRender.

Chapter 3: Physiological role of prolactin signaling in β cells during times of metabolic stress

3.1 Introduction

During pregnancy, maternal metabolism shifts from an insulin-sensitive state early in gestation, storing nutrients for the developing fetus, to an insulin-resistant state in mid/late gestation to divert nutrients to the developing fetus.[54] GDM occurs when mothers fail to compensate for increased insulin resistance during the later stages of gestation.[43,55] Many hormones play a role in maternal metabolism during pregnancy, such as: cortisol, estrogens, growth hormone (GH), human chorionic somatomammotropin, placental lactogen (PL), prolactin (PRL), and progesterone.[227] Rodent studies have shown a 3-4 fold increase in β cell mass through proliferation and hypertrophy during pregnancy followed by a reversion of β cell mass back to that observed in non-pregnant states postpartum via apoptosis.[40]

In mammals, PRLR expression is found in various tissues other than the mammary gland, including the Islets of Langerhans.[228] Two forms of PRLR exist, PRLR-L and PRLR-S isoforms, both expressed in the pancreas, but *Prlr*-L expression predominates.[200] PRLR is activated by various ligands (GH, PRL, PL) and the pathways activated by PRLR are the JAK2/STAT5, PI3K/Akt, and MAPK signaling cascades.[34,201,210] The primary pathway of PRLR activation is the JAK2/STAT5 pathway, where ligand binding causes JAK2 to phosphorylate STAT5, leading to pSTAT5 homodimerization and translocation to the nucleus to regulate target gene expression.[34,229]

Peak β cell proliferation during pregnancy coincides with an increase in lactogen levels (PRL and PL), and expression of PRLR is also increased 4-fold in β cells.[56,230] It has been shown *in vivo* that overexpressing PL in β cells increases β cell proliferation and β cell mass, whereas global deletion of PRLR during pregnancy reduces β cell mass.[38,206]. Postpartum, β cell mass returns to pre-pregnancy levels by increasing β cell apoptosis and decreasing β cell proliferation.[231] These findings suggest the importance of PRLR in glucose homeostasis and maternal β cell compensation during pregnancy.

The importance of PRLR during pregnancy has been studied extensively, but its role in glucose homeostasis outside of pregnancy has not. Clinical studies have suggested that very high or very low levels of PRL are deleterious to metabolism, whereas moderately high levels within normal range are beneficial.[232] Large cohort studies have found an inverse relationship between serum PRL levels and lower prevalence of T2D, suggesting PRL to play a role outside of pregnancy.[47,48] Obesity is the greatest risk factor to T2D, where increased levels of fatty acids, adipokines, and cytokines lead to insulin resistance in peripheral tissues.[63] Similar to GDM, β cells will attempt to compensate for the increased demand for insulin but will reach a tipping point, and consequently, chronic hyperglycemia ensues.[66]

To investigate the role of PRLR receptor in pancreatic β cells outside of pregnancy, we utilized a transgenic mouse with an inducible, β cell-specific conditional homozygous deletion of PRLR, namely, the *Pdx1*CreER:*Prlr*$^{fl/fl}$ mice (herein denoted as the cKO mice). Following tamoxifen administration, mice will undergo 2-3 pregnancies and then placed on either HFD or CD for 12

weeks. The rationale for the pregnancies followed by HFD is to the common practice of consuming a Western diet.

To determine whether PRLR regulates β cell adaptation to obesity, the diet induced obesity (DIO) model is most often used to mimic the Western diet, which is characterized by high content of fat and sugars.[233] HFD in rodents has been shown to disrupt secretion patterns of various hormones including PRL.[234] The physiological effects of HFD in rodents has been studied extensively, where HFD in mice increases body weight, worsens glucose tolerance, and increases insulin resistance.[235–237]

Within the endocrine pancreas, glucagon-secreting α cells and insulin-secreting β cells maintain glucose homeostasis. Glucagon signals the liver to release blood glucose, whereas insulin signals peripheral tissues to take up blood glucose, consequently lowering blood glucose.[8] Together, these antagonistic hormones maintain blood glucose in a narrow of 4-7mM in humans and 4-10mM in mice. When blood glucose rises, such as after a meal ingestion, two components dictate blood sugar back to normal levels: insulin sensitivity and the amount of insulin secreted.

Insulin resistance is observed in physiologic states, such as during pregnancy to divert nutrients to the developing fetus, and in obesity due to inflammatory signals mediated by elevated levels of fatty acids.[152,238] Insulin secretion from pancreatic β cells is biphasic: the first phase insulin secretion comes from immediate releasable (IR) pool, consists of less than 5% of insulin granules, occurring 5-10 minutes after exposure to glucose; this is followed by a slow and sustained second phase. [98,239] In addition to glucose, other insulin secretagogues, such as

nutrients (free fatty acids, amino acids), as well hormones and neuronal signals work in concert to modulate insulin secretion.[240]

In this chapter, we will investigate the physiological effects of PRLR receptor in both WT and cKO mice. We will measure mRNA expression of both isoforms of *Prlr* (long and short) after 12 weeks of diet using Real Time quantitative Polymerase Chain Reaction (RTqPCR). We will also measure activation of PRLR using phosphorylated signal transducer and activator of transcription 5 (pSTAT5) as a surrogate marker for PRLR.

To assess the physiological impact of PRLR in β cells (Aim 1), we will assess glucose homeostasis by an oral glucose tolerance test (OGTT), random and fasting blood glucose (FBG), and insulin sensitivity by an insulin tolerance test (ITT). In addition, we will measure changes in body weight during 12 weeks of HFD or CD. We hypothesize glucose homeostasis to be comparable between cKO and WT mice postpartum as β cell mass reverts to pre-pregnancy states postpartum.[204] Clinical studies have shown a role of serum PRL inversely associated with T2D risk; therefore, we hypothesize that activation of PRLR by PRL is important for maintaining normal glucose homeostasis in non-pregnant states. Moreover, exposure to HFD will likely exacerabate glucose intolerance in the cKO mice due to the known protective effects of PRL on β cells. Finally, as our model utilizes a β cell-specific deletion of PRLR, in which we expect to observe no difference in insulin resistance between WT and cKO mice because *Prlr* expression in insulin sensitive tissues are comparable.

3.2 Methods

3.2.1 Transgenic mice with an inducible β cell-specific deletion of prolactin receptor

This project utilized a transgenic mouse line with an inducible β cell-specific PRLR deletion, generated by the previous student Vipul Shrivastava.[46] Utilizing a tamoxifen-inducible Cre system, where Cre recombinase is fused with estrogen receptor (CreER) and driven by PDX1 as the promoter (*Pdx1*CreER).[241] We interbred sires that were heterozygous for *Pdx1*CreER and heterozygous for floxed exon 5 of *Prlr* (*Pdx1*CreER$^{+/-}$:*Prlr* LoxP-Exon 5-LoxP$^{+/fl}$) with dams that were heterozygous for floxed exon 5 of *Prlr* LoxP-Exon5-LoxP$^{+/fl}$ to generate offspring heterozygous for *Pdx1*CreER and homozygous for exon 5 floxed of *Prlr* (*Pdx1*CreER$^{+/-}$:*Prlr* LoxP-Exon5-LoxP$^{fl/fl}$). Following tamoxifen administration, CreER would be activated, removing LoxP-flanked exon 5 of *Prlr* to generate conditional knockout mice (*Pdx1*CreER: *Prlr*$^{-/-}$, herein denoted as cKO mice). We also generated *Pdx1*CreER$^{+/-}$:*Prlr*$^{+/+}$ as well as *Prlr*$^{fl/fl}$ mice, both of which would have intact *Prlr* expression after tamoxifen administration, hence we use both groups as wild type (WT) for comparison. The *Pdx1*CreER:*Prlr*$^{+/+}$ group would control for theoretical tissue non-specific expression of PDX1 and *Prlr* LoxP-Exon5-LoxP$^{fl/fl}$ group would control for the effect of LoxP insertion into the *Prlr* gene locus (Figure 3.1).

The *Pdx1* promoter was chosen to drive CreER expression because while it is expressed in the pancreatic bud during development, its expression is restricted to mature pancreatic β cells, pancreatic duct, duodenum, and stomach postnatally.[89,90] We have previously shown that it is minimally expressed in the hypothalamus and in our model, this minimal PDX1-CreER expression in the hypothalamus did not result in any change in *Prlr* expression.[46] At 8 weeks of

age, both WT and cKO mice received five dosages of tamoxifen (4mg/dose) orally every other day. All genotyping to detect the expression of CreER and *Prlr* LoxP-Exon5-LoxP$^{fl/fl}$ were performed by Kenichi Ito at the Centre for Genome Engineering, University of Calgary.

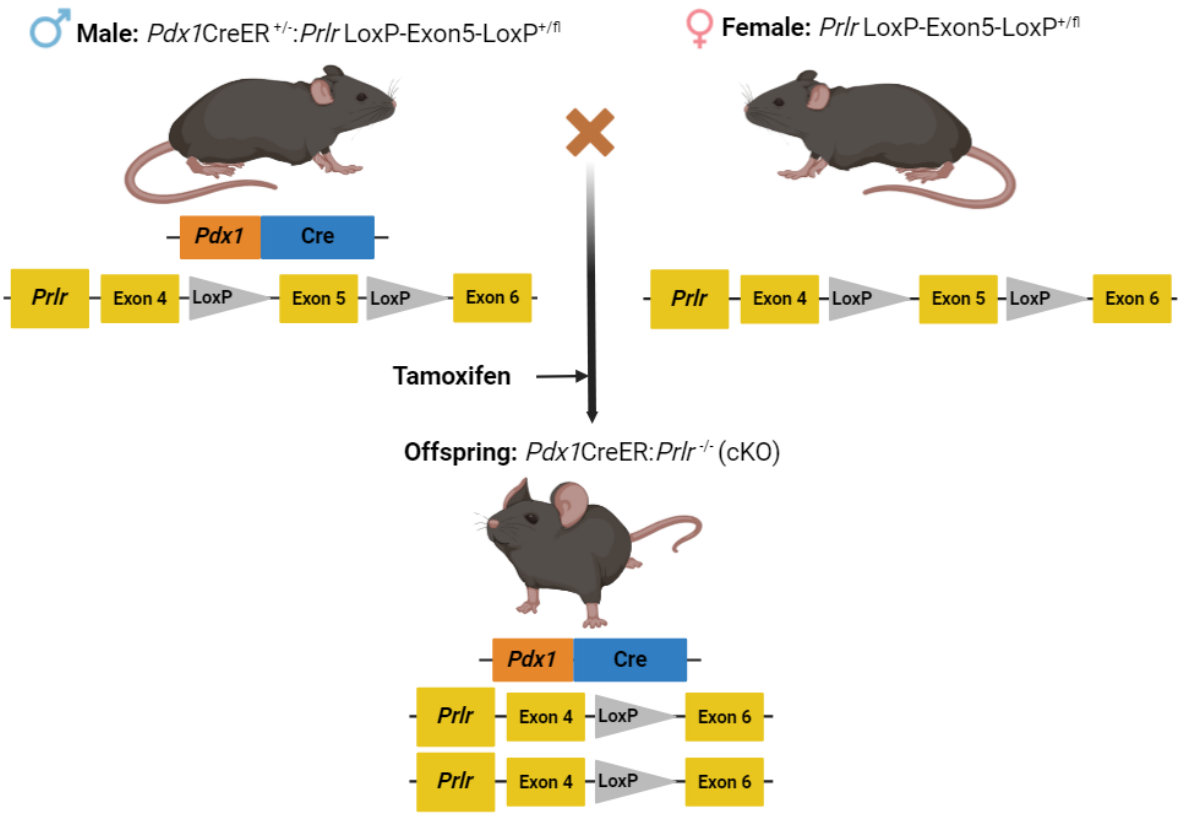

Figure 3.1 Generation of *Pdx1*CreER:*Prlr*$^{-/-}$ mice

*Pdx1*CreER: *Prlr* LoxP-Exon5-LoxP$^{fl/fl}$ mice were generated by crossing male mice heterozygous for Cre recombinase driven by *Pdx1* promoter and heterozygous for the LoxP floxed exon 5 of PRLR (*Pdx1*CreER$^{+/-}$:*Prlr* LoxP-Exon5-LoxP$^{+/fl}$) with female mice that were heterozygous for the LoxP floxed exon 5 of PRLR (*Prlr* LoxP-Exon5-LoxP$^{+/fl}$). Tamoxifen was administered to activate CreER and delete both copies of exon 5 of PRLR, resulting in the generation of β cell-specific PRLR knockout (*Pdx1*CreER:*Prlr*$^{-/-}$ or cKO) mice.

3.2.2 Timeline of experimental treatment

At 12 weeks of age, tamoxifen was administered to induce β cell-specific deletion of Prlr. It was administered to both WT and cKO mice. Female mice were then set up for 2-3 consecutive pregnancies. One week after their last litter, they were placed on either a high-fat diet (HFD), consisting of 60% of calories from fats, 20% from protein, and 20% from carbohydrates (Research Diets D12492) or a control diet (CD) with 10% of calories from fats, 20% from protein, and 70% from carbohydrates (D12450K) for 12 weeks. The diets are fully matched for all other ingredients with the exception of the fat and carbohydrate contents. Following 12 weeks of either HFD or CD, mice had their whole pancreas isolated for morphometric analyses via immunofluorescence, or their islets isolated for measurement of gene expression, *in vitro* glucose-stimulated insulin secretion (GSIS), and insulin content. (Figure 3.2).

To determine the whether PrlR in β cells affect β cell physiology during times of metabolic stress (Aim 1), we assessed glucose homeostasis with an OGTT, insulin sensitivity via an (ITT), and fasting blood glucose (FBG) at specific timepoints: before pregnancy (Virgin), after two pregnancies (Postpartum), and after 6- and 12-weeks of HFD or CD. To address how β cells compensate when PrlR is lost (Aim 2), we measured *in vivo* serum insulin at minutes 0, 10, and 30 during OGTT to capture FBG (0 minutes), first phase of insulin secretion (10 minutes), and second phase of insulin secretion (30 minutes). Pancreatic islets were isolated after 12 weeks of HFD, where a subset (~40 islets) from each mouse was used for *in vitro* GSIS to measure glucose-dependent insulin secretion (16mM glucose) and glucose independent insulin secretion (KCl). The whole pancreas was used to measured changes in β cell morphometrics (β cell proliferation, apoptosis, and mass). To identify the molecular mechanisms governing differences

in β cell compensation and function (Aim 3), the remaining isolated islets had total RNA isolated for Real-Time quantitative Polymerase Chain Reaction (RTqPCR) to determine expression of genes that regulate β cell growth, function, and survival.

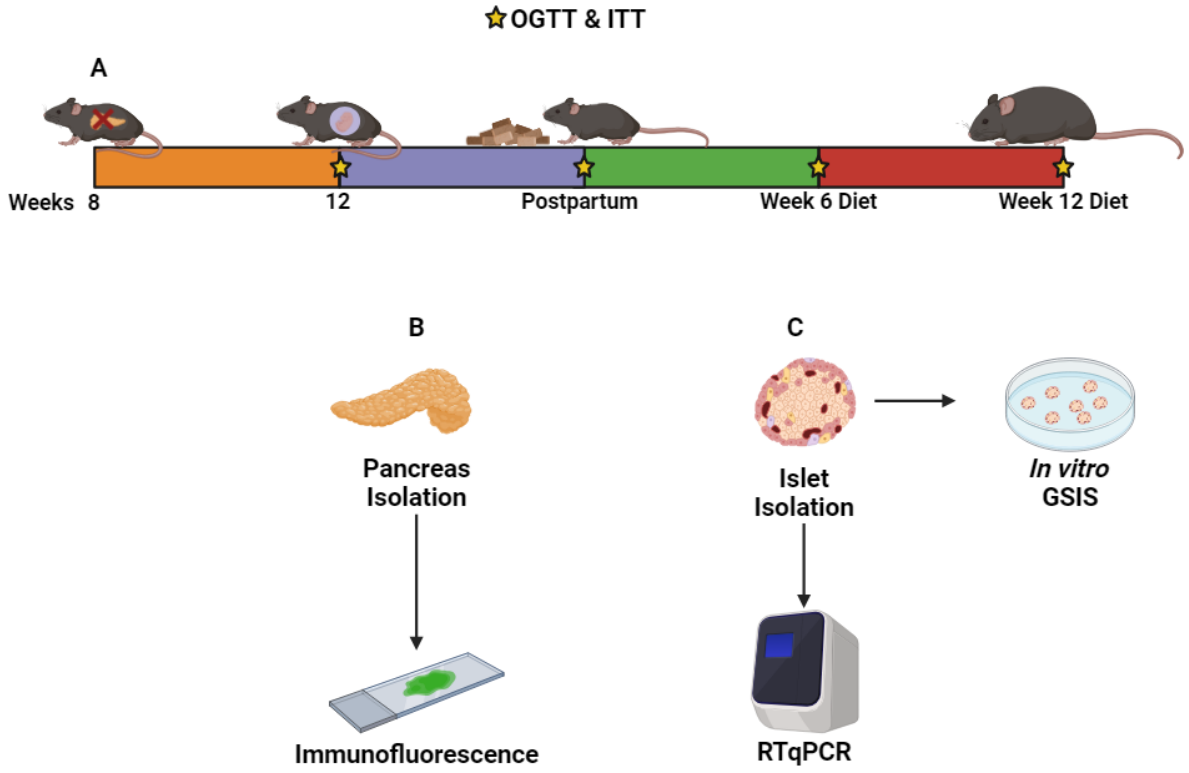

Figure 3.2 Timeline of experimental treatments

Timeline of experimental treatments:
A) At 8 weeks: Tamoxifen to induce β cell-specific deletion of PRLR. At 12 weeks: Mice set up for two pregnancies. Postpartum: Placed on HFD or CD for 12 weeks. Oral glucose tolerance tests (OGTT) and insulin tolerance tests (ITT) were performed at age 12 weeks (Virgin), one week after their second litter (Postpartum), 6 weeks and 12 weeks on HFD/CD, as indicated by the yellow stars. Subsequently, the mice will be divided into two groups:
B) Whole pancreas will be isolated for morphometric analyses using immunofluorescence.
C) Pancreatic islets will be isolated for *in vitro* glucose-stimulated insulin secretion (GSIS) experiments and measurement insulin content, while in the remaining islets RNA will be isolated for transcriptomic analyses using Real Time quantitative Polymerase Chain Reaction (RTqPCR).

3.2.3 Isolation of pancreatic islets

The pancreas were distended using collagenase P (Roche) (0.66 mg/ml in Hank's Balance Salt Solution, 2.5ml/pancreas), surgically removed, and then incubated at 37ºC for 15 minutes under constant agitation. During the digestion process, variables that can affect high-quality islet yield include the duration of digestion, temperature, collagenase concentration, and route of collagenase administration. Additionally, as isolated islets lose vascularity, this may lead to hypoxic conditions and possible necrosis.[242] Under-digested islets clump together with non-islet tissues such as acinar tissue, making it difficult to isolate islets and isolation of RNA or protein from these islets will be contaminated with non-islet tissues, while over-digested islets may not respond to insulin secretory stimulation and may not survive overnight culture.[242] Furthermore, reagents can be contaminated by endotoxins, and the physical digestion process itself, have been shown to release inflammatory cytokines that can lead to islet dysfunction and a reduction in insulin secretion during *in vitro* GSIS.[242,243]

To ensure consistency, islets were then hand-picked under a light microscope, and 40 intact islets of similar size from each mouse were set aside for *in vitro* GSIS experiments on the following day. Islets that were possibly necrotic or clumped with non-islet tissue were not collected for further experimentation. The islets for *in vitro* GSIS were cultured overnight in RPMI1640 supplemented with 10% fetal bovine serum (FBS) and penicillin/streptomycin. The remaining islets were flash frozen for total RNA extraction to determine gene expression by RTqPCR.

3.2.4 RNA extraction

100 µl of RLT buffer (Qiagen) containing 1% (v/v) β-mercaptoethanol was added to thaw the flash frozen islets on ice. 250 µl of TRIzol (Invitrogen) was added, and the solution was vortexed to lyse the islets, followed by incubation at room temperature for five minutes. Next, 50 µl of chloroform was added, and the solution was vortexed again and incubated at room temperature for an additional five minutes. The samples were then centrifuged at 12,500 rpm at 4ºC for 20 minutes, and the aqueous phase was transferred to a new tube. To this, 2 µl of RNA-grade Glycogen (ThermoFisher), $1/10^{th}$ volume of aqueous phase of 3M sodium acetate, and twice the volume of aqueous phase of 100% ethanol were added. After vortexing, the mixture was incubated at -80ºC overnight to precipitate nucleic acid.

The following morning, the samples were centrifuged at 12,500 rpm at 4ºC for 15 minutes to pellet nucleic acid. The supernatant was discarded, and samples were washed with 70% ethanol made in diethyl pyrocarbonate (DEPC)-treated H_2O before being centrifuged again at 12,500 rpm at 4ºC for 15 minutes. This washing step was repeated with 100% ethanol, followed by centrifugation at 12,500 rpm at 4ºC for 15 minutes. The remaining ethanol was allowed to evaporate in the fume hood, and the RNA was resuspended in 30 µl of DEPC-H_2O. The RNA concentration and purity was assessed using the NanoDrop spectrophotometer (ThermoScientific), where an absorbance ratio between 1.8-2.0 at 260nm/280nm was considered acceptable. These RNAs were subsequently used for reverse transcription into complementary DNA (cDNA) for RTqPCR.

3.2.5 Real-time quantitative Polymerase Chain Reaction

cDNA was prepared from 1 µg of RNA and reverse transcribed using the QuantiTect Reverse Transcription Kit (Qiagen) following the manufacturer's instructions for SYBR green quantitative PCR (Qiagen). Each reaction included sense primers (0.3µl at 10 µM per reaction), anti-sense primers (0.3µl at 10 µM per reaction), cDNA (4µl containing 10ng cDNA per reaction), and 2x SYBR green master mix (5 µl per reaction), the and 0.4µl of DEPC-H_2O for a final volume of 10 µl. Thermocycling was performed using Applied Biosystems QuantStudio 6 Flex Real-Time PCR System with the following conditions: 30 seconds enzyme activation at 95ºC, 40 cycles of denature at 95ºC for 5 seconds per cycle, annealing at 61ºC for 30 seconds, followed by melt curve analysis from 55-95ºC (Figure 3.3).

Primer sequence pairs were identified using NCBI Primer-BLAST tool, ensuring all primers were 18-22 base pairs in length and at least one primer sequence flanked an exon-exon junction of the gene. Primer pairs were chosen with a melting temperature close to 60ºC, a GC content of 50-60%, and a higher GC content near the 3' ends. All primers used in this thesis had a primer efficiency between 85-120%, calculated by running a serial dilution of cDNA to plot a standard curve where Primer efficiency = $(10^{(-1/slope)}-1) \times 100\%$. Sense and anti-sense primers used are listed in (Supplemental Table 1).

The $2^{-\Delta\Delta Ct}$ method was employed to measure relative fold changes in gene expression. This involved subtracting the cycle threshold (Ct) value of the housekeeping gene was subtracted from the Ct value of the gene of interest (ΔCt). The average ΔCt of the control sample was then subtracted from each individual sample (ΔΔCt) to calculate $2^{-\Delta\Delta Ct}$, representing the fold change

of the gene of interest expression between control and experimental samples. Inorganic pyrophosphate (PPA1) served as the housekeeping gene for measuring relative gene expression and normalization, as its expression showed the least variability between islets from pregnant vs. non-pregnant mice among housekeeping genes tested.[244]

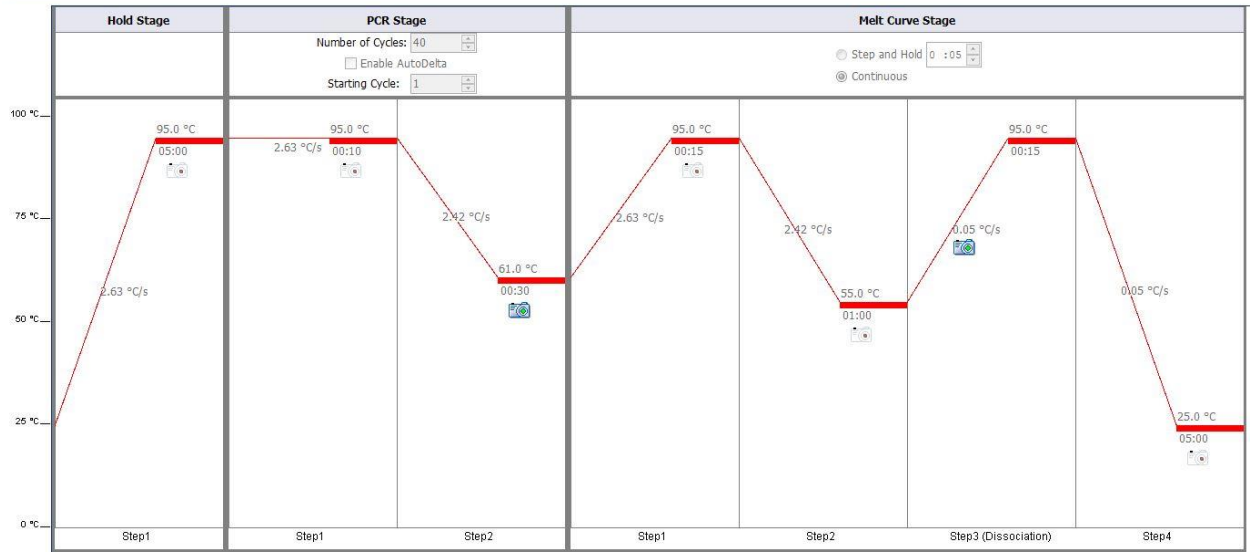

Figure 3.3 RTqPCR Thermocycle conditions

Thermocycling conditions during RTqPCR with Applied Biosystems QuantStudio 6 Flex Real-Time PCR System with the following conditions:
1) Hold stage: 30 seconds of enzyme activation at 95ºC
2) PCR stage: 40 cycles of denature at 95ºC for 5 seconds per cycle and annealing at 61ºC for 30 seconds
3) Melt curve stage: melt curve analysis from 55-95ºC.

3.2.6 Isolation of whole pancreas

Whole pancreases were isolated using blunt dissection, cleaned of blood and fat, and weighed. Subsequently, they were fixed in 4% paraformaldehyde overnight. The fixed pancreases underwent three washes in 1x phosphate buffered saline (PBS) for 20 minutes each, followed by daily dehydration in increasing concentrations of sucrose solutions (10, 20, and 30% sucrose/1x PBS each day). After being incubated in 30% sucrose/PBS for one day, the pancreases were set in optimal cutting temperature (OCT) compound for 1 hour at 4°C and flash frozen for long term storage at -80°C.

3.2.7 Immunofluorescence

Pancreas tissues were cut into 7-8µm thick sections using a cryostat machine and mounted on glass slides for immunofluorescence analysis. Prior to immunofluorescence, the frozen sections were thawed and rehydrated in 1x PBS, permeabilized in 0.1% Triton-X/1x PBS for 10 minutes, and blocked with 5% goat serum (GS)/1x PBS for 1 hour at room temperature (RT). Following this, they were incubated overnight with primary antibody diluted in 1% GS/1x PBS. The next morning, the slides were washed three times in 1x PBS and then incubated with secondary antibodies for 2 hours at RT. Details regarding the sources and dilutions of primary and secondary antibodies can be found in (Supplemental Table 2). Finally, the slides were mounted using mounting media (Dako), allowed to set overnight, and stored at 4°C before imaging.

The slides were imaged with an Axio Observer 7 microscope (Zeiss) and images were taken using Zen 2.6 Software (Zeiss). pSTAT5 was utilized as a surrogate marker of PRLR activation,

where β cells were considered pSTAT5-positive when pSTAT5 co-localized with the nuclei (Hoechst) surrounded by cytoplasmic insulin positivity.

3.2.8 Glucose tolerance

To evaluate glucose tolerance, we employed an OGTT at specific timepoints: Virgin, Postpartum, and at 6- and 12-weeks intervals after the start of HFD or CD. Mice underwent an overnight fast lasting 14-16 hours and were orally administered 2.0 g/kg of body weight of glucose (20% D-glucose in normal saline, Sigma). We chose an overnight fast because it results in a catabolic state in mice, depleting liver glucose stores and establishing a stable baseline blood glucose level with minimal fluctuations.[245] Blood glucose levels were measured from the saphenous vein at times 0, 10, 15, 30, 45, 60, and 120 minutes post-glucose administration using a blood glucometer (One Touch Verio Reflect). Additionally, 30 µL of blood was collected in blood collection tubes (BD Microtainer) at 0, 10, and 30 minutes during the OGTT to assess *in vivo* insulin secretion. Glucose excursion was determined by calculating the integrated area under the curve (AUC) throughout the 120 minute OGTT, with time 0 minutes serving as the baseline.

Furthermore, random fed blood glucose levels were measured bi-weekly between 8:00-10:00 AM, and body weight was measured weekly after the initiating the HFD or CD. Collected blood was allowed to coagulate for 30 minutes on ice, then centrifugated at 3000 RPM for 15 minutes at 4ºC. The separated serum was stored at -80 ºC for the subsequent measurement of serum insulin by enzyme-linked immunosorbent assay (ELISA), following the manufacturer's instructions (Crystal Chem, Elk Grove Village, IL, USA).

Fasting blood glucose (FBG) levels were measured at time 0 of either OGTT or IPGTT. In humans, a FBG of less than 100mg/dL (5.6 mM) is considered normal, between 100-124mg/dL (5.6-6.9mM) is considered prediabetic, and greater than 125mg/dL (6.9mM) is considered diabetic.[246] Inbred mouse strains have a FBG between 100-199mg/dL (5.6-11.0mM), which would be considered diabetic according to human criteria.[246] With no standardized criteria for diagnosing diabetes in mice, we utilized a FBG of less than 199mg/dL(11.0mM) as normal, 200-249mg/dL (11.1-13.8mM) as prediabetic, and greater than 250mg/dL (13.9mM) as diabetic.[246,247]

3.2.9 Insulin sensitivity

Insulin sensitivity was assessed using an ITT, which took place the day after the OGTT at specific time points: Virgin, Postpartum, and at 6- and 12-weeks intervals after the start of HFD or CD. Mice were fasted in the morning at 8:00 AM for 4-6 hours and then intraperitoneally administered 0.50 units/kg of body weight of insulin (NovoRapid insulin, Novo Nordisk) diluted in normal saline. Blood glucose levels were measured with glucometer from tail vein at times 0, 15, 30, 45, and 60 minutes after insulin administration. The ITT evaluates whole-body insulin action in response to a supraphysiologic dose of exogenous insulin, independent of the endogenous glucose-stimulated insulin release.[248]

3.2.10 *In vivo* and *in vitro* Insulin secretion

Insulin secretion occurs in in two phases: a rapid first phase followed by a sustained second phase. The first phase insulin secretion typically lasts around 5-10 minutes before the onset of the second phase.[239] To capture both phases of insulin secretion *in vivo*, blood samples were

collected from the saphenous vein during the OGTT at 10 minutes (first phase) and 30 minutes (second phase). Additionally, we calculated the insulinogenic index (IGI), a widely used measure of β cell function that assesses the change in blood glucose relative to the change in plasma insulin. Specifically, we calculated IGI both 0-10 minutes ($IGI_{0\text{-}10\ min}$) , and 0-30 minutes ($IGI_{0\text{-}30\ min}$) intervals, where $IGI_{0\text{-}10\ min} = \Delta\ Blood\ glucose_{0\text{-}10\ min} / \Delta\ Serum\ insulin_{0\text{-}10\ min}$ and $IGI_{0\text{-}30\ min} = \Delta\ Blood\ glucose_{0\text{-}30\ min} / \Delta\ Serum\ insulin_{0\text{-}30\ min}$.[249]

For *in vitro* insulin secretion analysis, pancreatic islets were isolated as described earlier. Two technical replicates of 19-20 islets were selected and cultured overnight in RPMI 1640 supplemented with glutamine and 10% Fetal Bovine Serum, 1U/100ml Penicillin-streptomycin at 37°C and 5% CO_2. The next day, the islets were preincubated twice for 30 minutes each in Krebs-Ringer Buffer (KRB) containing 2mM Glucose. To observe basal insulin secretion, the islets were transferred to microcentrifuge tubes containing 300µl of 2mM Glucose/KRB and incubated for 1 hour under the same conditions. After incubation, microcentrifuge tubes were briefly centrifuged at 500RPM at RT for 15 seconds, and 280µl of supernatant was collected and stored in -80°C for insulin measurement. Subsequently, 300 µl of 16mM Glucose/KRB was added, and incubation continued under the same conditions above, with supernatant collected afterward. Finally, 40mM KCl/2mM Glucose/KRB was added for 1 hour, and supernatant was collected again.

Following the collection of media after KCl incubation, 500µl of acid-ethanol (3% HCl, 75% EtOH) was added to microcentrifuge tubes, which were then vortexed to lyse cells. The next day, 250µl of the lysed sample was added to an equal volume of 1M Tris (pH=7.5) to neutralize the

HCl, and the mixture was stored in -80°C for total insulin content measurements. Total insulin content was calculated as the sum of insulin in the supernatant collected after 2mM Glucose, 16mM Glucose, 40mM KCl, and acid-ethanol treatments. Insulin secretion for the various 1-hour incubations are expressed as the percent of insulin secreted in each media condition relative to total insulin content.

3.2.11 Statistical Analyses

The data are presented as means $\pm$ standard error of the mean (SEM). An unpaired Student's t-test was employed to compare the means of two groups, while one-way analysis of variance (ANOVA) was utilized to compare the means of three or more groups. Furthermore, two-way ANOVA was used to compare means of three or more groups with two independent variables. Tukey's post hoc analysis was conducted to determine *p-values*, with statistical significance set at a $p\text{-value} < 0.05$. Tukey's multiple comparison test was employed to compare each experimental group with every control group. Outliers were identified and removed using the ROUT method with a Q value of 10%. All statistical analysis was done using GraphPad Prism Version 9.3.1.

3.3 Results

3.3.1 Validation of β cell-specific knockout of prolactin receptor

We have previously demonstrated a 90% reduction in *Prlr* mRNA expression in cKO mice during gestation day 15 (G15).[46] To confirm the knockout of PRLR in our transgenic mouse model, we evaluated mRNA expression of both long (*Prlr*-L) and short (*Prlr*-S) isoforms in islets of WT versus cKO mice after 12 weeks of HFD. *Prlr*-L primer pair was located on exon 10

whereas *Prlr*-S primer pair spanned exon 1 and exon 2 (Supplemental Figure 1). similar to our previous findings at G15, cKO mice exhibited an approximately 80% reduction in *Prlr*-L (*p=0.0003*) and a 90% reduction in *Prlr*-S (*p=0.001*) mRNA expressions compared to WT mice (Figure 3.4). Next, we investigated whether HFD affected *Prlr* mRNA expression in WT mice. Although not statistically significant, we observed a tendency towards increased *Prlr*-L and *Prlr*-S mRNA expression in WT HFD mice compared to WT CD mice (Figure 3.5).

During pregnancy, maternal pancreatic islet adaptations partly result from elevated prolactin signaling, including increased PRLR expression along with its ligands PRL, PL, and GH.[56,250] Due to limited availability of PRLR antibodies for protein-level assessment, we utilized pSTAT5, a downstream target of PRLR action, as an indicator for reduced PRLR activation.[34] (Figure 3.6). Given the substantial rise in PRLR action at G15, we employed immunofluorescence to assess pSTAT5 nuclear co-localization with β cells in the pancreas during G15.[38] Our preliminary results showed that during G15 WT mice displayed 70% pSTAT5-positive β cells compared to 4% in cKO mice (Figure 3.6). Following 12 weeks of HFD, WT mice exhibited a reduction in pSTAT5-positive β cells with 12% pSTAT5-positive β cells, whereas cKO mice showed only 2% pSTAT5-positive β cells (Figure 3.7).

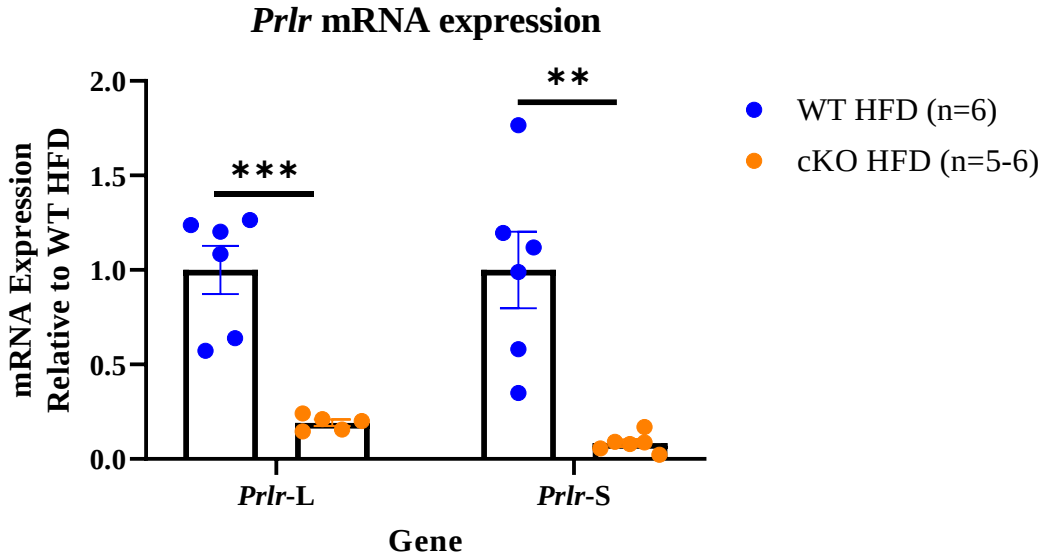

Figure 3.4 Islet *Prlr*-L and *Prlr*-S mRNA expression in WT and cKO mice after 12 weeks of HFD

mRNA expression of the prolactin receptor long isoform (*Prlr*-L) and short isoform (*Prlr*-S) was measured in WT and cKO mice after 12 weeks of HFD by RTqPCR. mRNA expression was normalized to *Ppa1* (housekeeping gene) and expressed relative to WT HFD mice. Each data point represents a mouse averaged from 3 independent experiments (n=5-6 mice/group). Results are presented as means ± SEM. Statistical analysis was done using an unpaired Student's t-test between groups (where ** $p<0.005$, *** $p< 0.0005$).

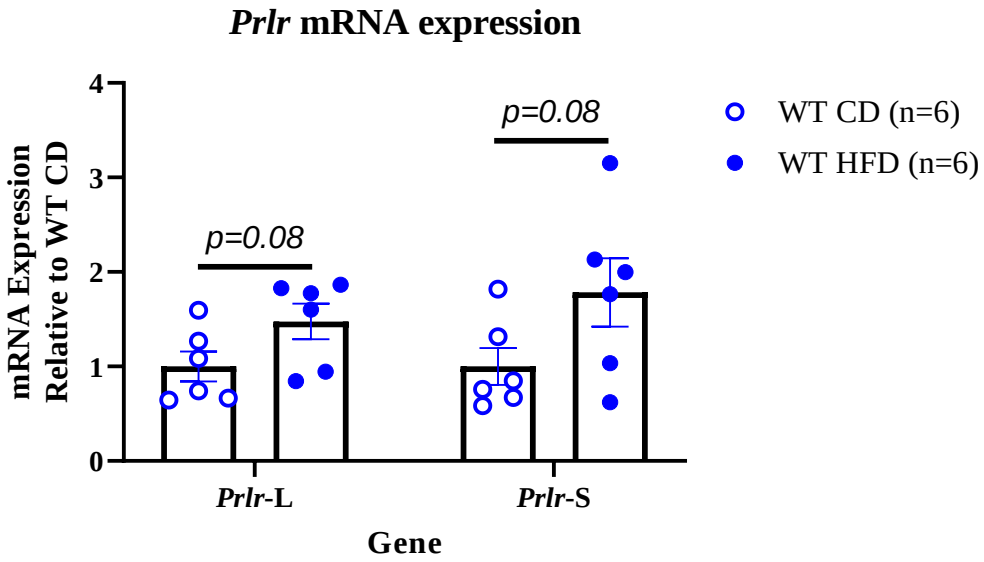

Figure 3.5 Islet *Prlr*-L and *Prlr*-S mRNA expression in WT mice after 12 weeks of CD or HFD

mRNA expression of prolactin receptor long isoform (PRLR-L) and short isoform (PRLR-S) was measured by RTqPCR in the islets of WT mice after 12 weeks of CD or HFD by RTqPCR. mRNA expression was normalized to *Ppa1* (housekeeping gene) and expressed relative to WT CD mice. Each data point represents a mouse averaged from 3 independent experiments (n=6 mice/group). Results are presented as means ± SEM. Statistical analysis was done using an unpaired Student's t-test between groups.

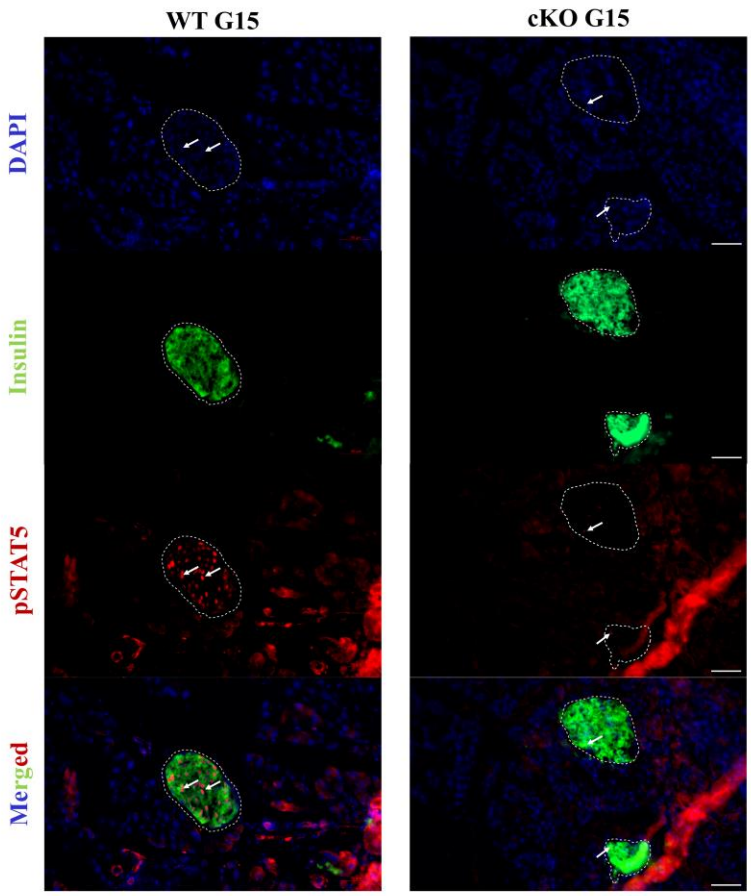

Figure 3.6 Representative image of phosphorylated STAT5 (pSTAT5) immunofluorescence in WT and cKO mice during gestational day 15 of pregnancy

This is a representative image of phosphorylated STAT5 (pSTAT5) immunofluorescence. The pancreas from WT mice (left) and cKO mice (right) during gestation day 15 (G15) was immunostained for Hoechst (blue), pSTAT5 (red), and Insulin (green). The dotted white lines outline an islet, white arrows indicate pSTAT5-positive and insulin-positive β cells, and the scale bars represent 50μm. Raneet Khalon performed immunofluorescence and took the images.

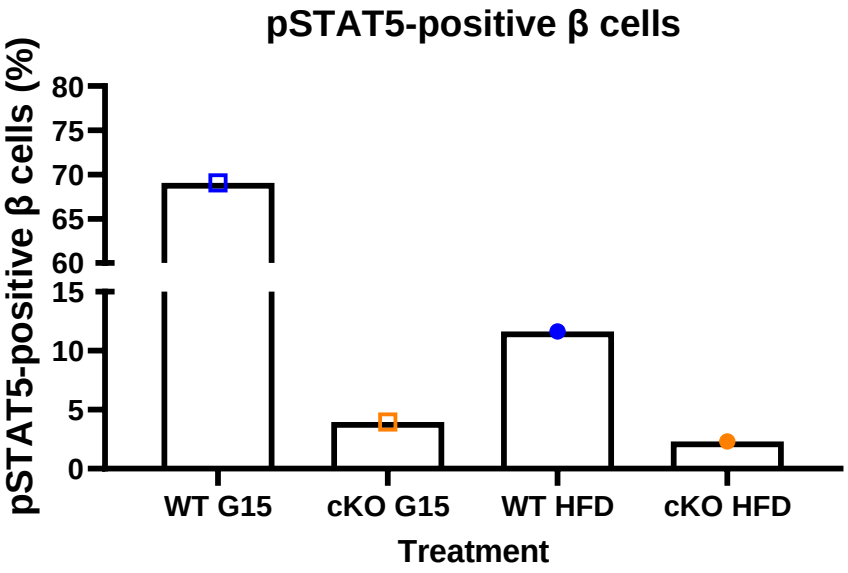

Figure 3.7 pSTAT5-positive β cells in WT versus cKO mice at G15 or HFD

The presence of pSTAT5-positive β cells was determined based on cells that were nuclear pSTAT5-positive, nuclear Hoechst-positive, and cytoplasmic Insulin-positive. At least 800 β cells were counted per mouse (n=1). No statistical analysis was performed between genotypes and treatments. The quantification of pSTAT5-positive β cells was done by Raneet Khalon.

3.3.2 Glucose homeostasis

Previous studies from the Huang Lab used whole-body and β cell-specific PRLR heterozygous mice to underscore the significance of PRLR in preserving glucose homeostasis during pregnancy.[38,46] This project utilized a β cell-specific homozygous knockout of PRLR to determine the effects of HFD on β cell function in multiparous mice. Both WT and cKO mice exhibited no statistically significant change in weight during 12 weeks of CD and gained similar amounts of weight after 12 weeks HFD (Supplemental Figure 2). No statistically significant differences were observed in biweekly fed blood glucose measurements between WT and cKO mice during 12 weeks of CD or HFD (Supplemental Figure 3).

Additionally, there was no statistically significant difference observed in FBG between WT and cKO mice across the timepoints: Virgin, Postpartum, 6 weeks of CD, 12 weeks of CD, 6 weeks of HFD, and 12 weeks of HFD (Supplemental Figure 4). However, a statistically significant difference in FBG was noted in WT mice after 12 weeks of HFD [7.6$\pm$0.4mM] compared to Virgin [5.1$\pm$0.3mM (*p=0.001*)], Postpartum [5.7$\pm$0.3mM (*p=0.006*)], and 12 weeks of CD [5.3$\pm$0.3mM (*p=0.002*)] (Figure 3.8). Similarly, in cKO mice, FBG was also elevated after 12 weeks of HFD [8.4$\pm$0.7mM] compared to Virgin [5.9$\pm$0.5mM (*p=0.002*)] and Postpartum [6.1$\pm$0.3mM (*p=0.002*)] (Figure 3.8).

To evaluate glucose homeostasis, an OGTT was conducted at specific time points: 4 weeks after the last dosage of tamoxifen before pregnancy (Virgin), one week after their second litter (Postpartum), and after 6- and 12-weeks of CD or HFD. It was observed that Virgin WT mice had elevated blood glucose levels compared to cKO mice at 10 minutes during OGTT

(Supplemental Figure 5A), although no difference in overall glucose excursion, measured as integrated AUC throughout the 120 minutes of OGTT, was noted (Supplemental Figure 5C). Postpartum, no statistically significant difference was found in blood glucose levels at any timepoint during OGTT and the AUC measurements were similar (Supplemental Figure 5 B&C).

Further investigations aimed to determine the effects of 12 weeks of CD in WT and cKO mice. It was observed that WT mice after 6 weeks of CD had higher blood glucose at 10 minutes during an OGTT compared to Postpartum (Supplemental Figure 6A). After 12 weeks of CD, WT mice had elevated blood glucose at 15 minutes during an OGTT compared to Postpartum (Supplemental Figure 6A). However, no statistically significant difference in AUC was observed in WT mice between the timepoints: Postpartum, 6-, and 12-weeks of CD (Supplemental Figure 6). cKO mice fed 12 weeks of CD displayed elevated blood glucose levels at 45 and 60 minutes compared to Postpartum (Supplemental Figure 7A). Similarly, WT mice fed CD, no statistically significant difference in AUC was observed in cKO mice at timepoints: Postpartum, 6- and 12-week CD (Supplemental Figure 7B). Comparing WT and cKO at 6- and 12-weeks of CD, no statistically significant difference in blood glucose levels was noted during OGTT at Week 6 of CD but at Week 12 of CD, cKO mice displayed increased blood glucose levels at 30, 45, and 60 minutes (Supplemental Figure 8A). However, no statistically significant difference in AUC was observed at both 6- and 12-weeks of CD between WT and cKO mice (Supplemental Figure 8B).

The impacts of 12 weeks of HFD were evident in both WT and cKO. In WT mice, blood glucose levels during OGTT were elevated at various time points during Week 6 and Week 12 of HFD compared to Postpartum (Figure 3.9A). Integrated AUC during OGTT increased from

Postpartum after exposure to both 6- and 12-weeks of HFD in WT mice [Postpartum: 666±40 mM x min vs. Week 6 HFD: 990±54 mM x min (*p=0.009*)] and persisted until 12 weeks of HFD [Postpartum: 666±40 mM x min vs. Week 12 HFD: 1070±58 mM x min, (*p=0.006*)] (Figure 3.9B). Similarly, in cKO mice, blood glucose levels during OGTT were elevated at multiple timepoints during Week 6 and Week 12 of HFD compared to Postpartum (Figure 3.10A). Integrated AUC also increased in Postpartum cKO mice after exposure to both 6- and 12-weeks of HFD [Postpartum: 650±40 mM x min vs. 6 Week HFD: 1525±95 mM x min (*p=0.000005*)] and persisted until 12 weeks of HFD [Postpartum: 650±40 mM x min vs. 12 Week HFD: 1399±93 mM x min, *p=0.00001*)] (Figure 3.10B).

Finally, comparing WT and cKO mice on HFD revealed that cKO mice were glucose intolerant compared to WT mice on HFD. At 6 Weeks of HFD, cKO mice had elevated blood glucose at 60 and 120 minutes (Figure 3.12 A) and increased AUC [WT: 990±54 mM x min vs. cKO: 1525±95 mM x min, *p<0.0001*)] (Figure 3.12 C). This difference became more apparent at 12 weeks of HFD as cKO mice had elevated blood glucose levels during OGTT at 30, 45, and 60 minutes (Figure 3.12 B) and increased AUC [WT: 1070±58 mM x min vs. cKO: 1399±93 mM x min, *p<0.0001*)] (Figure 3.12C).

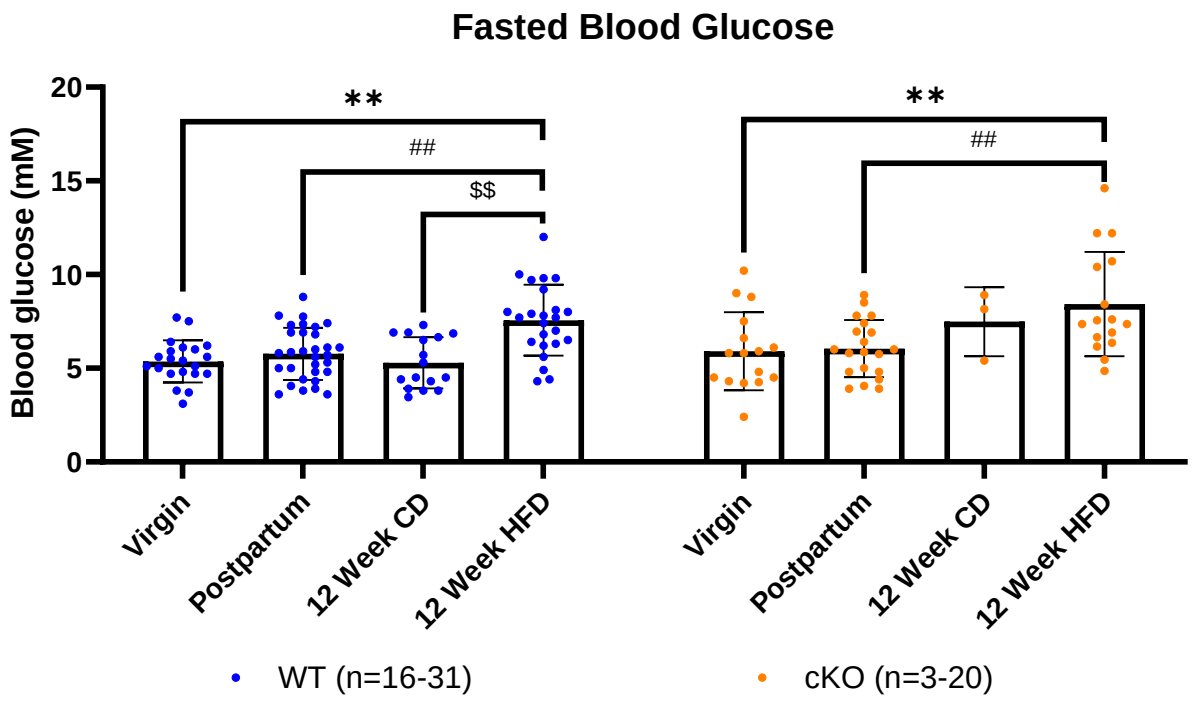

Figure 3.8 Fasted blood glucose (FBG) in WT and cKO mice at timepoints: Virgin, Postpartum, Week 12 CD, and Week 12 HFD

Fasted blood glucose (FBG) in WT and cKO mice at time points: Virgin, Postpartum, Week 12 CD, and Week 12 HFD. FBG were measured at the start of glucose tolerance tests OGTT and IPGTT. Blood glucose measurements were taken after a 14-16 hour fast at 08:00-09:00. Results are expressed as mean ± SEM. ANOVA was performed, and statistical significance was determined using Tukey's post hoc test where ns = not significant. Carol Huang assisted with data collection.

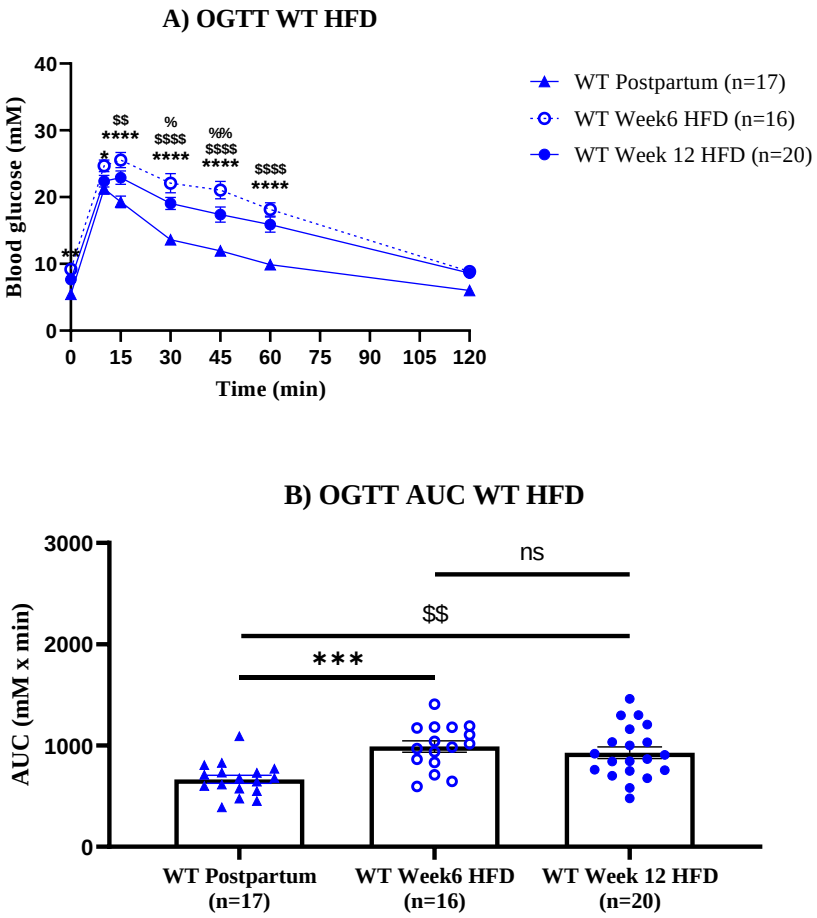

Figure 3.9 A) OGTT in WT mice Postpartum, 6- and 12-Week of CD and B) AUC

(A) Blood glucose levels in WT mice during OGTT at timepoints: Postpartum, 6- and 12-Week of HFD. After an overnight fast, glucose solution by oral gavage (2g glucose/kg) was administered and blood glucose was measured at 0, 10, 15, 30, 45, 60, 120 minutes. (B) AUC was calculated using trapezoidal method where time point 0 minutes as baseline. Results are means ± SEM (n=16-20). Two-way ANOVA was performed, and significance determined using Tukey's post hoc test where Postpartum vs. Week 6 HFD: * $p<0.05$, ** $p<0.005$, *** $p<0.0005$, **** $p<0.00005$, Postpartum vs. Week 12 HFD: $$ $p<0.005$, $$$$ $p<0.00005$, and Week 6 HFD vs. Week 12 HFD: % $p<0.05$, %% $p<0.005$. Carol Huang assisted with oral gavage and data collection.

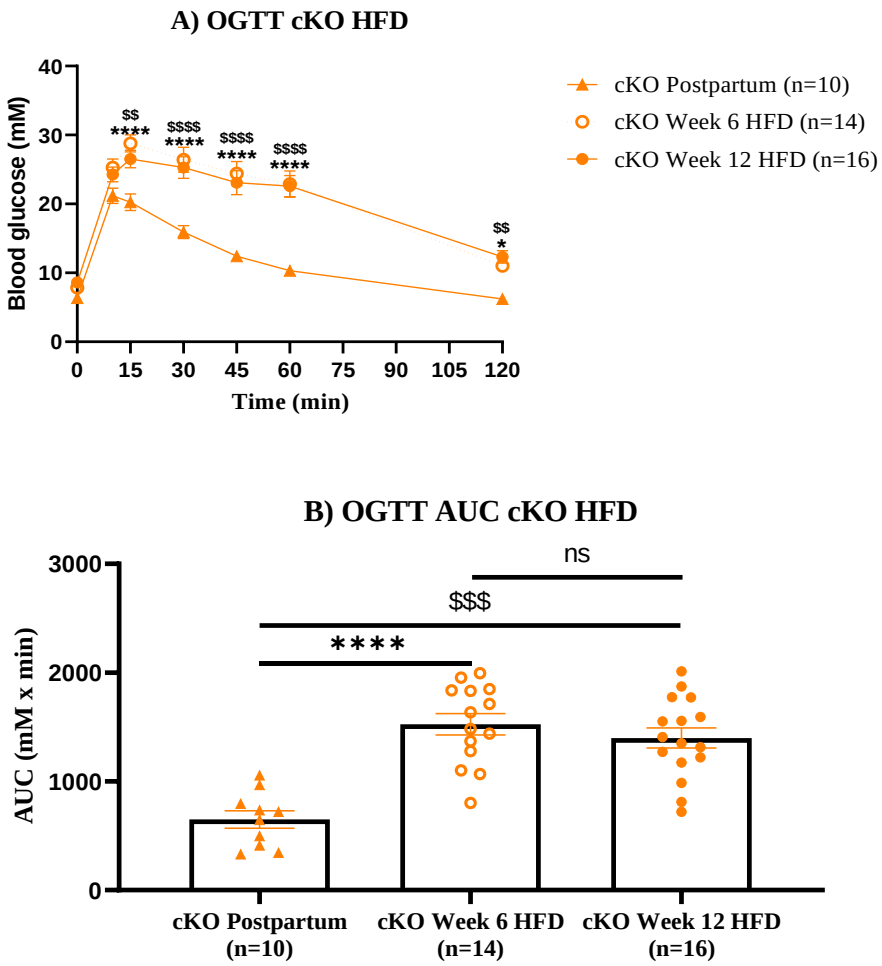

Figure 3.10 A) OGTT in cKO mice Postpartum, 6- and 12-Week of CD and B) AUC

(A) Blood glucose levels in WT mice during OGTT at timepoints: Postpartum, 6- and 12-Week of HFD. After an overnight fast, glucose solution by oral gavage (2g glucose/kg body weight) was administered and blood glucose was measured at 0, 10, 15, 30, 45, 60, 120 minutes. (B) AUC was calculated using trapezoidal method where time point 0 minutes as baseline. Results are means ± SEM (n=10-16). Two-way ANOVA was performed, and significance determined using Tukey's post hoc test where Postpartum vs. Week 6 HFD: * *p<0.05*, **** *p<0.00005*, Postpartum vs. Week 12 HFD: $$ *p<0.005*, $$$ *p<0.0005*, $$$$ *p<0.00005*. Carol Huang assisted with oral gavage and data collection.

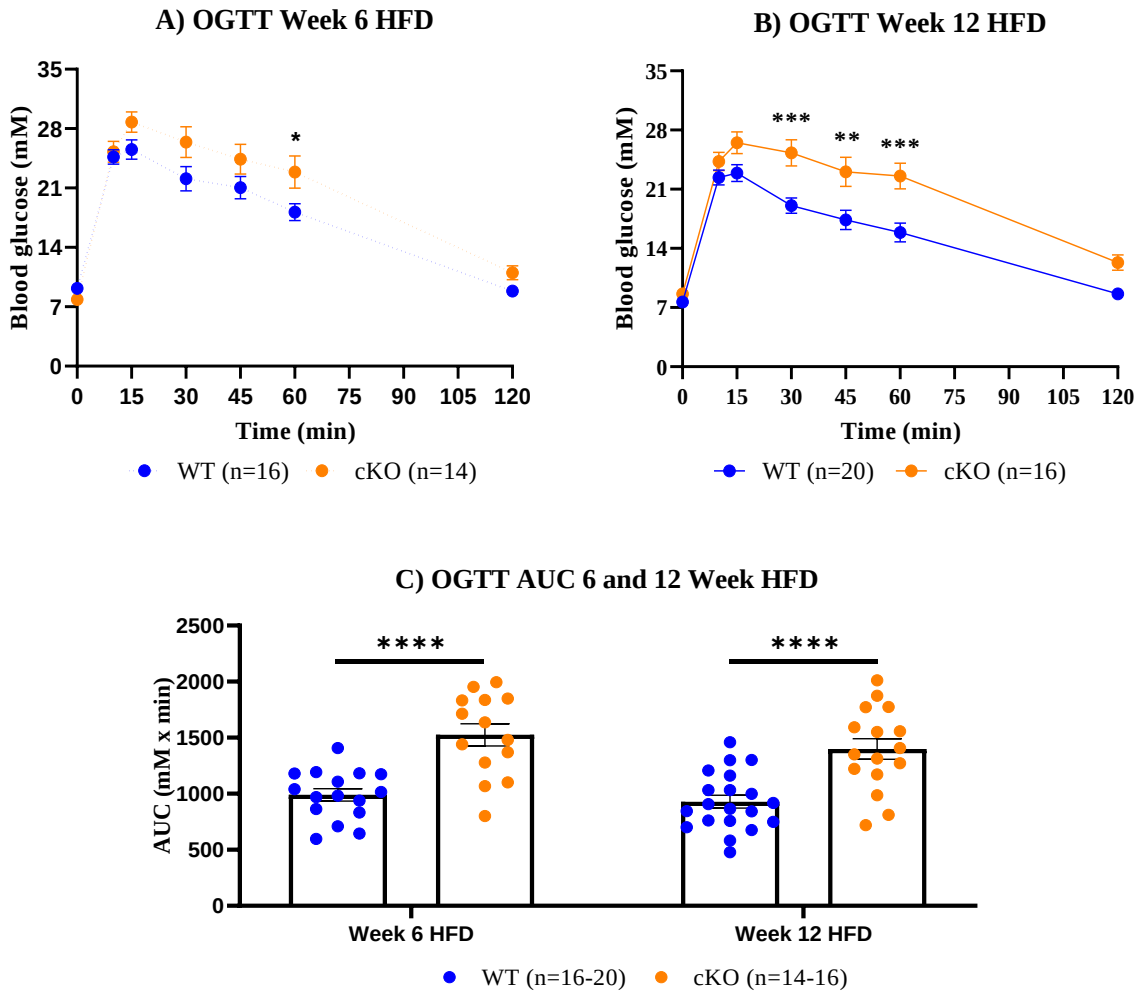

Figure 3.11 OGTT WT and cKO at A) 6 Week HFD, B) 12 Week HFD mice, and C) AUC

Blood glucose levels during OGTT at timepoints A) 6 Week HFD, B) 12 Week HFD, and C) AUC. After an overnight fast, glucose solution by oral gavage (2g glucose/kg body weight) was administered and blood glucose was measured at 0, 10, 15, 30, 45, 60, 120 minutes. Results are means ± SEM (n=14-20). Two-way ANOVA was performed, and significance determined using Tukey's post hoc test where WT vs. cKO: * $p<0.05$, ** $p<0.005$, *** $p<0.0005$, **** $p<0.00005$. Carol Huang assisted with oral gavage and data collection.

3.3.4 Insulin sensitivity

To assess how multiple pregnancies and subsequent exposure to CD and HFD afterwards affects insulin sensitivity, we conducted an ITT at time points: Virgin, Postpartum, Week 6 CD, Week 12 CD, Week 6 HFD, and Week 12 HFD. We found there was no statistically significant difference in blood glucose levels between WT and cKO mice at most time points, except during Week 6 HFD at 60 minutes, where WT HFD mice displayed higher blood glucose levels compared to cKO HFD mice (Figure 3.12E). However, we observed that in both WT and cKO mice, blood glucose levels were elevated at 15 minutes during Week12 of HFD compared to Postpartum [WT Postpartum: 5.0$\pm$0.4 mM vs. WT Week 12 HFD: 7.3$\pm$0.3 mM (*p=0.001*)] (Figure 3.13 A) and [cKO Postpartum: 4.9$\pm$0.4 mM vs. cKO Week 12 HFD: 7.7$\pm$0.7 mM (*p=0.0005*) (Figure 3.13B).

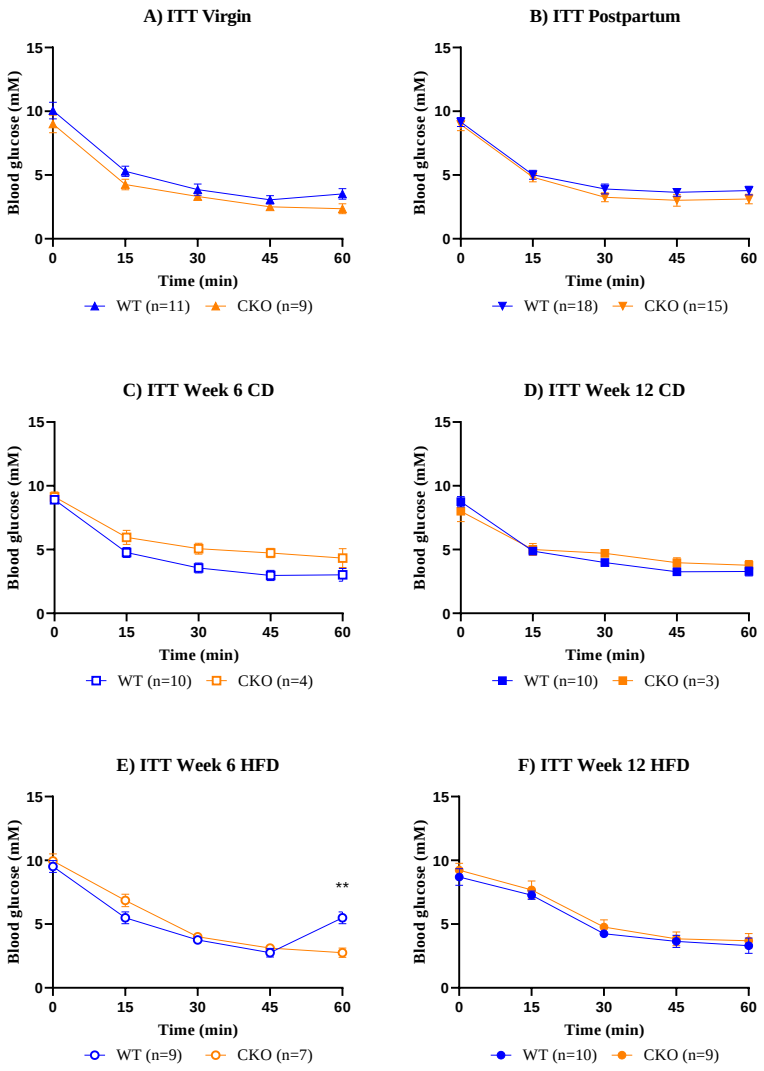

Figure 3.12 Insulin sensitivity measured by ITT in CD and HFD-fed mice

WT and cKO mice blood glucose levels during ITT were measured at timepoints A) Virgin, B) Postpartum, C) Week 6 CD, D) Week 12 CD, E) Week 6 HFD, and F) Week 12 HFD. After a 4-6 hour fast, insulin (0.5units/kg) was administered intraperitoneally, and blood glucose was measured at 0, 15, 30, 45, and 60 minutes. Results are presented as means ± SEM (n=3-18 mice/group). One-way ANOVA was performed, and statistical significance was determined using Tukey's post hoc test where ** $p<0.005$ WT vs cKO. Carol Huang assisted with intraperitoneal injection and data collection.

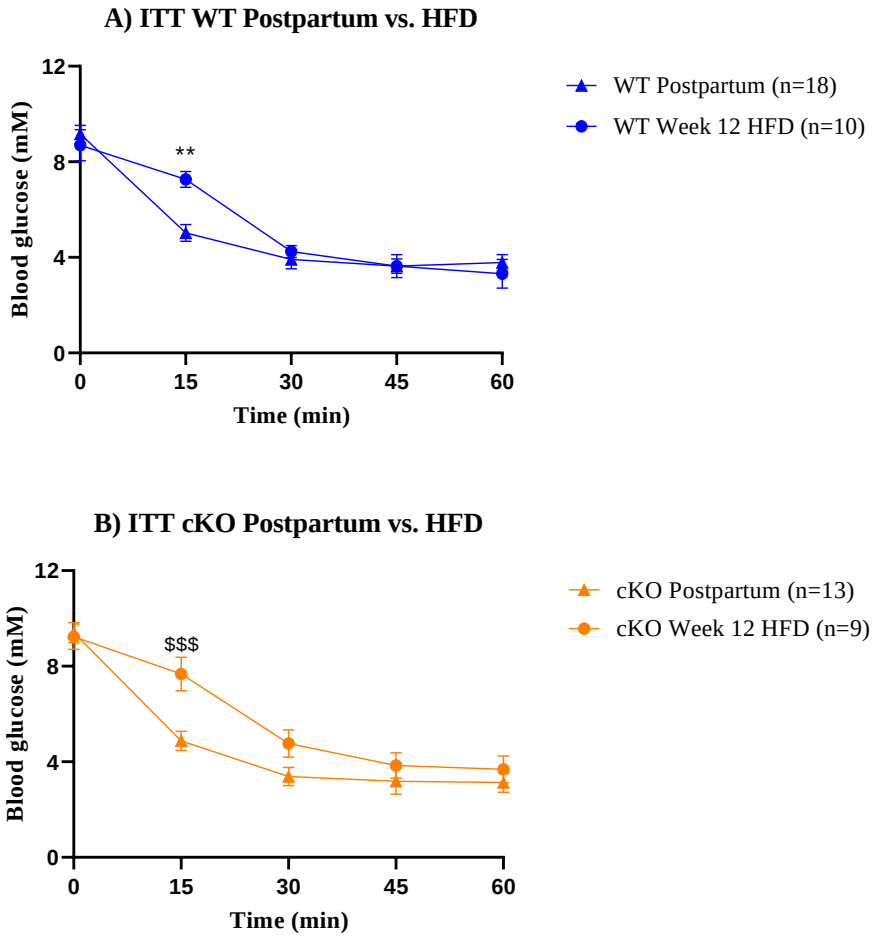

Figure 3.13 ITT Postpartum vs. Week 12 HFD in A) WT and B) cKO mice

A) WT and B) cKO mice blood glucose levels during ITT were measured at timepoints: Postpartum and Week 12 of HFD. After an 4-6 hour fast, insulin (0.5units/kg) was administered intraperitoneally and blood glucose was measured at 0, 15, 30, 45, and 60 minutes. Results are means ± SEM (n=3-18 mice/group). One-way ANOVA was performed, and statistical significance was determined using Tukey's post hoc test where ** $p<0.005$ WT Postpartum vs. WT Week 12 HFD and $$$ $p<0.0005$ cKO Postpartum vs. cKO Week 12 HFD. Carol Huang assisted with intraperitoneal injection and data collection.

3.3.5 *In vivo* and *in vitro* insulin secretion

We previously observed that cKO HFD mice exhibited glucose intolerance during an OGTT compared to WT HFD at 12 weeks of HFD (Figure 3.11). This glucose intolerance was unlikely due to differences in insulin sensitivity, as we found no statistically significant difference in blood glucose levels between WT and cKO during an ITT (Figure 3.12 F). Therefore, suspected that cKO mice secreted less insulin compared to WT mice after 12 weeks of HFD, which might explain the increased blood glucose levels during OGTT. To ascertain whether cKO mice have reduced insulin secretion, we measured both *in vivo* and *in vitro* insulin secretion.

In vivo insulin levels were measured from serum collected at 0, 10, and 30 minutes during the OGTT. Since insulin secretion is biphasic, the 10-minute time point aimed to capture the first phase, while the 30-minute time point was for observing the second phase of insulin secretion. Alongside measuring plasma insulin at these intervals, we calculated the IGI, a surrogate measure of β cell function derived from insulin change relative to glucose change during OGTT.[251]

Plasma insulin concentrations at 0 and 30 minutes showed no statistically significant difference between WT and cKO mice during OGTT at Week 12 HFD (Figure 3.13). Interestingly, cKO mice secreted had a reduction in plasma insulin at 10 minutes in comparison to WT mice [WT: 3.4$\pm$0.4 ng/ml vs. cKO: 2.2$\pm$0.2 ng/ml, n=16-17 (*p=0.002*)] (Figure 3.14). To further characterize this reduced *in vivo* insulin secretion, we computed IGI from 0 to 10 ($IGI_{0\text{-}10\ min}$) and 0 to 30 minutes ($IGI_{0\text{-}30\ min}$). While we saw no statistically significant difference in $IGI_{0\text{-}30\ min}$,

$IGI_{0\text{-}10\ min}$ was lower in cKO mice compared to WT mice [WT: 0.19$\pm$0.004 vs. cKO: 0.008$\pm$0.02, n=16-17, (*p=0.02*)] (Figure 3.15).

We aimed to determine whether there was an intrinsic defect in the ability of islets to secrete insulin, without the external influences of nutrients, hormones, and neuronal signals that are known to influence *in vivo* insulin secretion. To assess *in vitro* GSIS, pancreatic islets were isolated from all experimental mice, after 12 weeks of HFD or CD. Islets were sequentially incubated for 1 hour in the non-stimulatory conditions (2 mM glucose), stimulatory conditions (16 mM glucose), and glucose-independent stimulatory conditions (KCl). After each incubation, we collected media to quantify the amount of insulin secreted. We found no statistically significant difference in the amount of insulin secreted between WT and cKO islets from media collected after incubation in 2mM glucose, 16 mM glucose, and KCl (Figure 3.16).

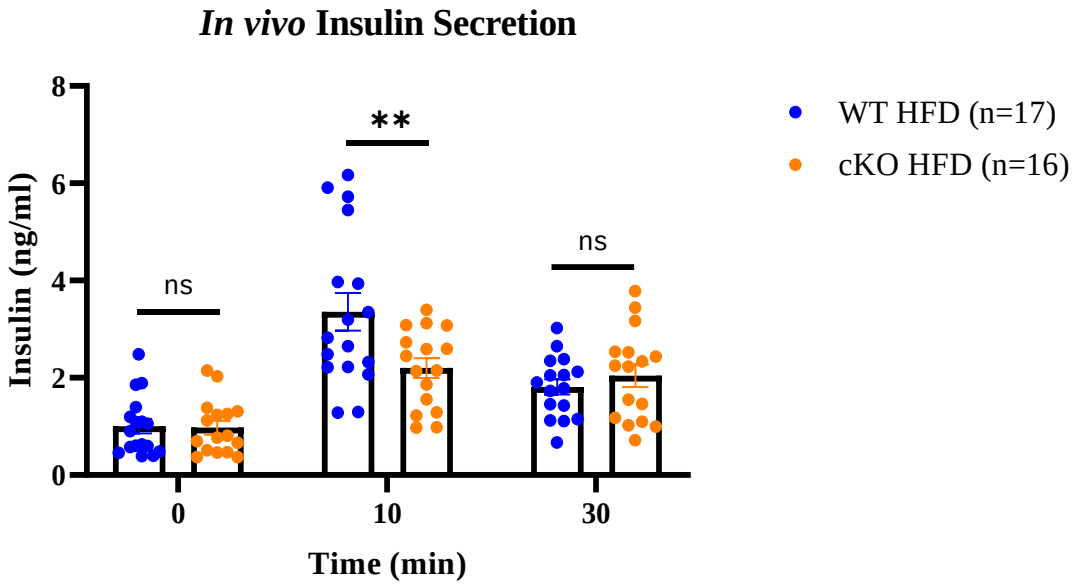

Figure 3.14. *In vivo* insulin secretion during OGTT after 12 weeks of HFD

Plasma insulin concentrations during the oral glucose tolerance test (OGTT) (2g/kg) following an overnight fast were compared between WT and cKO mice fed an HFD for 12 weeks. Blood was collected at 0, 10, and 30 minutes and measured by ELISA. Each data point represents a mouse (n=16-17). Results are expressed as means ± SEM. One-way ANOVA was performed, and statistical significance was determined using Tukey's post hoc test where ** $p<0.005$ WT vs. cKO. Carol Huang assisted with data collection.

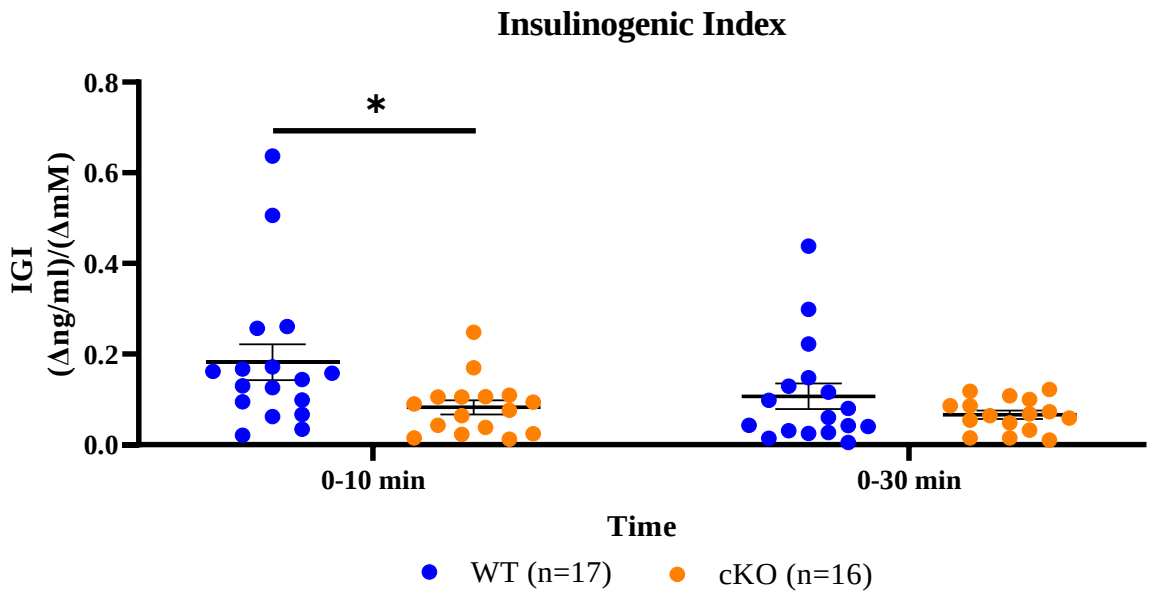

Figure 3.15. Insulinogenic index (IGI) at 10 and 30 minutes during OGTT after 12 Weeks of HFD

The insulinogenic index (IGI) was calculated after 12 weeks of HFD during OGTT, where $IGI_{0\text{-}10\ min}$ = (Δ blood glucose $_{0\text{-}10\ min}$) / (Δ insulin $_{0\text{-}10\ min}$) and $IGI_{0\text{-}30\ min}$ = (Δ blood glucose $_{0\text{-}30\ min}$) / (Δ insulin $_{0\text{-}30\ min}$). Each data point represents a mouse (n=16-17 mice/genotype). Results are expressed as means ± SEM (n=16-17 mice/group). One-way ANOVA was performed, and statistical significance was determined using Tukey's post hoc test where * $p<0.05$ WT vs. cKO. Carol Huang assisted with data collection.

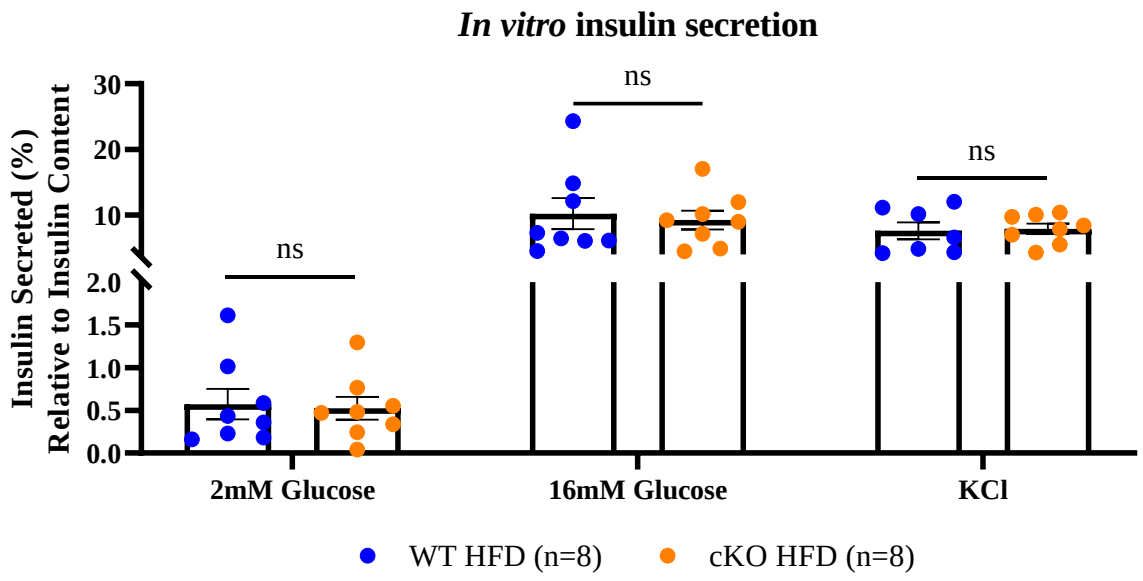

Figure 3.16. *In vitro* glucose stimulated insulin secretion in pancreatic islets after 12 weeks of HFD

In vitro glucose-stimulated insulin secretion (GSIS) was assessed using isolated pancreatic islets. The islets were cultured sequentially in 2mM glucose (non-stimulatory), 16mM glucose (stimulatory), and KCl (glucose-independent stimulation) for 1 hour each. Media was collected after each stimulus and the amount of insulin in media was normalized to total insulin content. Each data point represents the mean of two independent experiments of one mouse (n=8 mice/group). Data expressed as mean ± SEM. One-way ANOVA was performed, and statistical significance was determined using Tukey's post hoc test where ns = not significant.

3.4 Discussion

Our study aimed to examine the role of PRLR in pancreatic β cells in multiparous mice exposed to HFD. It has been shown that during pregnancy, there is maternal insulin resistance that shunts nutrients to the developing fetus.[54] To combat this increased demand of insulin, and prevent GDM, there are maternal β cell adaptations that enhance β cell mass, insulin production, and secretion, believed to be regulated in part by pregnancy-related hormones PL, PRL, estrogens, and GH. [43,55,56] Previous studies have shown that during pregnancy, PRLR has an important role in regulating β cell mass, through upregulation of β cell proliferation, allowing greater insulin secretion.[252] Previous work from our lab has shown *in vivo* evidence that PRLR is involved in the maternal increase in β cell mass during pregnancy, using transgenic mice with either global heterozygous deletion of PRLR or β cell-specific heterozygous and homozygous deletion of PRLR.[38,46] However, little work has been done to determine the role of PRLR in β cells outside of pregnancy.

In this chapter, we investigated whether PRLR in β cells affect β cell physiology during times of metabolic stress (Aim 1). We have previously showed that *Prlr* mRNA expression is reduced by 90% during G15 of pregnancy in cKO mice.[46] While pregnancy is marked with increased levels of PRL, PL, and GH, which have been shown to increase PRLR expression in pancreatic islets, these increases would not be observed in non-pregnant mice placed on HFD.[56,120] However, we still observed that multiparous cKO mice after 12 weeks of HFD had an 80% reduction in *Prlr*-L and 90% reduction in *Prlr*-S mRNA expressions compared to WT controls (Figure 3.4). We observed a trend towards increased *Prlr* expression (both *Prlr*-L and *Prlr*-S) after 12 weeks of HFD in WT mice compared to CD (Figure 3.5). A statistically significant difference was almost

reached, both p=0.08; therefore, a larger sample size would allow for us to determine if HFD increases PRLR mRNA expression in WT mice. Our PRLR mRNA expression results coincide with work done by Pepin et al. (2019), whose group also observed increased PRLR expression in mice with β cell-specific knockout of PRLR after exposure to HFD.[220]

At the protein level, we utilized a surrogate marker of PRLR activation, pSTAT5, because we could not find a reliable anti-PRLR antibody. pSTAT5 is activated by ligand binding to PRLR during the main JAK2/STAT5 signaling pathway, where JAK2 phosphorylates STAT5, leading to pSTAT5 homodimers translocating to the nucleus to influence transcription.[211] It is important to note that STAT5 is activated not just by PRLR but other hormones such as GH and cytokines with their respective receptors, suggesting these signals may contribute to the differences we observed.[253] To support our PRLR knockout at the mRNA-level in cKO mice, our preliminary results showed that during G15 of pregnancy, WT mice had nearly 70% pSTAT5-positive β cells while cKO mice had a 4% pSTAT5-positive β cells (Figure 3.7). In contrast, after 12 weeks of HFD, WT mice had 13% pSTAT5-positive β cells but islets from cKO mice only 2% of β cells were pSTAT5-positive (Figure 3.7). With only one mouse for each treatment and genotype, an increase in sample size is required to perform statistical analyses and determine the extent of pSTAT5 activation between these treatments.

Embryonic deletion of PRLR reduces β cell mass from birth, and a reduction β cell mass would potentially be an additional variable affecting glucose homeostasis, in addition to our experimental treatment of 1) multiparity and 2) HFD.[254] Furthermore, PRLR is expressed in many tissues other than pancreatic β cells, such as in endothelial cells in islets.[35–39] Therefore, an

inducible β cell-specific model would reduce these confounding variables and allow us to study the specific role of PRLR in β cell adaptation to metabolic stressors (pregnancy and HFD).

We used a tamoxifen-inducible Cre-LoxP system to induce β cell-specific deletion of PRLR, previously described.[46] Tamoxifen was given to both WT and cKO mice at age 8 weeks (after sexual maturity) to activate Cre recombinase in cKO mice and remove both copies of exon 5 of PRLR; the administration of tamoxifen did not result in any changes in glucose homeostasis between Virgin WT and cKO mice, as no statistically significant difference was observed in AUC during OGTT (Supplemental Figure 5C) and blood glucose levels during an ITT (Figure 3.12A). These results suggest that the effects of tamoxifen in both WT and cKO mice had no statistically significant difference in glucose homeostasis. Subsequently, female mice were then mated with WT males for two pregnancies.

As β cell mass reverts back to its pre-pregnancy state postpartum, we hypothesized that there will be no difference in glucose homeostasis between the cKO and WT mice following two pregnancies, as the ability to expand β cell mass during pregnancy accounted for the difference in their glucose tolerance during pregnancy.[204] As hypothesized, we observed similar levels of glucose homeostasis following two pregnancies in WT and cKO mice, as there were no statistically significant differences in blood glucose levels during an OGTT and AUC (Supplemental Figure 5B&C). Additionally, whole-body insulin sensitivity was similar in WT and cKO mice, as measured by an ITT (Figure 3.12B). We can conclude that two pregnancies did not affect glucose homeostasis and insulin sensitivity between cKO and WT mice following two pregnancies, but it has been shown that glucose intolerance during gestation increases the

risk of developing T2D later on in life.[53] Therefore, the absence of PRLR during pregnancy in cKO mice, which we have shown previously to be deleterious to glucose homeostasis, increases susceptibility to glucose intolerance when challenged with another metabolic stressor: HFD.

Following two pregnancies, WT and cKO mice were placed on either CD or HFD for a duration of 12 weeks to mimic mothers adopting a Western Diet following pregnancy. The die- induced obesity (DIO) model is most often used to simulate a Western Diet, characterized by high content of fat and sugars.[233] We chose a diet containing 60% of calories from fat, as mice on these diets become obese more quickly compared to diets with lower fat percentage, thus reducing the time needed for housing and consequently caging costs.[235,255] Additionally, female C57BL/6J mice exposed to varying fat concentrations ranging from 10-60% revealed that a HFD with 60% of calories coming from fat worsened glucose tolerance and insulin sensitivity to the greatest extent.[256]

In both WT and cKO mice fed CD for 12 weeks, no statistically significant difference in body weight was observed during weekly measurements (Supplemental Figure 2A). There was no statistically significant difference in fed blood glucose between WT and cKO over the course of 12 weeks on CD (Supplemental Figure 3A). At 6 and 12 weeks of CD, cKO mice had higher FBG, but statistical significance was not observed (Supplemental Figure 4). For WT mice, FBG at12 weeks of CD did not significantly differ from Virgin and Postpartum WT mice (Figure 3.8). cKO mice at the 12-week CD time point had a sample size of n=3 (Figure 3.8); therefore, an increase in the number of mice is needed to draw clearer conclusions about the effects of CD in cKO mice after two pregnancies

For WT mice, 12 weeks of CD did not appear to affect glucose homeostasis compared to the Postpartum period, as blood glucose levels at 6 and 12 weeks of CD did not significantly differ from Postpartum blood glucose levels during OGTT (Supplemental Figure 6A). No statistically significant difference was observed in AUC during OGTT in WT mice at time points: Postpartum, 6 weeks on CD, and 12 weeks on CD (Supplemental Figure 6B). In contrast, cKO mice on CD had elevated blood glucose levels during an OGTT at both 6 and 12 weeks of CD compared to Postpartum (Supplemental Figure 7). No statistically significant difference in AUC was observed during OGTT in cKO mice (Supplemental Figure 7B). The increase in blood glucose levels may be from the low sample size of cKO mice 12 weeks on CD (n=3-4), and experimental variance could also play a role. A larger sample size is required to observe whether 12 weeks of CD worsens glucose tolerance in cKO mice, postpartum. If cKO mice become glucose intolerant after exposure to CD postpartum, this may suggest that PRLR may have a role in aging, as conditional knockout of STAT5 in pancreatic β cells has been shown to induce mild glucose intolerance in aged (6 months) mice, possibly due in part to a STAT5-dependent decrease in β cell proliferation.[218,257] No statistically significant difference in blood glucose levels was observed during ITT between WT and cKO mice after 6- and 12-weeks of CD (Figure 3.12). This suggests that a difference in insulin sensitivity may not be responsible for the difference in glucose tolerance between WT and cKO mice challenged with CD.

The physiological effects of HFD in rodents has been extensively studied.[157,235–237,258–260] The effects of HFD in mice includes increasing body weight, worsened glucose tolerance, and

increased insulin resistance.[157,235–237,258–260] This occurs due to chronic elevations of glucose and FFAs that can lead to glucolipotoxicity in β cells.[29,184]

In both WT and cKO mice placed on HFD, no statistically significant difference was observed in body weight during weekly measurements, but a steady increase over the 12 weeks was noted (Supplemental Figure 2B). There was also no statistically significant difference in fed blood glucose between WT and cKO over the 12-week course of HFD (Supplemental Figure 3B). FBG between WT and cKO mice at 6- and 12-weeks of HFD were not significantly different (Supplemental Figure 4). However, we did observe that FBG increased in both WT [7.5±0.4 mM] and cKO [8.4±0.7 mM] compared to their earlier Virgin and Postpartum blood glucose levels but is still within the normal range of a FBG less than 11.0mM (Figure 3.8). [246,247]
To summarize, the effects of HFD in our model aligns with other rodent models of DIO where an increase in body weight and FBG is observed.

Glucose tolerance measured by an OGTT worsened in both WT and cKO mice after 6 and 12 weeks of HFD compared to Postpartum (Figures 3.9 & 3.10). We did observe that cKO mice were more glucose intolerant, indicated by increased blood glucose levels and AUC, compared to WT mice at 6 weeks of HFD, and this glucose intolerance persisted until 12 weeks (Figure 3.11). Our glucose tolerance results differ from Pepin et al, who found no difference in glucose tolerance between female mice with β cell-specific KO PRLR.[220] Previous work by Pepin et al. have shown that no difference in glucose tolerance was observed in female virgin mice with β cell-specific PRLR knockout compared to WT controls challenged with HFD at both 4 and 12 weeks.[220] The biggest difference between our findings and Pepin et al. is that they measured

glucose tolerance with an IPGTT whereas we performed an OGTT; an intraperitoneal administration of glucose would be physiologically abnormal as nutrient consumption occurs orally but is commonly used in this field to test glucose tolerance as oral administration requires more technical expertise and is more stressful for the animals.[245] An IPGTT tests the ability to secrete insulin in the absence of incretin hormones GIP and GLP-1 from the gut, whereas an OGTT would induce the secretion of GIP and GLP-1, which contributes to a significant amount of postprandial insulin release.[13–15] Additionally, our females were exposed to two pregnancies before HFD and this could have insulted β cells ability to compensate prior to HFD exposure. Finally, Pepin et al. generated β cell-specific PRLR KO using rat insulin promoter (RIP)-Cre, where the mere expression of RIP-Cre has been shown to develop glucose intolerance.[261]

Both WT and cKO mice displayed higher levels of insulin resistance, as blood glucose levels were increased at 15 minutes (Figure 3.13). Interestingly, we observed that WT mice at 6 weeks of HFD had a statistically significant increase in blood glucose levels at 60 minutes during an ITT (Figure 3.12 E). This may suggest that WT mice have increased α cell function at 6 weeks on HFD, whereby WT mice have increased glucagon release to combat the decreased blood glucose due to exogenous insulin. Further investigation whether a difference in α cell function or experimental variance is the cause of this difference and whether this phenotype is observed 6 weeks into HFD. However, at 12 weeks of HFD, WT and cKO mice had comparable blood glucose levels during the timepoints measured during the ITT (Figure 3.12F). These results suggest that while both WT and cKO mice experience worsened glucose tolerance and insulin sensitivity after exposure to HFD in comparison to Postpartum, cKO HFD-fed are more glucose intolerant with similar levels of insulin sensitivity compared to WT HFD-fed controls.

Finally, our aim was to measure insulin secretion both *in vivo* and *in vitro*, as our current results indicated a reduction in insulin secretion was responsible for the glucose intolerance in cKO mice after 12 weeks of HFD, given that no statistically significant difference was observed during an ITT. We found that *in vivo* insulin secretion was lower at 10 minutes of the OGTT, but no statistically significant difference was observed at times 0 and 30 minutes (Figure 3.14). Similarly, $IGI_{0\text{-}10\ min}$ was decreased, but no statistically significant difference was observed $IGI_{0\text{-}30\ min}$ in cKO mice compared to WT (Figures 3.15). These results suggest that cKO mice fed HFD may have a defect in first phase of insulin secretion during an OGTT after 12 weeks of HFD compared to WT controls. This is of importance as a reduction in first phase insulin secretion is considered one of the earliest detectable abnormalities in individuals developing T2D.[99,100]

Given that various insulin secretagogues, nutrients such as free fatty acids, amino acids, as well as hormones and neuronal signals integrate into the insulin secretion pathway to augment insulin secretion *in vivo*, conduction *in vitro* analyses would allow us to measure insulin secretion in the absence of these insulin secretagogues that would play a role *in vivo*.[240] We isolated pancreatic islets and cultured *in vitro* to observe glucose-dependent and glucose-independent insulin secretion. We found that there was no difference in the amount of insulin secreted from islets of cKO and WT mice at basal levels (2mM Glucose), in response to glucose-dependent (16mM Glucose), and glucose-independent (40mM KCl) stimuli (Figure 3.16). Although our method of data collection did not allow us to measure temporal (i.e. first and second phase) insulin secretion *in vitro*, the total insulin secreted in response to 2mM Glucose, 16mM Glucose, and

40mM KCl was no different between islets of WT and cKO mice after 12 weeks of HFD. Consequently, we can conclude that cKO mice exhibit a reduction in first phase of insulin secretion during an OGTT *in vivo*.

3.5 Conclusion

In conclusion, we have found evidence that PRLR required for maintaining glucose homeostasis in multiparous mice challenged with HFD. We have validated our knockout with decreased mRNA expressions of PRLR-L and PRLR-S, as well as a reduction in pSTAT5-positive β cells. cKO mice treated with HFD showed impaired glucose homeostasis as early as 6 weeks of HFD, worsened at 12 weeks. While both WT and cKO mice experienced worsened glucose tolerance after HFD, cKO mice were more glucose intolerant compared to WT controls during an OGTT. This difference in glucose tolerance could not be attributed to a difference in insulin resistance between WT and cKO mice, but rather a blunted first phase insulin secretion response in the cKO mice. Total insulin secreted during *in vitro* GSIS suggests that the intrinsic capabilities of β cells from WT and cKO are similar, and that an *in vivo* factor may be responsible for the reduction in first phase of insulin secretion during an OGTT.

Further investigation is needed to understand the underlying cause of blunted first phase of insulin secretion and to see if there are differences in β cell mass and function. During pregnancy, the role of PRLR signaling is to increase β cell mass, insulin content, and failure to do so in response to HFD could explain the reduction in insulin secretion observed in cKO mice. In Chapter 4, we will determine how β cells compensate when PRLR is lost (Aim 2) and identify the molecular mechanisms governing differences in β cell function and compensation (Aim 3).

We will examine the expression of genes involved in β cell function, such as key regulatory enzymes in the GSIS pathway, genes involved in β cell dysfunction like those involved in the UPR, and the incretin effect to determine which of these are responsible for the reduction in first phase of insulin secretion *in vivo*. Identification of targets that are differentially expressed will add to our understanding of the role of PRLR outside of pregnancy.

Chapter 4: β cell compensation during times of metabolic stress and the molecular mechanisms responsible

4.1 Introduction

In Chapter 3, we observed how the absence of PRLR in pancreatic β cells negatively affected glucose homeostasis in multiparous mice challenged with HFD. cKO mice fed HFD were more glucose intolerant compared to WT mice during an OGTT (Figure 3.10). This discrepancy in glucose tolerance did not stem from a difference in insulin sensitivity (Figure 3.12F) but rather from a decrease in the first phase of insulin secretion *in vivo* (Figure 3.14). In this chapter, we will explore how PRLR enables β cells to compensate during times of metabolic stress (Aim 2) and the molecular mechanisms that may be responsible (Aim 3).

β cells undergo compensatory mechanisms to meet the increased demand for insulin and maintain stable blood glucose levels during times of insulin resistance, as see in obesity. One of these mechanisms is to increase insulin biosynthesis. The amount of insulin (insulin content) in β cells has been implicated in β cell function, as insufficient insulin may lead to hyperglycemia and/or diabetes.[262,263] In humans, autopsy analyses have found that T2D subjects have a two-thirds insulin content compared to non-diabetic controls in humans.[264]

Unlike humans who have one insulin gene, mice have two insulin genes: *Ins1* and *Ins2*. Although both contribute to insulin production, the *Ins2* gene is more functionally important compared to *Ins1*.[85] Insulin gene expression is controlled by various transcription factors such as NEUROD1, NKX6.1, MAFA, PAX6, and PDX1.[81,91] Chronic exposure to nutrients requires

greater insulin biosynthesis and may lead to the accumulation of unfolded proinsulin, triggering the UPR. During the UPR, the ER chaperone, BIP, binds to unfolded proteins, activating the PERK, ATF6, and IRE1α pathways.[165] Downstream targets of UPR, such as *Xbp1*-S, decrease insulin transcription and if UPR is not resolved, ER stress ensues, possibly leading to apoptosis of the β cell.[157] The activation of all three branches of the UPR leads to the upregulation of CHOP, where CHOP promotes apoptosis by regulating the pro-apoptotic proteins in the BCL-2 family of proteins in the intrinsic apoptosis pathway.[173] In the BCL-2 family, the ratio of BAX:BCL-2 represents a cell death switch, where an increased ratio of BAX:BCL-2 pushes the cell towards apoptosis, while a decreased ratio of BAX:BCL-2 pushes the cell away from apoptosis.[172]

Another compensatory mechanism to meet the increased demand for insulin is to increase β cell mass. Studies in rodents have reported a 3- to 4-fold increase, but in contrast, humans have been shown to only have a 1- to 2-fold increase in β cell mass.[38,40,153–155] The increase in β cell mass is partly regulated by nutrients such as glucose and FFAs in addition to hormones such as GIP, GLP-1, insulin, PL, PRL, and GH.[22–24,211,212] While β cell proliferation plays an important aspect in increasing β cell mass, β cell apoptosis is a key contributor to the pathogenesis of T2D, as β cell apoptosis may lead to a reduction in β cell mass and consequently, insulin deficiency.[17] Studies in young male rodents have suggested that β cell proliferation occurs early (3 to 7 days) during exposure to HFD, decreasing over time, with little to no evidence of β cell apoptosis after 16 weeks of HFD.[156,157]

In response to HFD in rodents, there is an increase in the expression of genes involved in β cell function such as *Gck*, *Glut2*, *Pc*, *Gipr*, and *Glp-1r*.[157] GLUT2 allows the rapid entry of glucose into β cells, where upon glucose entry, GCK phosphorylates glucose allowing entry into glycolysis. PC converts oxaloacetate into pyruvate to enter the TCA cycle, these transporters and enzymes increase glucose metabolism and consequently, increase GSIS.[102–104] FFAs have also been shown to amplify insulin secretion through FFAR1 by causing Ca^{2+} from the ER.[112,113] Finally, the incretin hormones GIP and GLP-1 and their respective receptors GIPR and GLP-1R are one of the most important non-glucose insulin secretagogues, accounting for up to 80% of insulin secreted after a meal, called the incretin effect.[13–15]

The incretin effect is a physiological observation where oral glucose elicits greater insulin secretion compared to intravenous administration.[12] The incretins, play an important role in both first phase of insulin secretion and postprandial insulin secretion.[13–15,122] Both GIPR and GLP-1R are GPCRs, and their activation results in the increase in intracellular cAMP.[23] The increase in cAMP activates EPAC, which increase intracellular Ca^{2+} to promote insulin granule exocytosis.[23,126] There exists two isoforms of EPAC (EPAC1 and EPAC2), both down stream of GIPR and GLP-1R, and have been found to directly impact the effect of incretins on β cells.[131] Additionally, the activation of GLP-1R has been shown to induce PDX1 nuclear translocation in a cAMP-dependent manner.

Regulation of both GIPR and GLP-1R expressions is under the control of various stimuli and transcription factors. Chronic elevation in glucose and lipids has been shown to decrease incretin hormone expression and the actions of GIP and GLP-1.[27,28,133,134] The transcription factor

PPARG has been shown to regulate the expression of *Gipr*, whereas transcription factors E2F1, MAFA, and NKX6.1 have been shown to regulate *Glp-1r* expression.[91,137,139,141,265] Finally, PAX6 and TCF7L2 have been shown to regulate expressions of both *Gipr* and *Glp-1r*.[136,138]

In this chapter, we will examine how β cells respond to HFD after two pregnancies when prolactin signaling is lost (Aim 2). We measured insulin content from the pancreatic islets isolated for *in vitro* GSIS and used immunohistochemistry to observe whether there are differences in β cell proliferation, apoptosis, and mass. Finally, we used RTqPCR to measure genes involved in β cell functions and measured glucose tolerance with an IPGTT to observe the incretin effect. To identify the molecular mechanisms governing differences in β cell function and compensation (Aim 3), we used a candidate gene approach to identify genes that regulate insulin gene expression, genes involved in the UPR, genes involved in the incretin effect, and transcription factors that regulate incretin hormone receptor expressions.

We hypothesize that cKO mice fed 12 weeks of HFD will exhibit a reduction in insulin content and β cell mass, as PRLR-null mice manifest these phenotypes.[207,208] As HFD induces insulin resistance in both WT and cKO mice, we anticipate an increase in the expressions of the UPR-related genes compared to mice fed a CD. Previous research in our lab has demonstrated that LRRC55 expression increases during pregnancy in a PRLR-dependent manner. Additionally, overexpression of LRRC55 has been shown to protect β cells from FFA-induced apoptosis *in vitro*.[219] Therefore, we expect to observe increased β cell apoptosis in cKO mice compared to WT controls.

Treatment of pancreatic islets with PRL have shown an increase in the expressions of GLUT2 and GCK.[205] Consequently, we anticipate the downregulation of these genes in cKO mice compared to WT controls. Pepin et al. have previously shown that mice with β cell-specific KO of PRLR have similar glucose homeostasis compared to WT controls fed HFD for 12 weeks.[220] Therefore, we expect glucose tolerance, as measured by an IPGTT, to be similar between WT and cKO mice fed HFD.

4.2 Methods

4.2.1 Measurement of insulin content

Insulin content was measured using islets that underwent *in vitro* GSIS, and data was normalized to DNA. To measure DNA, samples were centrifuged at 12,500 rpm at 4ºC for 10 minutes to pellet all cell contents, and the supernatant (~200µl) was removed. Then, 500µl of Phenol:Chloroform:Isoamyl Alcohol (25:24:1 v/v) (Invitrogen) was added, and the tubes were inverted 10 times. After centrifugation at 12,500 rpm at 4ºC for 10 minutes, the aqueous layer was collected into a new tube. Next, 640µl of isopropanol was added, and tube was inverted 20 times to precipitate the nucleic acid. Following centrifugation at 12,500 rpm at 4ºC for 15 minutes, the supernatant was removed. The samples were then washed with 150µl of 70% ethanol and centrifuged at 12,500 rpm at 4ºC for 15 minutes. After removing the supernatant, the remaining ethanol was allowed to evaporate in the fume hood. Subsequently, the samples were resuspended in 100µl of Tris EDTA buffer, and the DNA concentration was measured by NanoDrop spectrophotometer (ThermoScientific). The data were expressed as the sum of insulin (ng/dL) in supernatant collected during the 2mM Glucose, 16mM Glucose, 40mM KCl

incubations of the GSIS assay, and the insulin extracted from these islets by (acid-ethanol method), normalized to the total DNA content.

4.2.2 Measurement of genes involved in β function and ER stress

To assess whether β cells lacking PRLR are more susceptible to ER stress and consequently apoptosis, we utilized RTqPCR to quantify mRNA expression of genes involved in the UPR. RNA was extracted from pancreatic islets following the procedure outlined in Chapter 3.2.4. The RTqPCR conditions are detailed in Chapter 3.2.5, and the primer sequences used are listed in Supplemental Figure 1. We evaluated the expression of UPR genes: splicing of X-box Binding Protein 1 (Xbp1), and C/EBP homologous protein (CHOP). During UPR, IRE1α mediates the splicing of Xbp1 mRNA, leading to the upregulation of UPR genes.[266] CHOP, downstream of PERK, serves a dual role in the UPR, acting protectively during ER stress; however, prolonged activation of the UPR may induce apoptosis by increasing CHOP expression.[267]

4.2.3 β cell morphometrics

The pancreas was processed as described in Chapter 3.2.6, and the immunofluorescence protocols are outlined in Chapter 3.2.7. Total pancreas images were taken with Leica DM E (Leica) and images were taken using Infinity Analyze Version 6.5 (Lumenera). Stitching of total pancreas images was performed using the Automate feature in Photoshop (Adobe), and total pancreas area was quantified using ImageJ software (NIH). For detection of β cell apoptosis, proliferation, PDX1-positive β cells, sections were imaged with an Axio Observer 7 microscope (Zeiss) and images were acquired using Zen 2.6 software (Zeiss).

Caspase 3 is activated upon cleavage, leading to apoptosis by catalyzing the cleavage of important cellular proteins, which results in DNA fragmentation. Caspase 3 is commonly used as a marker for apoptosis.[268] To quantify β cell apoptosis, cryosections were co-stained for cleaved caspase 3 and insulin. Apoptotic β cells were identified by cleaved caspase 3-positivity in the nuclei with cytoplasmic insulin, with at least 5000 β cells counted per mouse. Hoechst was used to visualise nuclei in during immunofluorescence.

The nuclear protein Kiel 67 (KI67) labels cells in G1, S, G2, and M phases and is expressed in all mammalian species. This is in contrast to 5-bromo-2-deoxyuridine (BrdU), which specifically labels cells during the S phase.[269] Proliferating β cells were defined by KI67-positivity in the nuclei with cytoplasmic insulin, with at least 3000 β cells counted per mouse.

GLP-1 has been shown to regulate transcription factor PDX1, resulting in the translocation of PDX1 into the nucleus in a cAMP/PKA-dependent manner.[127] PDX1-positive β cells were defined by PDX1-positivity in the nuclei with cytoplasmic insulin with at least 1000 β cells were counted per mouse.

The average number of β cells was determined as the number of insulin-positive cells per pancreas area (mm^2), while the average β cell size was calculated by dividing the insulin-positive area (μm^2) by the total number of insulin-positive cells. At the islet-level, the average number of islets, defined as a clusters of insulin-positive cells, was calculated as the total number of islets relative to total pancreas area (mm^2). The average islet size was determined by the total insulin-positive area (μm^2) relative to the total number of islets counted. β cell mass was calculated by

multiplying the β cell fraction insulin-positive area (μm^2) relative to the total pancreas area (μm^2) by the pancreas weight after whole pancreas dissection. Islet size distribution was categorized as follows: very small islets (less than $30\mu m^2$), small islets ($30\text{-}50\mu m^2$), medium islets ($50\text{-}150\mu m^2$), and large islets (greater than $150\mu m^2$), with measurements represented as a percentage of at least 200 islets counted per mouse. At least 5 sections, 200 µm apart, were counted per mouse. This ensured that the same islet was not measured twice, considering that the average diameter of islets in all mammals is usually between 100 and 200µm.[270]

4.2.4 Intraperitoneal glucose tolerance test

To evaluate glucose homeostasis in the absence of nutrient-induced incretin hormone release, we conducted an IPGTT in both WT and cKO mice. Mice were subjected to an overnight fast (14-16 hours) and then received an intraperitoneal injection of 2.0 g glucose/kg of body weight (20% D-glucose in normal saline, Sigma).

Upon administration of 2.0g glucose/kg of body weight, blood glucose levels reached 33.3mM in both WT and cKO mice on HFD, which is the maximum reading possible with the blood glucometer (One Touch Verio Reflect) (data not shown). In order to distinguish blood glucose levels between WT and cKO mice, we opted to reduce the dosage to 1.0g glucose/kg of body weight. Blood glucose levels were monitored from the saphenous vein at 0, 10, 15, 30, 45, 60, and 120 minutes post-administration using the blood glucometer (One Touch Verio Reflect). Additionally, 30 µL of blood was collected at 0, 10, and 30 minutes to measure *in vivo* insulin secretion. The AUC was calculated as the integrated AUC during the 120-minute IPGTT, with blood glucose at 0 minutes serving as a baseline.

4.2.5 Statistical analysis

The data are presented as means ± standard error of the mean (SEM). An unpaired Student's t-test was employed to compare the means of two groups, while one-way analysis of variance (ANOVA) was utilized to compare the means of three or more groups. Furthermore, two-way ANOVA was used to compare means of three or more groups with two independent variables. Tukey's post hoc analysis was conducted to determine *p-values*, with statistical significance set at a $p\text{-value} < 0.05$. Tukey's multiple comparison test was employed to compare each experimental group with every control group. Outliers were identified and removed using the ROUT method with a Q value of 10%. All statistical analysis was done using GraphPad Prism Version 9.3.1.

4.3 Results

4.3.1 Insulin Content

To investigate whether a decrease in insulin content was responsible for the observed reduction in insulin secretion observed during OGTT, we measured insulin content from islets isolated for *in vitro* GSIS. A reduction in insulin content can lead to reduced insulin secretion, as β cells have less insulin available to be released in response to stimuli. We found that the islets of cKO HFD mice had a lower insulin content in comparison to WT HFD mice [WT: 4387±848 ng insulin/µg DNA vs. cKO: 1847±196 ng insulin/µg DNA ($p=0.03$)] (Figure 4.1).

We then assessed whether the mRNA expression of *Ins1* and *Ins2* differed between the WT and cKO mice after HFD. We found that the expression levels of both insulin genes were lower in

cKO HFD mice [*Ins1*: 45% reduction (*p=0.*02) and *Ins2*: 40% reduction (*p=0.001*)] (Figure 4.2). Exposure of WT mice to HFD led to an increase in the expression levels of *Ins1* and *Ins2* mRNA when compared to WT mice fed a CD, but this increase was not statistically significant (Supplemental Figure 9).

To determine if transcription factors involved in insulin gene transcription were differentially regulated in WT vs. cKO mice, we measured the expression levels of *MafA*, *NeuroD1*, *Nkx6.1*, *Pax6*, and *Pdx1*. Expression levels of *Mafa, Neurod1, Nkx6.1*, Pax6 were all downregulated in cKO mice in comparison to WT mice after 12 weeks of HFD but only the expression levels of *Nkx6.1* (*p=0.003*) and *Pax6* (*p=0.0001*) reached statistical significance (Figure 4.3).

Next, we aimed to measure the mRNA expression of genes involved in the UPR, as UPR can lead to ER stress and consequently decrease insulin biosynthesis. We found that the mRNA expressions of *Bax:Bcl-2*, *Bip¸Chop*, *Ire1α*, *Lrrc55*, and *Xbp1*-S:*Xbp1*-U were all downregulated in cKO HFD mice compared to WT HFD mice (Figure 4.4). Statistically significant differences were only observed in the mRNA expressions of *Bip* (*p=0.01*) and *Lrrc55* (*p<0.000001*). No statistically significant differences in the expressions of *Bax:Bcl-2, Bip¸Chop, Ire1α, Lrrc55*, and *Xbp1*-S:*Xbp1*-U were observed between WT HFD and WT CD mice after 12 weeks of diet (Supplemental Figure 10).

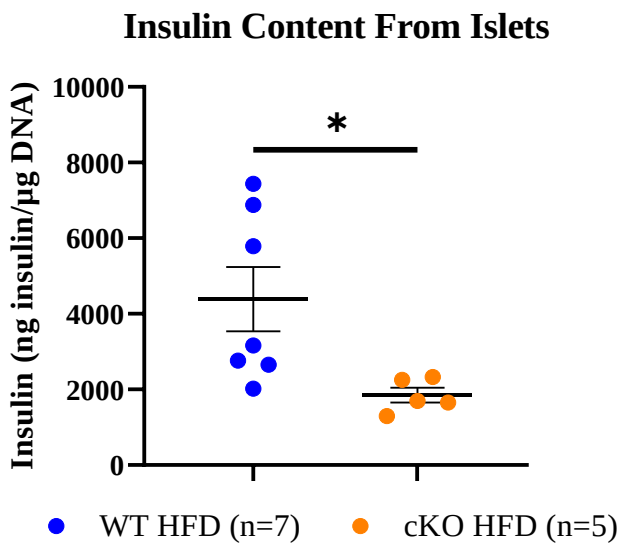

Figure 4.1 Insulin content from pancreatic islets after *in vitro* GSIS

The insulin content of isolated islets was assessed after one day of culture, followed by *in vitro* GSIS. Here, insulin content was determined as the sum of insulin secreted after *in vitro* incubation in 2mM glucose, 16mM glucose, and KCl. Subsequently, the islets were lysed with acid-ethanol to measure remaining insulin. Insulin content was normalized to µg of DNA and expressed as mean ± SEM; n = 5-7 mice/group. Statistical analysis was performed using an unpaired Student's t-test: ***** $p < 0.05$.

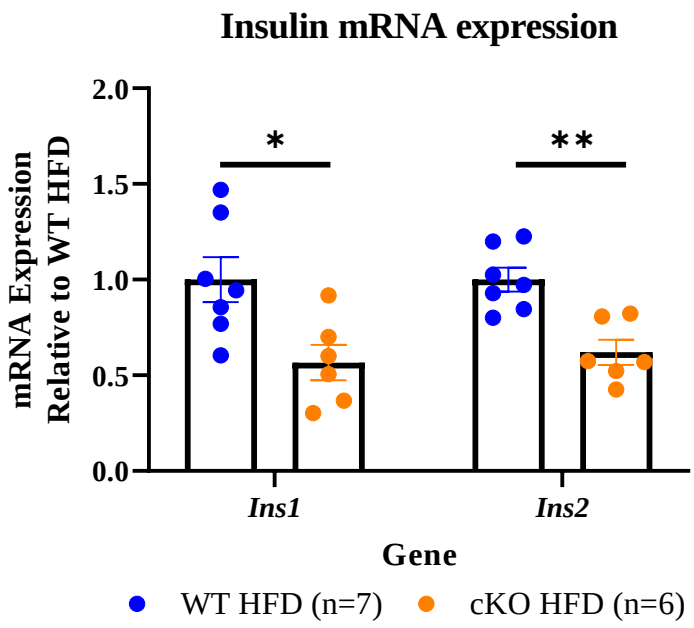

Figure 4.2 Islet *Ins1* and *Ins2* mRNA expression in WT and cKO mice after 12 weeks of HFD

mRNA expression of *Ins1* and *Ins2* was measured in WT and cKO mice after 12 weeks of HFD by RTqPCR. The expressions of *Ins1* and *Ins2* were normalized to the expression of *Ppa1* (a housekeeping gene) and expressed relative to WT HFD mice. Each data point represents a mouse (n=6-7 mice/group), averaged from 3 independent experiments. Results are presented as means ± SEM. Statistical analysis was done using an unpaired Student's t-test where: "*" $p<0.05$, "**" $p<0.005$.

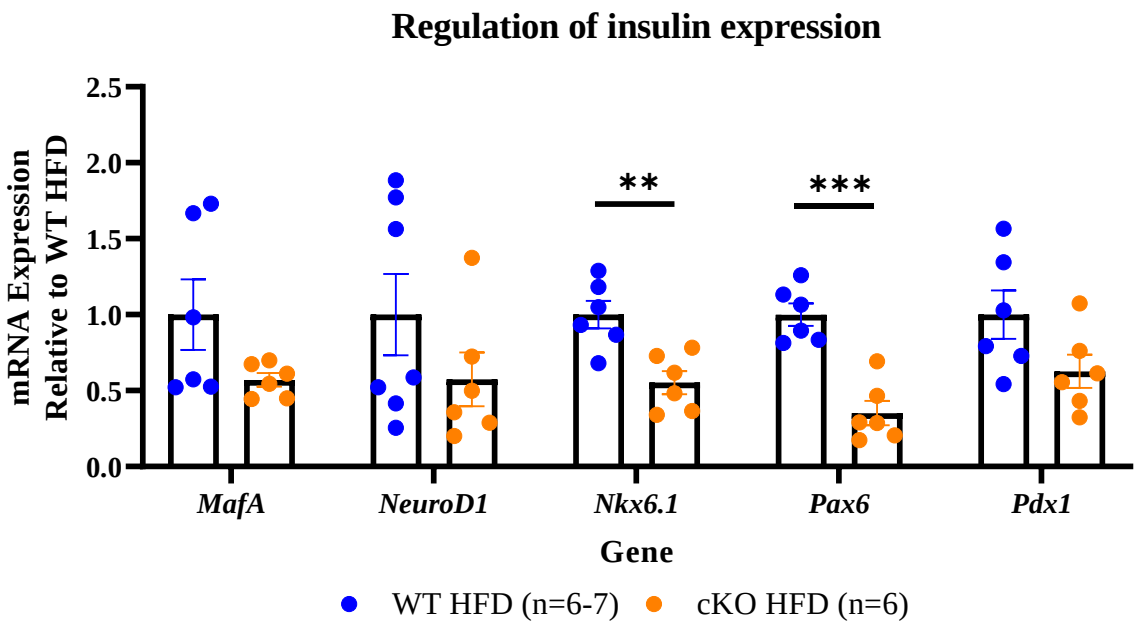

Figure 4.3 Islet mRNA expression of transcription factors that regulate insulin gene expression in WT vs. cKO mice after 12 weeks of HFD

mRNA expression of *MafA*, *NeuroD1*, *Nkx6.1*, *Pax6*, and *Pdx1* was measured in WT and cKO mice after 12 weeks of HFD by RTqPCR. mRNA expression was normalized to *Ppa1* (housekeeping gene) and expressed relative to WT HFD mice. Each data point represents a mouse averaged from 3 independent experiments (n=6-7 mice/group). Results are presented as means $\pm$ SEM. Statistical analysis was done using an unpaired Student's t-test: "**" indicates $p<0.005$ and "***" indicates $p<0.0005$.

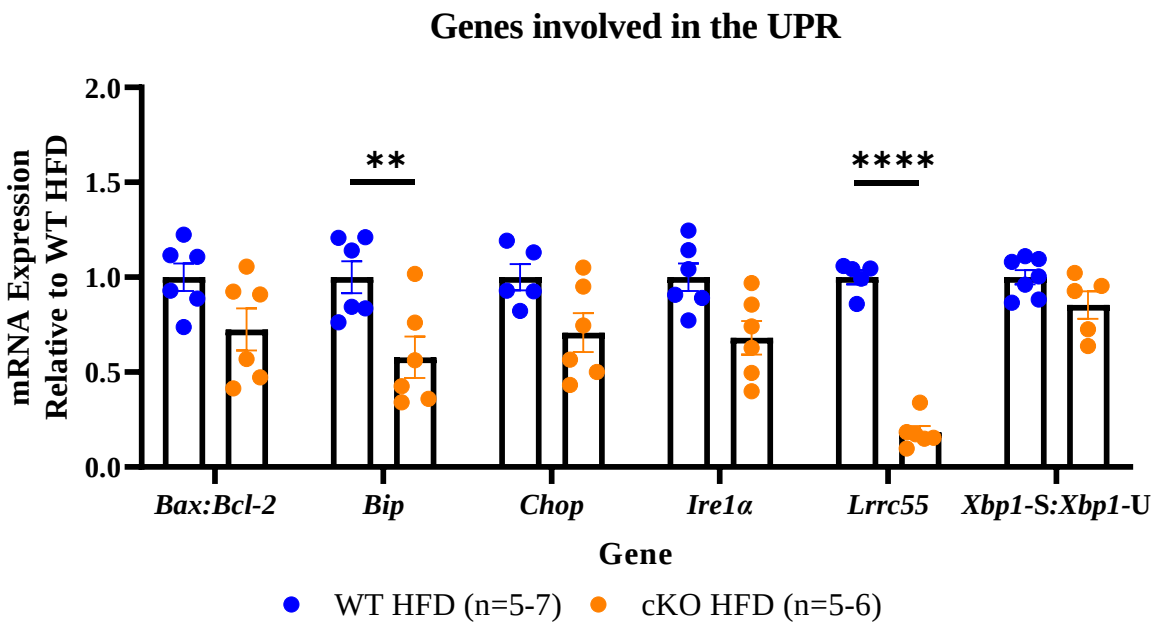

Figure 4.4: Islet mRNA expression of genes involved in UPR in WT HFD vs. cKO mice after 12 weeks HFD

mRNA expressions of *Bax*:*Bcl-2*, *Bip*, *Chop*, *Ire1α*, *Lrrc55*, and *Xbp1*-S:*Xbp1*-U were measured in the islets of WT and cKO mice after 12 weeks of HFD by RTqPCR. mRNA expression was normalized to *Ppa1* (housekeeping gene) and expressed relative to WT HFD mice. Each data point represents a mouse (n=5-7 mice/group). Results are presented as means ± SEM of 3 independent experiments. Statistical analysis was done using an unpaired Student's t-test between groups where "*" = $p<0.05$ and "****" = $p<0.000005$.

4.3.2 β cell morphometrics

To date, most of the data on the role of PRLR in β cells have focused on its role during pregnancy. [40–45] During pregnancy, there is an increase in β cell mass through β cell proliferation and a return back to pre-pregnancy state through β cell apoptosis.[25] This increase in β cell mass is in part regulated by PRLR.[42] Additionally, studies shown that lactogens protect β cells against glucolipotoxicity in both rodents and humans.[271] Therefore, to determine the impact of PRLR deletion on β cell proliferation and apoptosis, we used KI67 as a marker for proliferation (Figure 4.5) and cleaved caspase 3 as a marker for apoptosis (Figure 4.6).

We discovered that cKO HFD mice exhibited decreased β cell proliferation after 12 weeks of HFD, where [WT: 0.55±0.06% KI67-positive vs. cKO: 0.4-0±0.01% KI67-positive β cells (*p=0.03*)] (Figure 4.7A). In WT mice, no statistically significant differences in β cell proliferation were observed at time points: week 1 HFD, week 12 HFD, and week 12 of CD (Supplemental Figure 11). Additionally, we observed a trend towards more apoptotic β cell in cKO HFD mice after 12 weeks of HFD [WT: 0.12±0.03% cleaved caspase 3-positive vs. cKO: 0.25±0.05% cleaved caspase 3-positive β cells (*p=0.07*)] (Figure 4.7B).

Other morphometric data at the β cell level showed no statistically significant difference in the average number of β cells and average β cell size between WT and cKO mice after 12 weeks of HFD (Figure 4.8). At the islet level, we observed no statistically significant difference in the average number of islets and average islet size between WT and cKO after 12 weeks of HFD (Figure 4.9). No statistically significant difference was observed in the percentage of very small, small, medium, and large islets between WT and cKO mice after 12 weeks of HFD (Figure

4.10). In contrast, WT mice fed CD showed a statistically significant difference in the percentage of very small and large islets compared to WT HFD mice [WT CD very small: 22.5±4.7% vs. WT HFD very small: 42.2±5.6% (*p=0.04*) and WT CD large: 17.8±2.8% vs. WT HFD large: 8.2±0.8% (*p=0.008*)] (Figure 4.11). We did observe a trend toward reduced β cell mass in cKO mice, but statistical significance was not reached [WT: 3.13±0.14 mg vs. cKO: 2.52±0.30 mg (*p=0.07*)] (Figure 4.12). No statistically significant difference was observed in β cell mass in WT mice after 12 weeks of HFD or CD (Supplemental Figure 12).

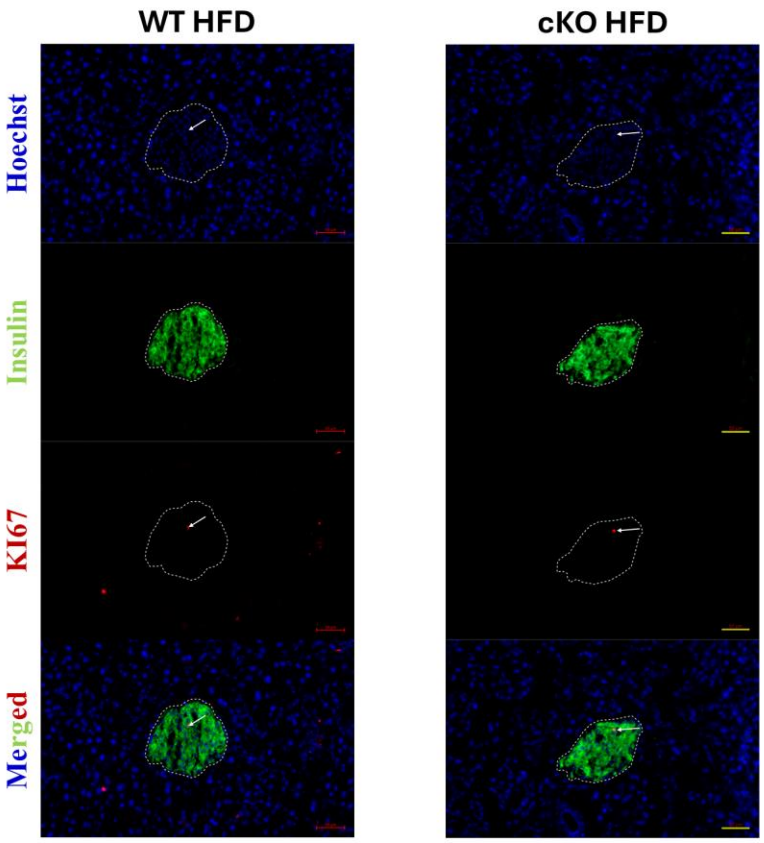

Figure 4.5: Representative KI67 immunofluorescence in WT and cKO mice after 12 weeks of HFD

A representative image of KI67 immunofluorescence is presented. Pancreas from WT (left) and cKO (right) mice were immunostained after 12 weeks of HFD for Hoechst (blue), KI67 (red), and insulin (green), where proliferating β cells were identified as nuclei co-localizing of Hoechst and KI67, along with cytoplasmic insulin positivity. Dotted white lines outline of an islet, while the white arrows indicate proliferating β cells. Scale bars represent 50μm.

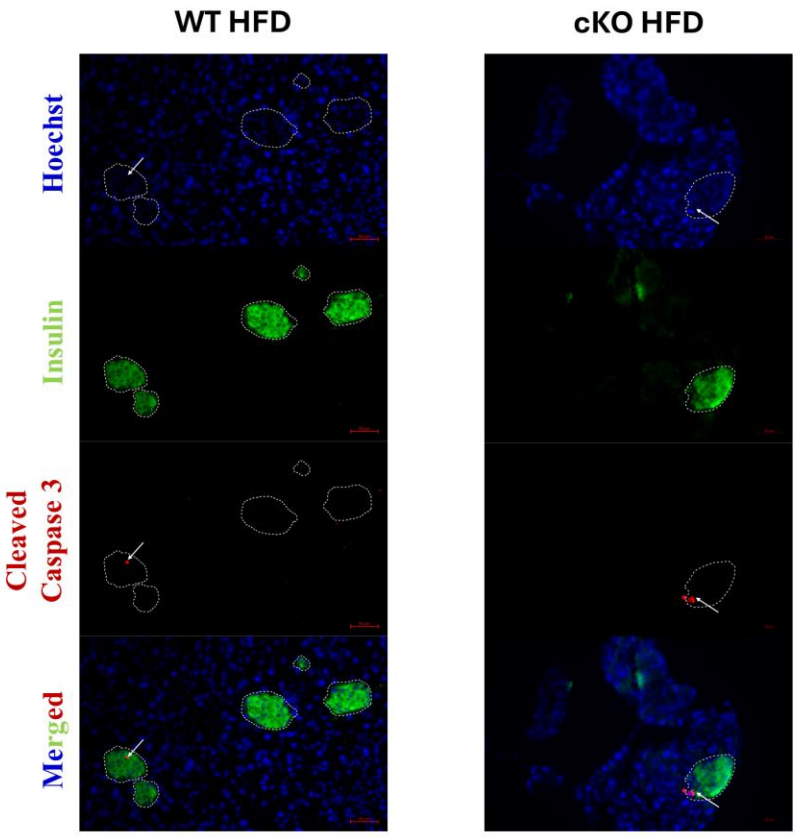

Figure 4.6: Representative Cleaved caspase 3 immunofluorescence in WT and cKO mice after 12 weeks of HFD

A representative image of Cleaved caspase 3 immunofluorescence is presented. Pancreas from WT (left) and cKO (right) mice were immunostained for Hoechst (blue), Cleaved caspase 3 (red), and insulin (green), where apoptotic β cells were identified as nuclei co-localizing with Hoechst and Cleaved caspase 3, along with cytosolic insulin positivity. Dotted white lines outline of an islet, white arrows indicate apoptotic β cells. Scale bars represent 50μm.

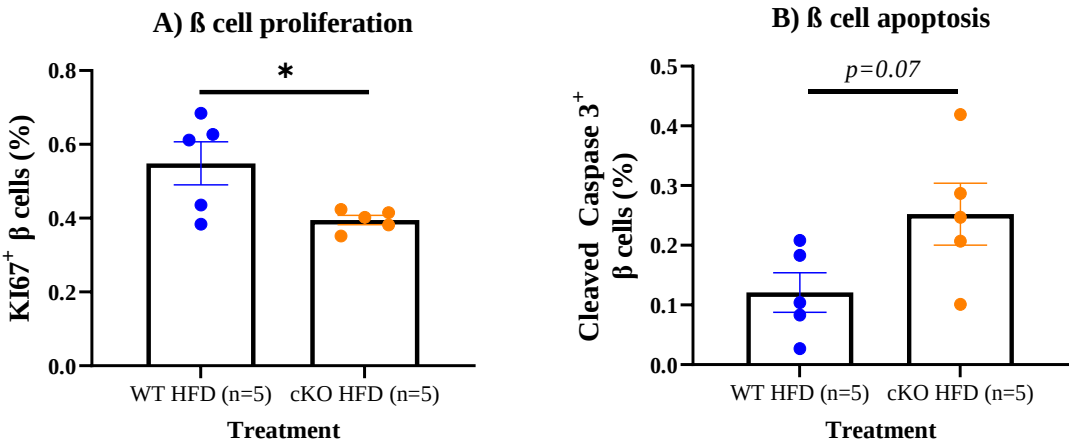

Figure 4.7 β cell A) Proliferation and B) Apoptosis after 12 weeks of HFD

After 12 weeks of HFD, immunofluorescence of pancreas sections to determine A) β cell proliferation and B) β cell apoptosis. β cell proliferation was determined by KI67-positive insulin-positive cells per total insulin$^+$ cells x 100%, with at least 6000 β cells per mouse counted across 3 sections. β cell apoptosis was determined by cleaved caspase 3-positive insulin-positive cells per total insulin-positive cells x 100%, with at least 3000 β cells per mouse counted across 3 sections. Each data point represents a mouse (n = 5 mice/group). Statistical analysis was conducted using an unpaired Student's t-test between groups where: **"*"** $p < 0.05$ WT HFD versus cKO HFD. Raneet Khalon, Sristi Dey, and Valerie Ho assisted with immunofluorescence, imaging, and quantification.

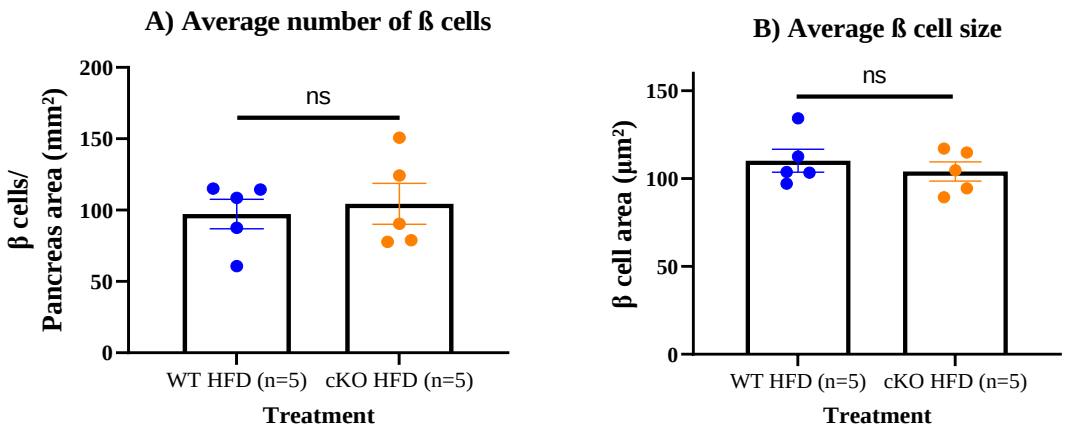

Figure 4.8: A) Average number of β cells and B) Average β cell size after 12 weeks of HFD

A) The average number of β cells was determined by the ratio of insulin-positive cells relative to the total pancreas area (mm^2). B) The average β cell size was determined by number of insulin-positive area (μm^2) relative to insulin-positive cells. At least 4 sections were quantified per mouse, with sections being at least 200 µm apart. Each data point represents a mouse (n = 5 mice/group). Statistical analysis was done using an unpaired Student's t-test between groups compared where: "ns" no statistical significance. Raneet Khalon, Sristi Dey, and Valerie Ho assisted with immunofluorescence, imaging, and quantification.

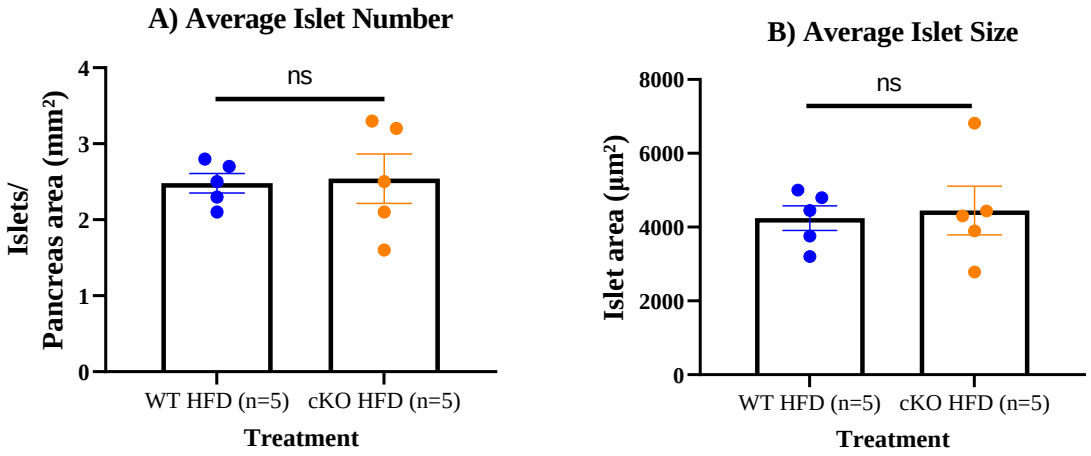

Figure 4.9: A) Average number of islets and B) Average islet size after 12 weeks of HFD

A) The average islet number was determined by the ratio of islets relative to the total pancreas area. B) The average islet size was determined by the total insulin-positive area relative to the total number of islets. At least 4 sections were quantified per mouse with sections being at least 200 µm apart. Each data point represents a mouse (n = 5 mice/group). Statistical analysis was done using an unpaired Student's t-test between groups compared where: "ns" no statistical significance. Raneet Khalon, Sristi Dey, and Valerie Ho assisted with immunofluorescence, imaging, and quantification.

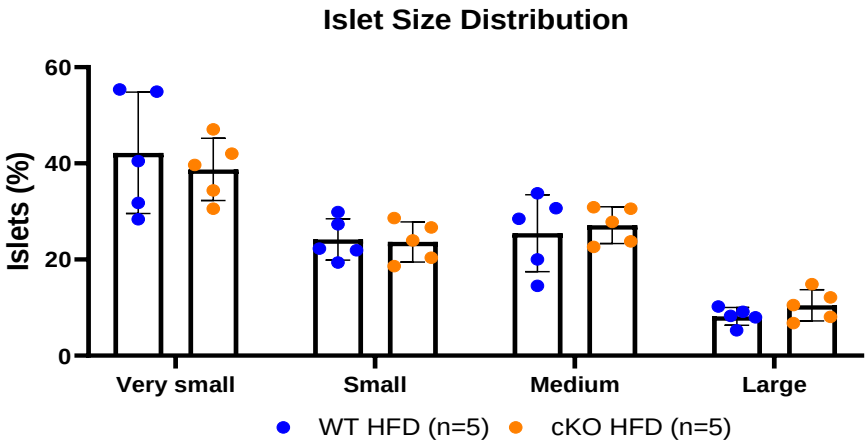

Figure 4.10: Islet size after 12 weeks of HFD in WT vs. cKO mice

Islet size distribution between WT and cKO mice after 12 weeks of HFD. Islet size was measured by the area of islets, categorizes as follows: very small islets (less than 30μm^2), small islets (30-50μm^2), medium islets (50-150μm^2), and large islets (greater than 150μm^2). Islet size is represented as a percentage of the total islets counted. Each data point represents a mouse (n=5/group) and at least 200 islets were counted per mouse. Statistical analysis was done using an unpaired Student's t-test. Raneet Khalon, Sristi Dey, and Valerie Ho assisted with immunofluorescence, imaging, and quantification.

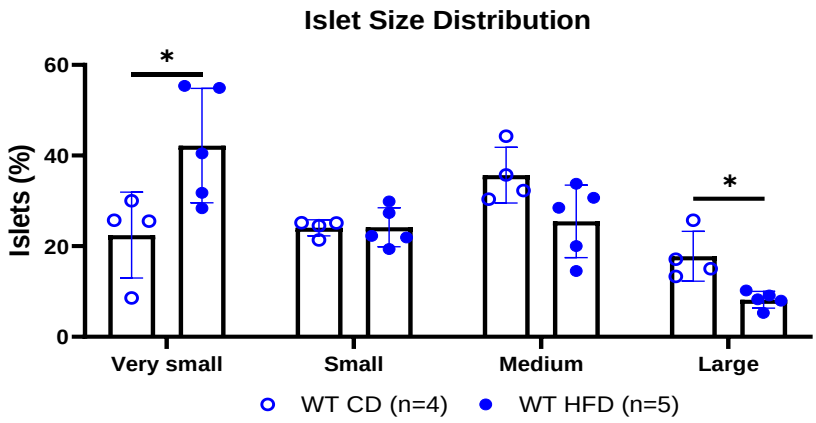

Figure 4.11: Islet size distribution after 12 weeks of HFD or CD in WT mice

Islet size distribution in WT mice after 12 weeks of HFD or CD. Islet size was measured by the area of islets where: very small islets (less than 30µm^2), small islets (30-50µm^2), medium islets (50-150µm^2), and large islets (greater than 150µm^2). Islet size is represented as a percentage of the total islets counted. Each data point represents a mouse (n=4-5/group) and at least 200 islets were counted per mouse. Statistical analysis was done using an unpaired Student's t-test where: "*" $p<0.05$. Raneet Khalon, Sristi Dey, and Valerie Ho assisted with immunofluorescence, imaging, and quantification.

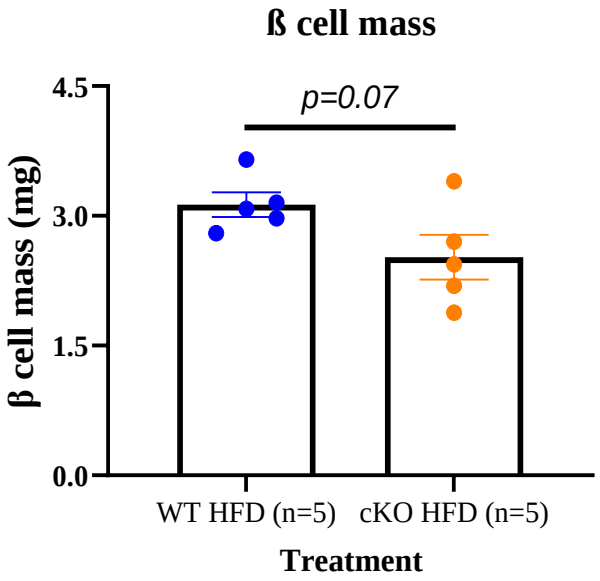

Figure 4.12: β cell mass after 12 weeks of HFD

β cell mass after 12 weeks of HFD in WT and cKO mice was measured. β cell mass was determined by multiplying the pancreas weight by the insulin-positive area and dividing it by the total pancreas area. At least three sections were examined, with 6000 β cells per mouse across 4 sections 200 µm apart. Each data point represents a mouse (n = 5 mice/group). Statistical analysis was done using an unpaired Student's t-test. Raneet Khalon, Sristi Dey, and Valerie Ho assisted with immunofluorescence, imaging, and quantification.

4.3.3 β cell function

While we observed a decrease in insulin content, only approximately 20 % of the total insulin content was secreted in response to a two-hour stimulation *in vitro* (1-hour 16mM Glucose followed by 1-hour 40mM KCl) in both WT and cKO mice (Figure 3.15). This represents a small fraction of insulin content. Consequently, we assessed the expression of key transporters and enzymes involved in GSIS: *Gck*, *Glut2*, and *Pc*. Additionally, we measured the expression of *Ffar1*, which enhances insulin secretion in the presence of FFAs. Furthermore, we evaluated the expressions of *Gipr* and *Glp-1r*, as the incretin effect represents the most potent *in vivo* non-glucose stimulus for insulin secretion.

We found a 65% reduction in the mRNA expression of *Glut2* ($p=0.02$), *Pc* ($p<0.000008$), as well as a 40% reduction in *Ffar1* ($p=0.009$) in cKO HFD mice compared to WT HFD mice (Figure 4.13). Both *Gipr* ($p=0.02$) and *Glp-1r* ($p=0.03$) mRNA expressions were reduced by 50% in cKO HFD mice in comparison to the WT HFD mice (Figure 4.13). In WT mice, HFD per se had no effect on the expression of genes involved in β cell function measured (Figure 4.14). However, the mRNA expressions of *Ffar1* and *Gipr* were slightly increased in WT HFD mice compared to WT CD mice (Figure 4.14).

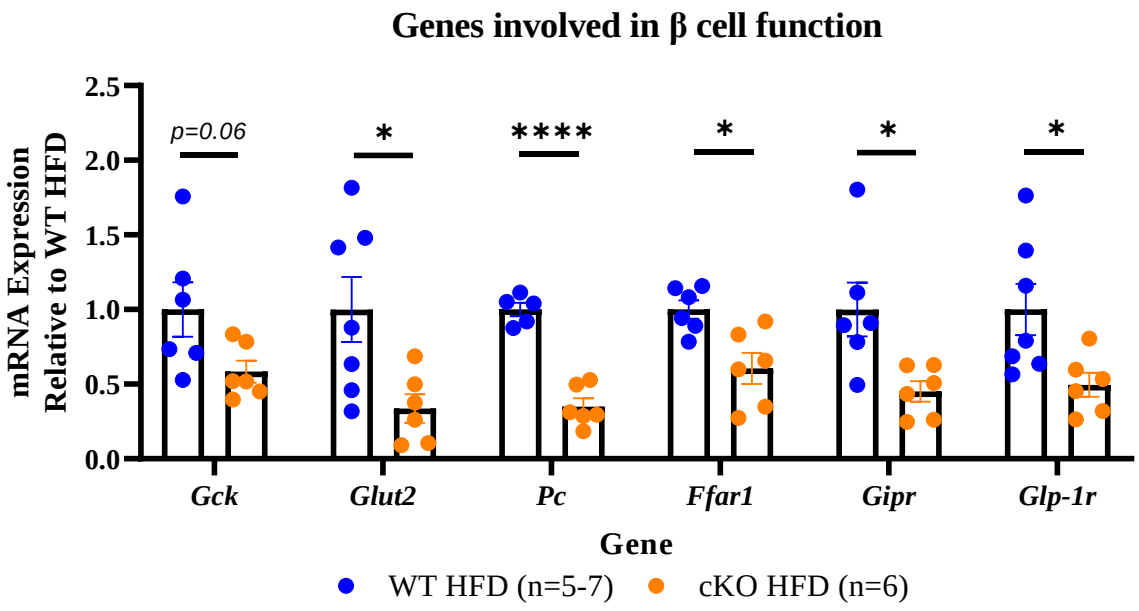

Figure 4.13 Islet mRNA expression of *Gck, Glut2, Pc, Ffar1, Gipr*, and *Glp-1r* in WT and cKO mice fed 12 weeks of HFD

Islet mRNA expression of *Gck*, *Glut2*, *Pc*, *Ffar1*, *Gipr*, and *Glp1-r* were measured by RTqPCR in WT and cKO HFD mice. mRNA expression was normalized to the expression of *Ppa1* (housekeeping gene) and expressed relative to WT HFD mice. Each data point represents a mouse averaged from 3 independent experiments (n=5-7 mice/group). Results are presented as means ± SEM. Statistical analysis was done using an unpaired Student's t-test where: "*" $p<0.05$ and "****" $p<0.00005$.

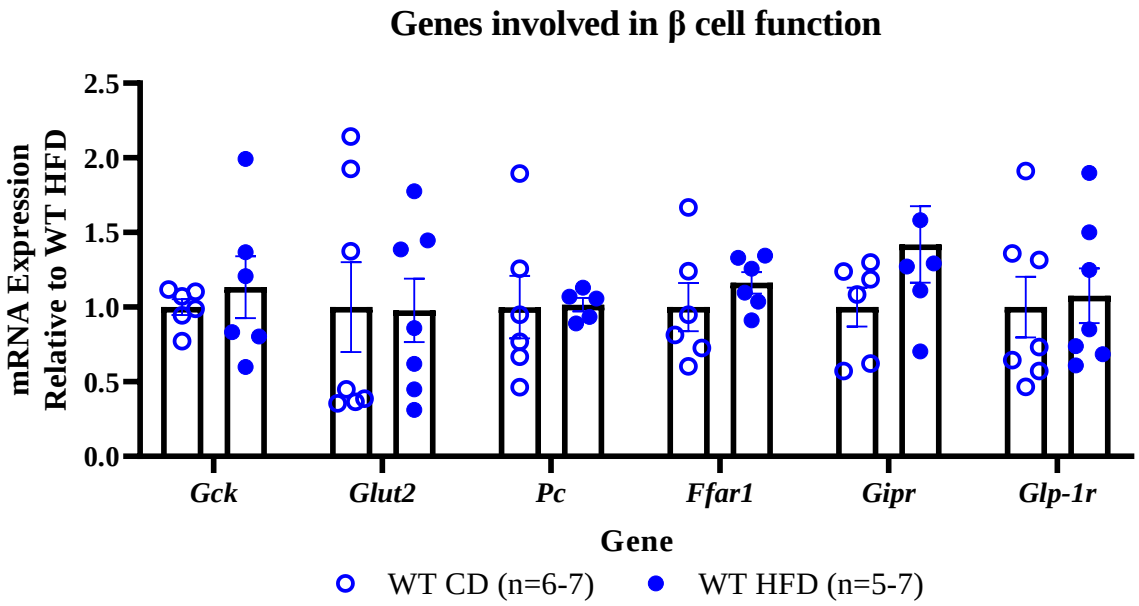

Figure 4.14 Islet mRNA expression of *Gck*, *Glut2*, *Pc*, *Ffar1*, *Gipr*, and *Glp-1r* in WT CD vs. HFD mice after 12 weeks of diet

Islet mRNA expression of *Gck*, *Glut2*, *Pc*, *Ffar1*, *Gipr*, and *Glp1-r* were measured by RTqPCR in WT mice after 12 weeks of CD and HFD. mRNA expression was normalized to the expression of *Ppa1* (housekeeping gene) and expressed relative to WT CD mice. Each data point represents a mouse averaged from 3 independent experiments (n=6-7 mice/group). Results are presented as means ± SEM Statistical analysis was done using an unpaired Student's t-test between groups where: "*" $p<0.05$.

4.3.4 Incretin Effect

To investigate whether cKO HFD mice exhibit a reduction in the incretin effect, we assessed glucose homeostasis with an IPGTT. Initially, we compared an OGTT vs. an IPGTT within each genotype. We observed that WT mice displayed higher blood glucose levels at 30, 45, 60, and 120 minutes during an IPGTT compared to an OGTT (Figure 4.15A). Conversely, cKO mice exhibited increased blood glucose levels at 60 and 120 minutes during an IPGTT compared to an OGTT (Figure 4.15B). Notably, both WT and cKO demonstrated higher glucose excursion during an IPGTT when compared to an OGTT, as indicated by the integrated AUC during the glucose tolerance tests (Figure 4.15C). Upon comparing glucose tolerance measured by IPGTT between WT and cKO mice after 12 weeks of HFD, we observed no statistically significant difference in blood glucose levels (Figure 4.16A) nor in AUC (Figure 4.16).

Regarding *in vivo* insulin secretion between WT and cKO mice, no statistically significant differences were observed at minutes 0, 10, and 30 in serum insulin during an IPGTT after 12 weeks of HFD (Figure 4.17). However, WT mice displayed a statistically significant reduction in serum insulin during IPGTT compared to OGTT at 10 minutes, whereas cKO mice displayed a statistically significant reduction in serum insulin at 10 and 30 minutes during IPGTT compared to OGTT (Figure 4.17).

To ascertain whether EPAC, downstream of GIPR and GLP-1R, contributes to the decrease in the incretin effect, we measured mRNA expression of both isoforms of this gene (*Epac1* and *Epac2*). We found that cKO HFD mice had a 60% reduction in *Epac1* expression ($p=0.02$) and a 40% reduction in *Epac2* expression compared to WT HFD mice (Figure 4.13). To further

investigate the downstream effects of GIPR and GLP-1R activation, we measured nuclear PDX-1-positive β cells using immunofluorescence (Figure 4.19). We found that cKO HFD mice had a reduction in nuclear PDX1-positive β cells compared to WT HFD mice [WT: 54.6±1.6% vs. cKO: 48.8±1.2 (*p=0.02*)] (Figure 4.20).

Finally, we noted a decrease in mRNA expression of both *Gipr* and *Glp-1r* in cKO HFD mice compared to WT HFD mice. We employed a candidate gene approach to identify transcription factors that have been shown to regulate the expression of *Gipr, Glp-1r*, or both incretin hormone receptors. The transcription factor PPARG has been implicated in regulating *Gipr* expression, E2F1 in regulating *Glp-1r* expression, while TCF7L2 regulates both *Gipr* and *Glp-1r*.[136,139,141] We observed that mRNA expression in cKO HFD mice had a 65% reduction in *E2f1* (*p=0.0009*), a 45% reduction in *Pparg (p=0.02*), and a 55% reduction in *Tcf7l2* (*p=0.002*) compared to WT HFD mice (Figure 4.21). In contrast, *E2f1* expression was increased 200% in WT HFD mice compared to WT CD mice after 12 weeks of diet while no statistically significant differences in *Pparg* and *Tcf7l2* was observed (Supplemental Figure 13).

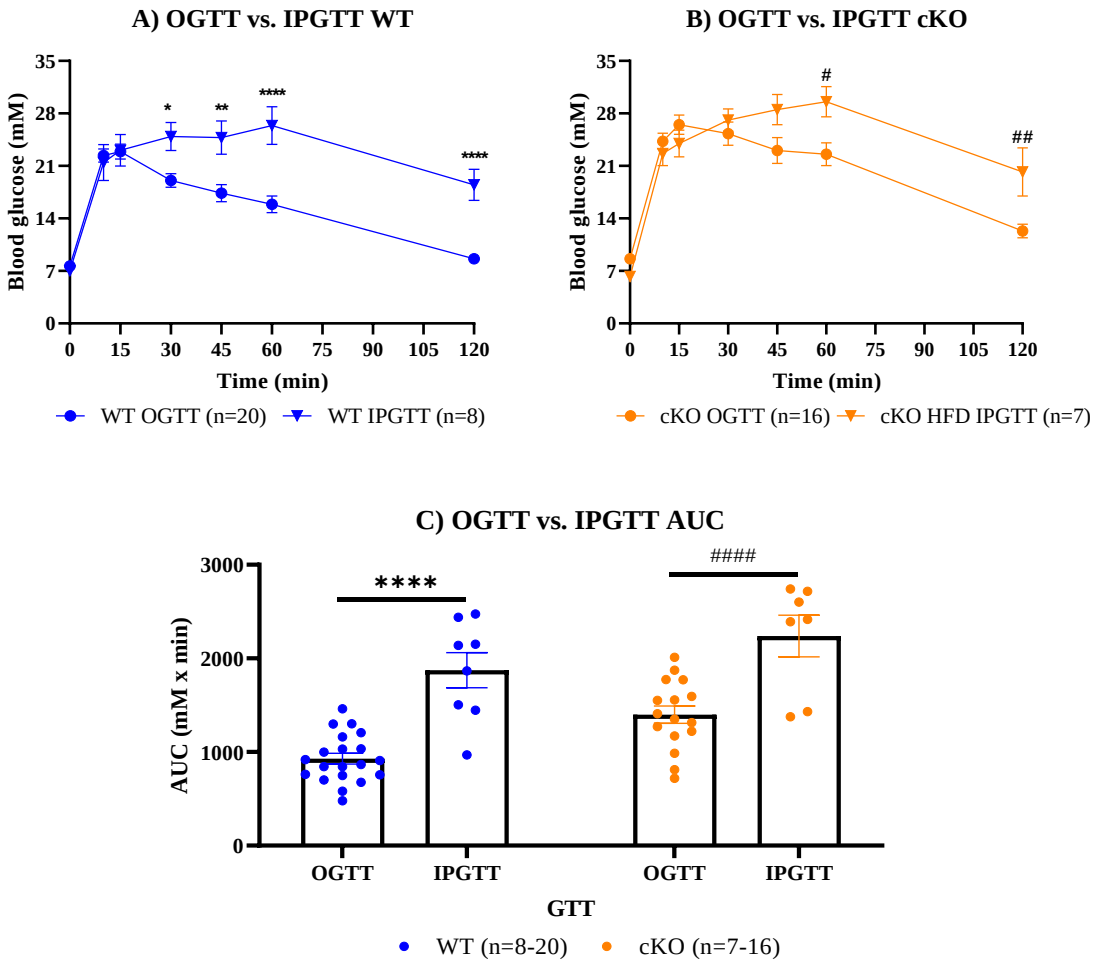

Figure 4.15 OGTT vs. IPGTT in A) WT and B) cKO mice after 12 Weeks of HFD, and C) AUC

Blood glucose levels during an OGTT and an IPGTT were measured in A) WT and B) cKO mice after 12 weeks of HFD. Following an overnight fast, a glucose solution was administered by either oral gavage (2g glucose/kg body weight) or intraperitoneal injection (1g glucose/kg body weight), and blood glucose levels were measured at 0, 10, 15, 30, 45, 60, 120 minutes. Results are means ± SEM (n=7-20 mice/group and treatment). Two-way ANOVA was conducted, and significance determined using Tukey's post hoc test, WT OGTT vs. IPGTT where: "*" $p<0.05$, "**" $p<0.005$, "****" $p<0.00005$ and cKO OGTT vs. IPGTT where: "#" $p<0.05$, "##" $p<0.005$, "####" $p<0.00005$. Carol Huang assisted with intraperitoneal injection and data collection.

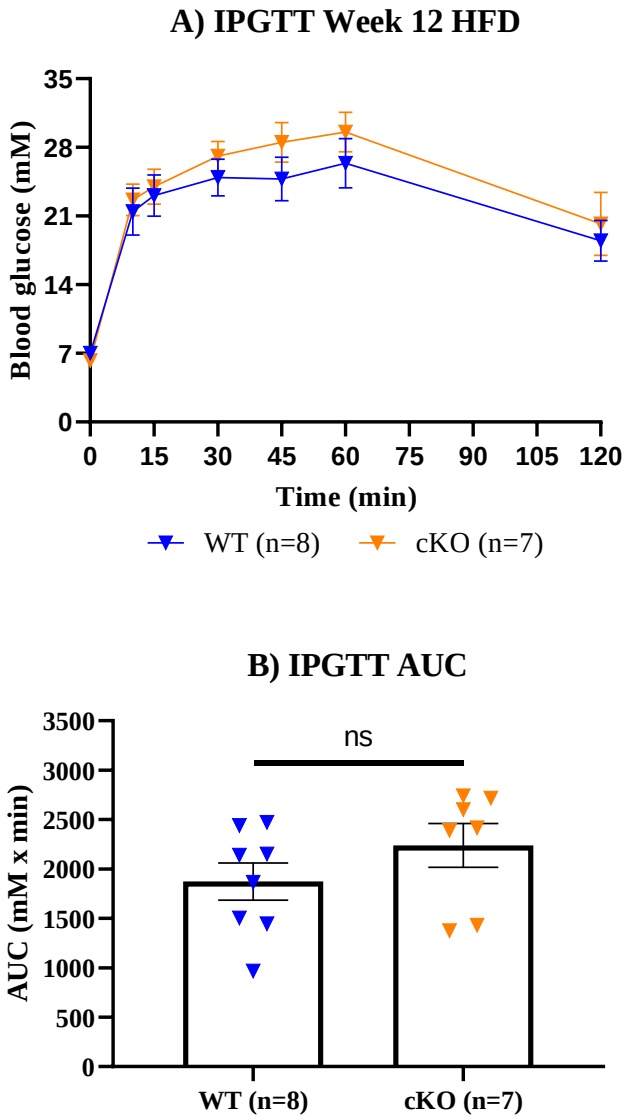

Figure 4.16 A) IPGTT in WT and cKO mice after 12 Weeks of HFD and B) AUC

Blood glucose levels during IPGTT after 12 Weeks of HFD and B) AUC were assessed. Following an overnight fast, a glucose solution (1g glucose/kg body weight) was administered intraperitoneally, and blood glucose was measured at 0, 10, 15, 30, 45, 60, 120 minutes. Results are means ± SEM (n=7-8). Two-way ANOVA was conducted, and significance determined using Tukey's post hoc test where: "ns" not significant. Carol Huang assisted with intraperitoneal injection and data collection.

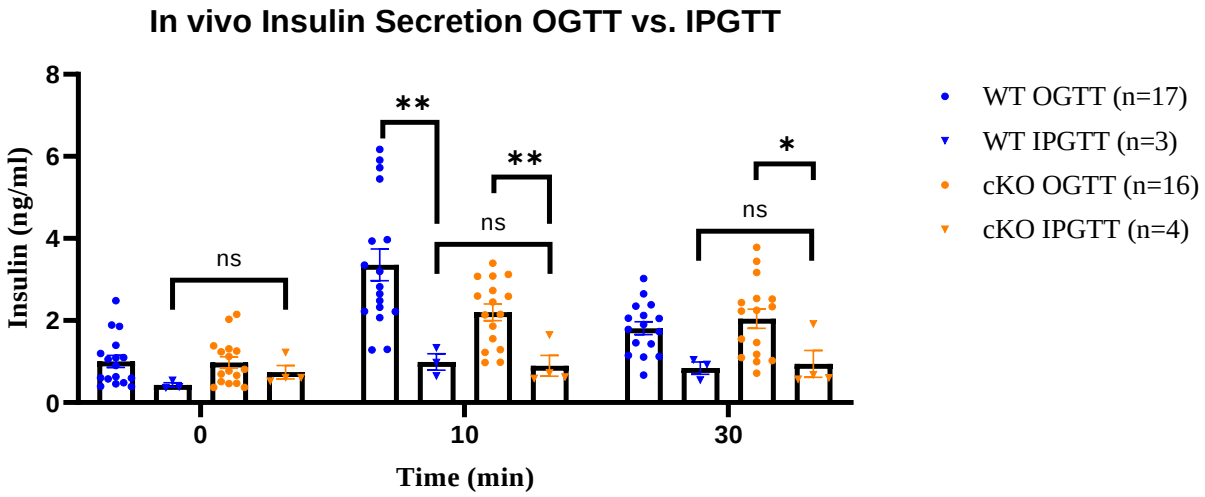

Figure 4.17: *In vivo* insulin secretion during OGTT and IPGTT after 12 weeks of HFD in WT and cKO mice

Plasma insulin concentrations during OGTT (2g glucose/kg body weight) and IPGTT (1g glucose/kg body weight) were examined following an overnight fast in WT and cKO mice fed HFD for 12 weeks. Blood samples were collected at 0, 10, and 30 minutes and insulin was measured by an ELISA. Results are expressed as means ± SEM (n=3-17 mice/group). Two-way ANOVA was conducted and statistical significance was determined using Tukey's post hoc test where: "*" $p<0.05$, "**" $p<0.005$ OGTT vs. IPGTT, and "ns" not significant. Carol Huang assisted with data collection.

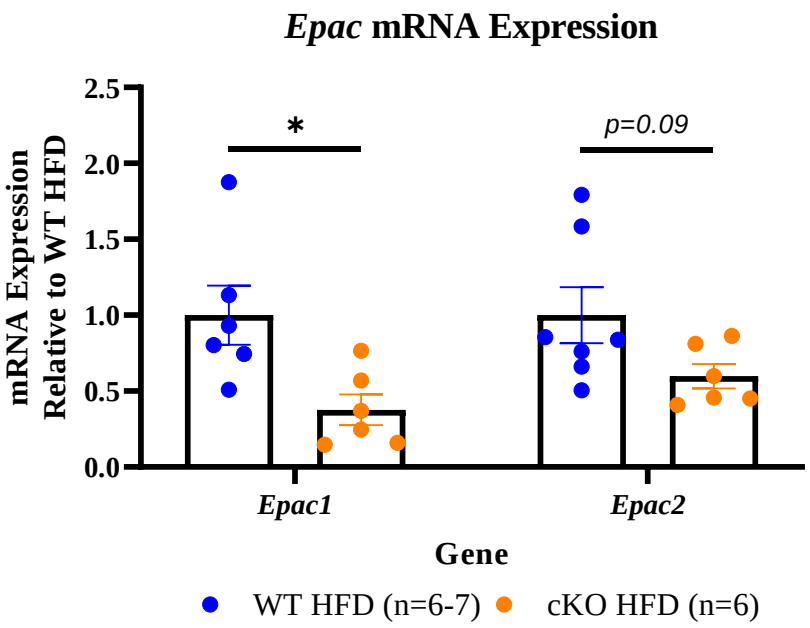

Figure 4.18: Islet mRNA expression of *Epac1* and *Epac2* in WT and cKO mice after 12 weeks of HFD

mRNA expression of *Epac1* and *Epac2* was measured using RTqPCR. mRNA expression levels were normalized to *Ppa1* (housekeeping gene) and expressed relative to WT HFD mice. Each data point represents a mouse averaged from 3 independent experiments (n=6-7 mice/group). Results are presented as means ± SEM. Statistical analysis was done using an unpaired Student's t-test between groups where: "*" $p<0.05$.

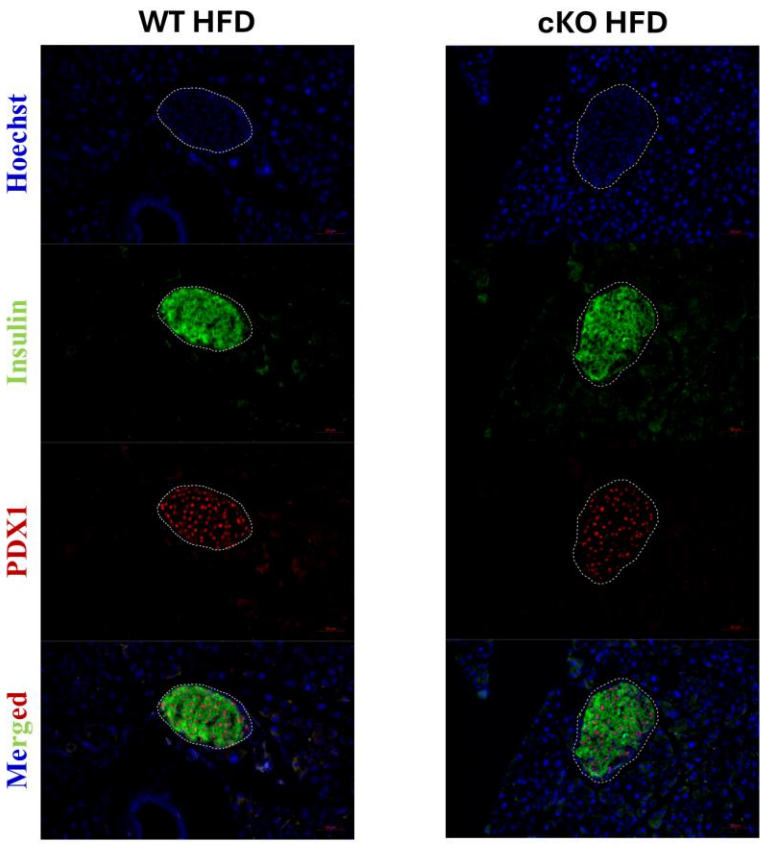

Figure 4.19: Representative PDX1 immunofluorescence in WT (left) and cKO (right) mice after 12 weeks of HFD

Representative images of PDX1 immunofluorescence are presented. Pancreases from WT (left) and cKO (right) mice were immunostained for Hoechst (blue), PDX1 (red), and Insulin (green). PDX1-positive β cells were identified as nuclei showing co-localization of Hoechst and PDX1 along with cytosolic insulin-positivity. Dotted white lines outline pancreatic islet. Scale bars represent 50μm. Images were taken by Raneet Khalon.

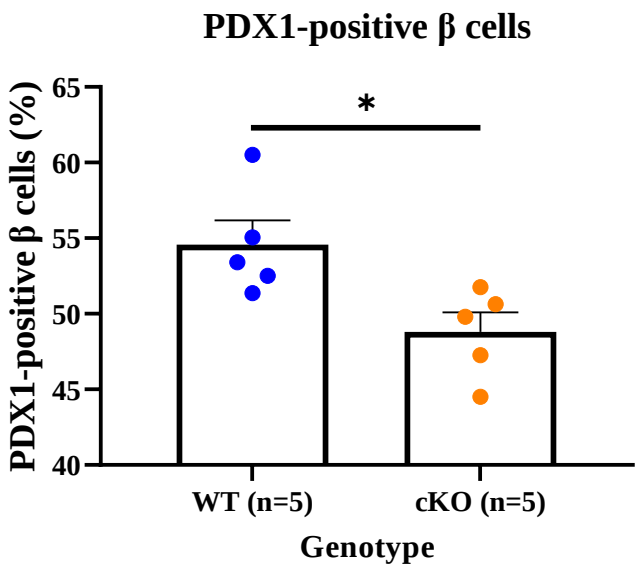

Figure 4.20: Nuclear PDX1-positive β cells in WT and cKO mice after Weeks 12 of HFD

The pancreas of WT and cKO mice after 12 weeks of HFD were labeled for PDX1 and insulin. The percentage of nuclear PDX1- positive β cells was determined by PDX1-positive β cells identified as nuclei showing co-localization of Hoechst and PDX1 along with cytosolic insulin-positivity relative to the total β cells counted. Each data point represents a mouse (n = 5 mice/group). At least 1000 β cells were counted per mouse. Statistical analysis was done using an unpaired Student's t-test between the means where" "*" $p < 0.05$. Quantification of PDX1 nuclear co-localization was done by Raneet Khalon.

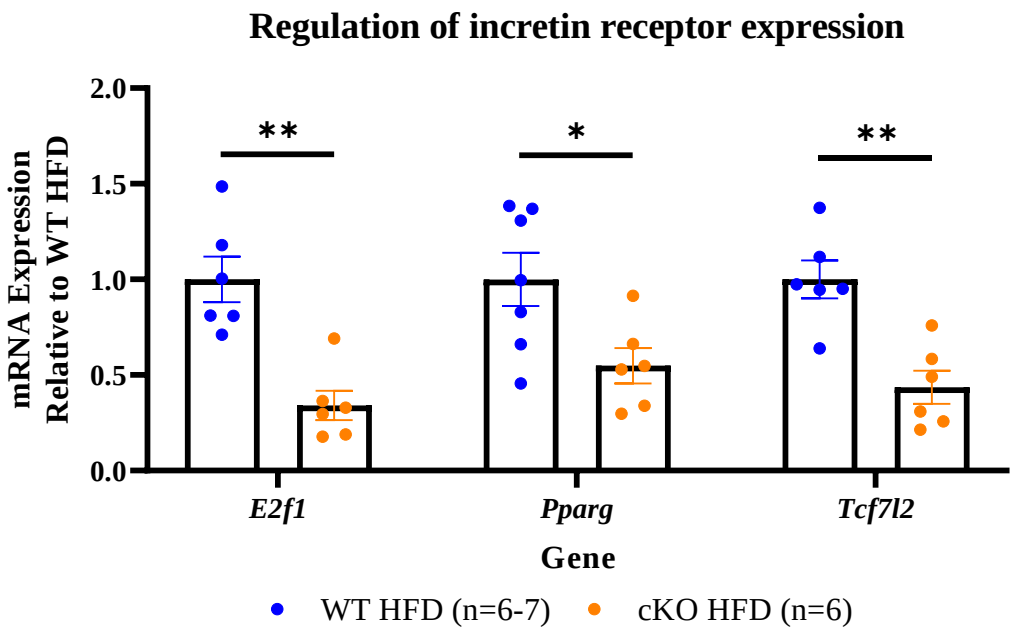

Figure 4.21: Islet mRNA expression of transcription factors that regulate incretin hormone receptor expression in WT and cKO mice after 12 weeks of HFD

mRNA expression of *E2f1*, *Pparg*, and *Tcf7l2* was assessed by RTqPCR. mRNA expression was normalized to *Ppa1* (housekeeping gene) and expressed relative to WT HFD mice. Each data point represents a mouse (n=6-7 mice/group). Results are presented as means ± SEM of 3 independent experiments. Statistical analysis was done using an unpaired Student's t-test between groups where: "*" $p<0.05$ and "**" $p<0.005$.

4.4 Discussion

Previous work from the Huang lab has demonstrated that PRLR in pancreatic β cells is necessary to maintain glucose homeostasis during pregnancy.[38,46] This study aimed to determine whether the PRLR-mediated protective mechanism is observed in multiparous mice challenged with an HFD, which mimics mothers adopting a Western Diet following pregnancy. In the Chapter 3, we observed no statistically significant difference in glucose tolerance between WT and cKO mice postpartum following two pregnancies (Supplemental Figure 5). However, as early as 6 weeks after the start of an HFD, cKO mice became glucose intolerant in comparison to WT mice and this glucose intolerance worsened at 12 weeks of HFD (Figure 3.11). This glucose intolerance could not be attributed to a difference in insulin sensitivity, as we observed that HFD increased insulin resistance to a similar extent in both WT and cKO mice (Figures 3.12F and 3.13). We also noted a reduction in first phase insulin secretion *in vivo*, seen at the 10-minute during an OGTT in cKO HFD mice compared to WT HFD at 12 weeks of HFD (Figure 3.14). However, we observed no difference in *in vitro* GSIS between the islets of cKO and WT mice (Figure 3.16). In this chapter, our aim was to determine why the *in vivo* first phase of insulin secretion was impaired and to explore the molecular mechanisms that may explain the maladaptive insulin response in cKO mice.

Quantification of insulin content from isolated islets after 12 weeks of HFD revealed that cKO mice had a reduction in insulin content in comparison to WT mice (Figure 4.1). To support this observation, cKO HFD mice had a reduction in mRNA expression of both *Ins1* and *Ins2* compared to WT mice (Figure 4.2). Next, we investigated key transcription factors known to directly regulate insulin gene transcription: *MafA*, *NeuroD1*, *Nkx6.1*, *Pax6*, and *Pdx1*. We found

decreased mRNA expressions in all these transcription factors, but statistical significance was observed only for *Nkx6.1* and *Pax6* (Figure 4.3). Our results suggest that cKO mice fed HFD have a reduction in insulin content, insulin gene expression, and transcription factors that regulate insulin gene expression compared to WT controls. Further work is required to determine whether some or all the transcription factors measured are responsible for the reduction in insulin content. Although, both the islets of cKO and WT mice after 12 weeks of HFD secreted 20% of their insulin content during *in vitro* GSIS, suggesting that the β cells of cKO HFD mice and WT HFD mice have similar insulin secretory capacity under *in vitro* conditions. Insulin content may contribute to the reduction in the first phase of insulin secretion *in vivo* as each β cell has a smaller pool of IR insulin granules but a more likely explanation is a reduction in total β cell mass.

During times of nutrient excess, β cells are required to increase synthesis of insulin, which can activate the UPR, known to inhibit insulin biosynthesis at the transcriptional and translational levels.[167] Surprisingly, cKO mice fed HFD displayed a reduction in the mRNA expressions of all the genes measured involved in the UPR compared to WT mice fed HFD (Figure 4.4). Our lab has previously shown that the overexpression of Lrrc55 in pancreatic islets protected them from FFA-induced apoptosis and hypothesized that cKO mice would upregulated UPR-related genes.[219] We observed a statistically significant decrease in *Lrrc55* mRNA expression in cKO HFD mice compared to WT HFD mice (Figure 4.4), as *Lrrc55* increases in a PRLR-dependent manner during pregnancy. The decreased expression of *Lrrc55* in cKO mice supports the knockout of PRLR in model. Contrary to our hypothesis, our results suggest that the UPR may be more active in WT HFD mice compared to cKO HFD mice. In WT mice fed CD or HFD, no

statistically significant differences were observed in the mRNA expression of genes involved in the UPR (Supplemental Figure 10). Gupta et al. have shown that in 8-week-old male mice, the greatest transcriptional changes in UPR-related genes are observed at 16 weeks.[157] Therefore, our 12 week duration of HFD may not have been long enough to observe differences in gene expression, in addition to the sex differences as males are more susceptible to developing diabetes.[85]

PRLR has also been shown to be protective against apoptosis.[272] In line with this, cKO HFD mice did display increased apoptotic β cells, but no statistically significant difference in β cell apoptosis was observed compared to WT HFD mice (Figure 4.7A) This finding is consistent with current literature that PRL protects β cells from apoptosis, and further experiments are needed to confirm whether this is true in our model by increasing the sample size and measuring other markers of apoptosis.[272] We did observe a statistically significant decrease in β cell proliferation in cKO HFD mice compared to WT HFD mice (Figure 4.7B), which may be explained by a reduction in the expressions of *Nkx6.1* and *Ire1α* (Figures 4.3 and 4.4). Rat bone marrow mesenchymal stem cells treated with PRL have been shown to increase the expression of NKX6.1 *in vitro*, but no studies have observed reported in insulin-producing cell lines.[273] NKX6.1 has been proposed to indirectly affect β cell proliferation by regulating the expression of Cyclin D2.[91] In contrast, IRE1α has been shown to promote proliferation by regulating the expression of Cyclin A1 through XBP-1.[274]

Literature has also suggested that in rodents, β cell proliferation peaks early (Week 1) after exposure to HFD, around 1.5% of β cells being KI67-positive or 8% BrdU-positive.[156,275] We

examined β cell proliferation from WT mice after 1 week of HFD. Interestingly, there was no statistically significant difference in β cell proliferation across time points: 1 week of HFD, 12 weeks of HFD, and 12 weeks of CD (Supplemental Figure 11). Further studies observing proliferation after two pregnancies and before the start of HFD or CD will be required to determine whether β cell proliferation is decreased when mice have litters before HFD. The absence of increased HFD-induced β cell proliferation early during HFD may be explained by the older age of our mice when placed on HFD (averaged 5-6 months old), which coincides with current literature as in both rodents and humans, the ability of β cells to proliferate decreases with age.[32,33]

Our morphometric results found no statistically significant difference in the average number of β cells or average β cell size between WT and cKO after 12 weeks of HFD (Figure 4.8). At the islet level, no statistically significant difference in the number of islets or islet size was observed between WT and cKO mice (Figure 4.9). We also observed no statistically significant difference in the percentage of very small, small, medium, and large islets between cKO and WT mice fed HFD (Figure 4.10). In contrast, WT mice fed HFD has a greater percentage of very small islets and a smaller percentage of large islets compared to WT mice fed CD (Figure 4.11). A higher proportion of very small islets in WT mice fed HFD may suggest the generation of new islets (neogenesis) from non-β cell sources such as the duct epithelium precursors.[155,175,276,277] Further work into the location of insulin-positive cells near duct epithelium would support these findings.

WT mice fed 12 weeks of CD or HFD did not result in a statistically significant difference in β cell mass (Supplemental Figure 12), cKO mice fed HFD had a trend towards decrease β cell

mass compared to WT mice fed HFD (Figure 4.12). We observed small changes in both β cell apoptosis (difference of 0.13%) and β cell proliferation (difference of 0.15%) between WT and cKO mice fed HFD, representing a very small fraction of β cells. Taken together, unlike pregnancy, where the main role of PRLR is to increase in β cell mass through proliferation, in our model where multiparous mice exposed to HFD, an increase in β cell mass was not as evident, suggesting a different compensatory mechanisms may be present.[43,204] This is in line with current transcriptomic analyses where PRLR-induced genes in pancreatic islets during pregnancy versus HFD showed very little overlap, suggesting that these pregnancy and HFD activate different mechanisms of compensation.[220]

We then investigated genes involved in β cell function that play an important role GSIS: GLUT2, GCK, and PC. First, GLUT2 transports glucose into β cells with a high Michaelis constant (K_m) and transport ability, allowing quick entry of glucose into the β cell.[9,103] Once glucose enters, it is phosphorylated by the rate-limiting enzyme GCK, which plays a pivotal role in GSIS.[278] Finally, pyruvate can enter the mitochondrial tricarboxylic acid (TCA) cycle through two pathways controlled by either PC or PDH pathways. In β cells, evidence suggests that PC, rather than PDH, controls pyruvate entry into the TCA cycle.[279–281] Since our model utilized an HFD, we expected to observe elevated production and release of FFAs into the plasma, whereby FFAs can amplify insulin secretion through FFAR1.[27,112,113] In addition, the incretin hormone receptors GIPR and GLP-1R were of interest, as the incretin effect accounts for up to 80% of insulin secretion in response to oral glucose ingestion and plays an important role in the first phase of insulin secretion.[13–15,122]

We observed no statistically significant differences in the expression of genes involved in β cell function between WT mice fed CD compared to WT mice fed HFD (Figure 4.14). Gupta et al. also found no differences in the expression of these genes in male mice fed HFD at 12 weeks, except for an increased expression of *Pc*. We found that the islets of cKO mice had reduced expressions of: *Gck*, *Glut2*, *Pc*, *Ffar1* as well as incretin hormone receptors *Gipr* and *Glp-1r* (Figures 4.13 & 4.14). The reduction in mRNA expression of *Gck* and *Glut2* is expected, as *in vitro* culture of islets with PRL have been shown to upregulate protein expressions of GLUT2 and GCK.[205] It has been shown that hyperglycemia results in changes in the gene expression in β cells, including *Pc*; it could be that the impaired glucose tolerance in cKO mice reduces *Pc* expression.[282] *Ffar1* has also been shown to contain transcription start sites for the STAT family, which is activated by PRLR in the JAK2/STAT5 pathway.[283]

Many of the genes involved in β cell function measured in the islets of cKO HFD mice compared to WT HFD mice were downregulated. This may suggest that the β cells of cKO mice have undergone dedifferentiation compared to WT mice placed on HFD. During dedifferentiation, β cells lose their identity, resulting in decreased expression of key transcription factors such as MAFA, NEUROD1, NKX6.1, and PDX1, as observed in Figure 4.3.[30,31] These transcription factors regulate the expression of β cell function genes, and β cells lose their ability to both synthesize and secrete insulin. Deleterious states such as oxidative stress, ER stress, inflammation, hypoxia, and hyperglycemia have been implicated in β cell dedifferentiation and contributes to the pathogenesis of diabetes.[284] Further work is needed to both confirm that β cells of cKO mice are more dedifferentiated compared to WT mice in our model and to determine which of the deleterious states PRLR may play a role in.

The incretin effect is not well studied during the context of pregnancy as medications such as GLP-1 agonists and sodium-glucose co-transporter-2 inhibitors have been found to result in adverse offspring effects in both animal and human studies.[285] Furthermore, the role of PRLR in β cells has primarily been studied in β cells during pregnancy.[40–45] A reduction in incretin hormone receptors, *Gipr* and *Glp-1r*, and possibly the incretin effect would be a novel finding as PRLR has never been implicated in regulating the incretin effect.

Therefore, we studied the incretin effect by comparing glucose tolerance with an OGTT vs. an IPGTT. We found that glucose excursion, calculated as integrated AUC during the 120-minute GTTs, was higher during an IPGTT compared to an OGTT in both WT and cKO (Figure 4.15C). Moreover, both WT and cKO mice secreted more insulin at the 10-minute time point during an OGTT compared to IPGTT, confirming the presence of an incretin effect (Figure 4.17). Surprisingly, we did not observe a statistically significant difference in glucose excursion between WT and cKO mice measured as integrated AUC during the 120-minute IPGTT (Figure 4.16B) and no statistically significant difference in serum insulin was observed during the 0, 10, and 30 minutes between WT and cKO mice after 12 weeks of HFD (Figure 4.17). An increase in sample size for both cKO and WT mice are required to determine if there is no statistically significant difference in glucose tolerance and insulin secretion between WT and cKO during IPGTT.

Here we displayed the incretin effect whereby an oral, but not intraperitoneal, administration of glucose elicits a greater insulin secretory response in WT HFD mice compared to cKO HFD

mice. A reduction in *Gipr* and *Glp-1r* expressions could explain how no statistically significant difference was observed in the insulin secretory capacity between islets of WT and cKO mice after 12 weeks of HFD *in vitro* as well as during an IPGTT, where there would be little to no GIP and GLP-1 present. One important distinction is that dosages during IPGTT (1g glucose/kg) were different than OGTT (2g glucose/kg). The rationale for this decision was that 2g/kg IPGTT resulted in blood glucose levels reaching 33.3 mM (upper limit of the glucometer). Therefore, to correctly compare WT HFD and cKO HFD mice glucose tolerance measured by an OGTT and an IPGTT further studies administering 1g/kg of body weight orally will be needed.

EPAC1 and EPAC2 are downstream effectors of both GIPR and GLP-1R signaling pathways in pancreatic β cells and are partly responsible for the insulin secretory effects observed during the incretin effect. Activation of GIPR and GLP-1R results in cAMP production and the activation of both PKA and EPAC, both of which enhance insulin secretion by priming insulin granules and closing K_{ATP} channels leading to membrane depolarization.[23,126,131] Both EPAC isoforms have been shown to mobilize intracellular Ca^{2+} stores in the ER to further increase intracellular Ca^{2+} levels, promoting insulin granule exocytosis, in addition to extracellular Ca^{2+} influx via the closure of K_{ATP} channels.[131] In the islets of rodents, it has been shown that the downregulation of EPAC2 diminishes the insulin stimulatory actions of GLP-1.[132]

We found that both *Epac1* and *Epac2* mRNA expressions were decreased in cKO HFD mice in comparison to WT HFD mice (Figure 4.16). To further investigate whether downstream signaling molecules would be affected, we used immunofluorescence to measure nuclear PDX1-positive β cells. GLP-1 has been shown to increase the mRNA expression of PDX1 and result in

nuclear translocation of PDX1 in a cAMP/PKA-dependent manner *in vitro*.[127] We observed that cKO HFD mice had a reduced number of nuclear PDX1-positive β cells compared to WT HFD mice (Figure 4.20). Although statistical significance was found, the difference is very small, and the biological significance is unknown. Taken together, we have observed a decrease in the expressions of *Epac1* and *Epac2* as well as less PDX1 nuclear co-localization, which may contribute to the reduction in the incretin effect we observed in cKO HFD mice compared to WT HFD mice. Further studies to delineate whether these differences are observed at the protein and functional levels and whether a decrease in incretin hormone receptors (GIPR and GLP-1R) or downstream effectors such as EPAC1 and EPAC2 contribute to the decreased insulin secretion observed in our model.

Finally, the transcription factors: *E2f1*, *MafA*, *Nkx6.1*, *Pax6*, *Pparγ*, and *Tcf7l2* have been shown to regulate the expression of GIPR and/or GLP-1R.[141,157,286–288] We found no statistically significant difference in mRNA expression of *MafA*, but expressions of *E2f1*, *Nkx6.1*, *Pax6*, *Pparg*, and *Tcf7l2* were decreased in cKO mice compared to WT mice (Figures 4.3 and 4.21). Comparing WT mice on CD or HFD, we found that only *E2f1* expression was upregulated in WT HFD mice (Supplemental Figure 13). The expressions of all the transcription factors measured have been associated with β cell adaptation during HFD. [141,157,286–288] Of these, only E2F1 and PPARG are known to be downstream of PRLR.[212,289]

During pregnancy, it has been shown during pregnancy that PRL promotes the phosphorylation of retinoblastoma proteins (Rbs) and E2F1 upregulation in a STAT5-dependent manner.[212] The transcription factor E2F1 has been shown to modulate GLP-1 action and expression of *Glp-1r* in

β cells. Whereas Bourouh et al. showed that *E2f1* knockdown in Min6 cells was shown to blunt GSIS *in vitro* in response to 20mM glucose and decreased insulin was secreted in response to 20mM glucose and Exendin-4, a synthetic GLP-1 analog. Furthermore, they observed pancreatic islets from E2F1 knockout mice and human islets treated with E2F pan inhibitor HLM006474 had decreased insulin secretion in response to glucose and Exendin-4 compared to controls, and this defect in insulin secretion could be rescued by forskolin treatment. Using chromatin immunoprecipitation-qPCR experiments, they were able to show that E2F1 binds directly to the *Glp1-r* promoter in both mouse and human islets in a phosphorylated retinoblastoma protein (pRB)-dependent manner.[139]

The transcription factor PPARG is part of a nuclear hormone receptor superfamily of ligand-activated transcription factors, where ligand binding results in the heterodimerization with retinoid X receptors, recruitment of co-factors, and binding to peroxisome proliferator response elements (PPREs).[141] TZDs are PPARG agonists and have been used for clinical treatment of T2D to enhance insulin sensitivity in the liver, adipose tissue, and skeletal muscle.[143] However, there is growing evidence that TZDs could also improve the insulin secretory capacity of β cells.[143,290–292] It has also been found that GIPR has PPREs and that Cre-Lox mediated knockout of PPARG in β cells leads to a 70% reduction in GIPR protein expression compared to Cre-negative WT littermate controls.[148] In NIH-3T3 cells, a mouse fibroblast cell line, it has been observed that PRL enhances the mRNA expression of *Pparg*.[289]

4.5 Conclusion

In conclusion, we have found that PRLR in β cells is required for maintaining glucose homeostasis in multiparous mice exposed to HFD. In Chapter 3, we found that cKO mice were glucose intolerant after exposure to HFD, and this difference was due to a reduction in first phase insulin secretion in response to oral glucose challenge. While previous studies have shown the role of PRLR during pregnancy is to increase β cell mass. In our model of HFD, no statistically significant difference was observed between the β cell mass cKO and WT mice. Since our *in vitro* GSIS results suggested that pancreatic islets from WT and cKO mice had no difference in their intrinsic ability to secrete insulin, we hypothesized that an *in vivo* factor was responsible for this discrepancy. This led us to measure mRNA expression of incretin hormone receptors *Gipr* and *Glp-1r* as well as look at whether the incretin effect was affected.

We found that both *Gipr* and *Glp-1r* mRNA expression as well as the mRNA expressions of downstream effectors *Epac1* and *Epac2* were downregulated in the islets of cKO HFD mice compared to WT HFD mice. To study the incretin effect, we challenged mice to an IPGTT, but no statistically significant difference in glucose tolerance and insulin secretion was observed between WT HFD and cKO HFD mice after 12 weeks of HFD. Using a candidate gene approach, we looked at transcription factors that regulate the expression of *Gipr* and *Glp-1r* and identified the downregulation of *E2f1* and *Pparg*, both of which are involved in β cell adaptation to HFD and are both downstream of PRLR. Here we propose that female multiparous mice with β cell-specific deletion of PRLR challenged with HFD exhibit expressions of *E2f1* and *Pparg*, which in turn decreases the expressions of incretin hormone receptors *Gipr* and *Glp-1r*, blunting the incretin effect.

Chapter 5: Conclusion and Future directions

5.1 Introduction

The incidence of diabetes has risen drastically and is expected to continue to rise worldwide.[1] Diabetes is a metabolic disorder wherein pancreatic β cells are unable to meet the body's insulin requirements. Current treatments aim to manage the diabetes through a dietary, lifestyle, and therapeutic approaches.[2,3] For the most severe form of diabetes, T1D, islet transplantation exists but is limited to patient eligibility and cadaveric donor islet availability.[4] A promising approach is to use stem cell-derived β cells, but currently, they lack the mature insulin secretory responses found in mature islets and may face challenges with immunogenicity.[6,7] Therefore, any strategies that can enhance our understanding of increasing β cell mass and function, whether applied to pre-existing or stem cell-derived β cells could hold therapeutic potential.

During the later stages of gestation, maternal insulin resistance develops to channel nutrients to the developing fetus.[152] To adapt to maternal insulin resistance, there is an increase in β cell mass to augment the amount of insulin that can be secreted.[42] Evidence suggests that lactogenic hormones PRL and PL, mediated by PRLR, regulate these pregnancy-associated adaptations in β cells.[40–42] Previous work in our lab has demonstrated *in vivo* that these pregnancy-associated adaptations occur through PRLR.[38,46] While most of PRLR research during diabetes focuses on its role during β cell adaptation during pregnancy, a growing body of clinical evidence suggests it may have a role outside of pregnancy. Serum prolactin levels outside the normal range have been associated with higher prevalence of T2D and insulin resistance.[47–49] Therefore, we hypothesized that PRLR plays a role in maintaining glucose homeostasis outside of pregnancy.

Using a β cell-specific knockout of PRLR, this hypothesis was evaluated by the following three aims:

1. How does PRLR in β cells affect β cell physiology during times of metabolic stress
2. How do β cells compensate when prolactin receptor is lost?
3. What are the molecular mechanisms governing differences in β cell function and compensation?

5.2 Strengths and limitations

5.2.1 *In vivo* model

One of the major strengths of this project was the use of an *in vivo* model of inducible, β cell-specific PRLR-null mouse to study the effects of PRLR in pancreatic β cell adaptation to HFD in multiparous mice. This new mouse model approach was necessary because mice with global PRLR deletion (i.e. $Prlr^{-/-}$ mice) cannot complete pregnancies due to a placental implantation defect; therefore, we cannot use it to study the role of PRLR during pregnancy. Moreover, $PRLR^{-/-}$ mice exhibit decreased β cell mass and function at birth, which could potentially bias our results.[207,208] Researchers have therefore resorted to using global PRLR-null mice treated with progesterone to rescue the implantation defect, and heterozygous PRLR-null mice to study the effects of PRLR, and they have found PRLR is required for normal glucose homeostasis during pregnancy.[38,42,209,293] However, a limitation of the model used in these studies is that PRLR is expressed in various other metabolic tissues, and the absence of PRLR could directly or indirectly influence β cell function.[35–39]

Our transgenic mice used the Cre-LoxP method to enable both temporal and tissue-specific deletion of PRLR.[241] The PDX1 promoter was chosen to drive CreER expression because it is

expressed in the pancreas during development, but its expression is restricted to mature pancreatic β cells, pancreatic duct, duodenum, and stomach postnatally.[89,90] In theory, CreER would be expressed in the aforementioned cells and tissues, residing in the cytoplasm bound to heat shock protein 90 (HSP90) with a mutated form of estrogen receptor preventing endogenous estrogen from binding to CreER-HSP90 complex.[294] Tamoxifen promotes the dissociation of CreER from HSP90, resulting in the translocation of CreER to the nucleus to bind to *loxP* sites flanking exon 5 of PRLR, thereby leading to the deletion of exon 5 and consequently a non-functional PRLR.

PDX1 expression is also observed in the duodenum, where enteroendocrine K and L cells, which synthesize and secrete the incretin hormones GIP and GLP-1, respectively.[13] Regions of the small intestine have been shown to express PRLR.[36] Activation of CreER and subsequent deletion of PRLR in K and L cells could potentially influence the production and secretion of GIP and GLP-1, which may be responsible for the reduction in incretin effect observed in cKO mice. Additional experiments will need to be performed to determine serum levels of GIP and GLP-1. Of note, we found a significant reduction in *Gipr* and *Glp-1r* in the islets from cKO mice given 12 weeks of HFD, in comparison to the WT mice. In most cases, a reduction of a hormone will lead to an up-regulation of its receptor, as the body attempts to compensate for the lower hormone level by maximizing receptor expression. Hence, a reduction in GIP and GLP-1 in K- and L-cells is not likely the cause of reduced *Gipr* and *Glp-1r* expression we observed.

Various limitations of the Cre-LoxP system have been demonstrated *in vivo*. Firstly, CreER recombination has been observed to occur in mice independently of tamoxifen (referred to as

"leaky" Cre). This suggests that ectopic Cre recombinase activity might have deleted PRLR during development, resulting in a reduction in both β cell mass and function, akin to what is observed in whole body PRLR-null mice.[207,208,295] For example, in mice that uses the rat insulin promoter (RIP) to drive Cre expression (the RIP-Cre mice), RIP expression is observed not only in β cells but also in hypothalamic neurons, which are an important regulator of glucose and energy homeostasis.[296–299] To address this issue, researchers have chosen to drive CreER expression using PDX1 as a promoter. PDX1 has been shown to have a more limited expression in adult mice, mostly in mature β cells and small parts of the GI tract.[89,90] However, many of these PDX1 Cre mouse lines have been found to exhibit mosaic Cre-mediated recombination.[300]

To investigate the spatial deletion of PRLR, we have previously interbred *Prlr*$^{fl/fl}$ mice with ROSA$^{mT/mG}$ reporter mouse line, which express tdTomato (red) and, upon CreER recombination, express green fluorescent protein (green), enabling the visualization of Cre activity (Figure 5.1). We observed no GFP expression in the brain, and *Prlr* mRNA expression was not reduced in metabolic tissues such as the hypothalamus, fat, and liver, when compared to WT mice (*Pdx1*CreER:*Prlr*$^{fl/fl}$ and *Prlr*$^{fl/fl}$).[46]

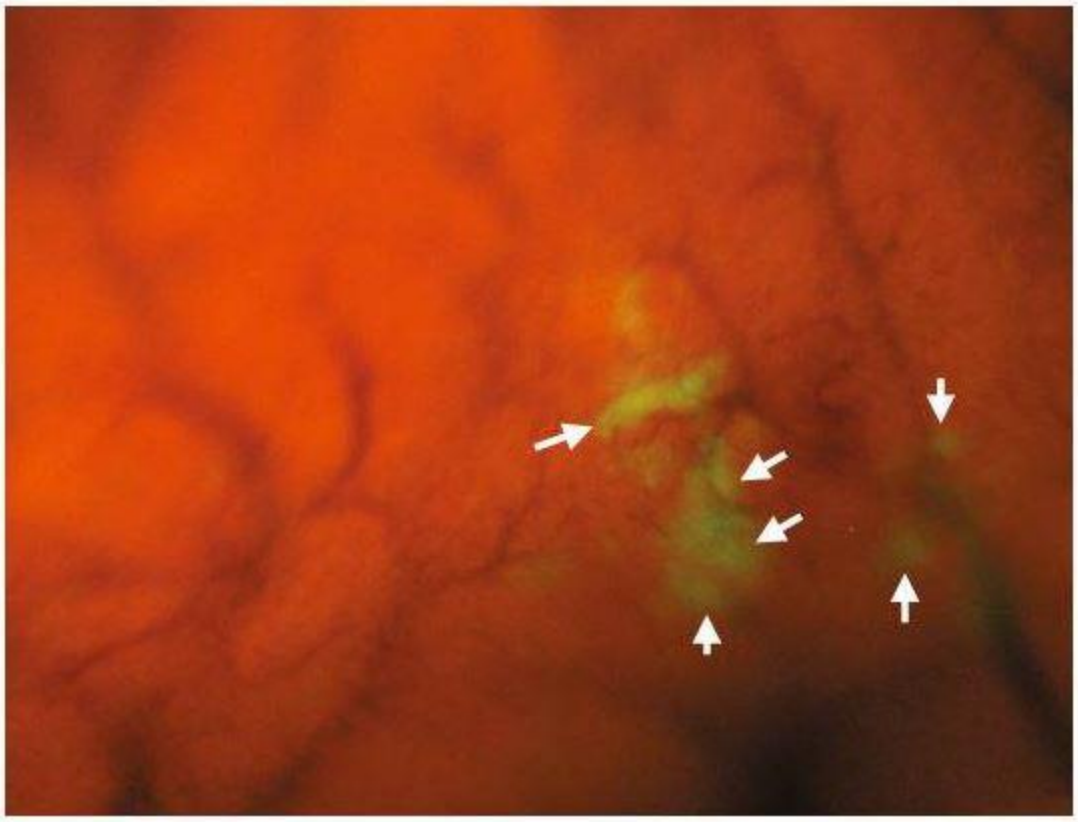

Figure 5.1 GFP expression in the pancreas of βPRLR$^{fl/fl}$:ROSA^{mTmG} mouse

βPRLR$^{fl/fl}$ mice were crossed with the ROSA$^{mT/mG}$ reporter mouse line, which express tdTomato (red) and upon Cre recombination, express green fluorescent protein (green), enabling the visualization of Cre activity.[46] White arrows indicate green fluorescent protein. Image taken by Vipul Shrivastava.

Studies have also shown that there are differences in Cre recombination frequencies within the same cell population and multiple dosages of tamoxifen may be required to achieve Cre recombination.[301,302] These studies suggest that Cre recombination may not be consistent within all β cells, which have been shown to exhibit heterogeneity themselves.[196,303] All mice in this study were given five dosages of tamoxifen (4mg/dose) to achieve Cre recombination in pancreatic β cells, but the effects of Cre recombination in cells such as pancreatic ductal cells, duodenum, and stomach and their relevance to the phenotypes observed remain to be answered.

The presence of Cre recombinase in mammalian cells has also been shown to inhibit growth and induce DNA damage.[304] Cells can both detect and repair DNA damage, but failure to repair DNA damage will result in apoptosis.[305] Therefore, the presence of CreER in β and non-β cells may have influenced the phenotypes observed. To observe whether CreER induced DNA damage, a comet assay of metabolically relevant tissues may be performed.[306]

5.2.2 Physiological results

Another strength of this project is the number of mice for each genotype of mice on HFD, as our Week 6 and Week 12 HFD OGTT results show great statistical significance. Our physiological data strongly support the notion that cKO mice are more glucose intolerant compared to WT mice after HFD during an OGTT. However, a limitation is our low sample size in cKO mice fed CD with an (n=3-4), and mice that underwent an IPGTT (n=7-8). Therefore, more mice are needed for these genotypes and treatments. Another limitation was that our glucometer, used to read blood glucose levels, had a maximum reading of 33.3mM, which was reached during both OGTT and IPGTT. This was the rationale for administering a lower dosage of 1g glucose/kg

body weight during IPGTT at Week 12 of HFD. Further studies with a glucometer with a higher range, as well as identical dosages for both OGTT and IPGTT, would be needed to truly compare these results.

Furthermore, in HFD-fed mice, changes in body mass are primarily due to alterations in fat mass, with small changes in lean mass (muscle, brain, and liver). Lean mass tissues are responsible for the short-term uptake of glucose, and obese mice receive a disproportionately large amount of glucose for the similar lean body mass.[245] Further experiments can employ a 1g glucose/kg body weight for OGTT to see if the glucose intolerance in cKO mice is still observed at lower dosages.

Additionally, our *in vitro* GSIS was static, and insulin from media only measured the total insulin secreted in response to different stimuli, unable to capture the first and second phases of insulin secretion. To observe temporal insulin secretion *in vitro*, electrophysiological studies would have to be performed, or media collected at specific time points during the assay.

5.2.3 Transcriptomic results

We used a candidate gene approach to identify differentially expressed genes and may have missed genes not tested that would have been captured in other methods such as bulk- or single-cell RNA sequencing. A difference in gene expression does imply a difference at both the protein and functional levels, as seen when β cells are treated with palmitic acid reduced *Glut2* mRNA expression by 40%, but no effect was observed in protein expression.[307] Therefore further experiments to support our transcriptomic results at the protein level using Western immunoblotting are required.

Furthermore, the mRNA expression data presented thus far between WT and cKO mice after 12 weeks of HFD were all downregulated in cKO mice compared to WT mice. These results could stem from artifact amplification due to mispriming, leading to non-specific product amplification or self-hybridization of primers resulting in the formation of primer-dimers.[308] To overcome artifact biases during qPCR, we ensured that the melting peaks had one product, and the primer efficiencies of all genes measured were within between 85-120%. This was calculated by running a serial dilution of cDNA to plot a standard curve where Primer efficiency = $(10^{(-1/\text{slope})}-1) \times 100\%$. To verify that our RTqPCR experiments amplified the intended product, gel electrophoresis of samples can be performed to detect the presence of a band of DNA at the correct base pair length and sent for sequencing.

We also measured the mRNA expression of the gene Transcription factor 7 (*Tcf7*) that encodes the T cell-specific transcription factor-1 (TCF1), as β cell-specific knockout of Gipr had decreased islet expression of *Tcf7*.[309] It was found that GIP promotes β cell *Tcf7* expression through cAMP-independent and extracellular signal-regulated kinase (ERK)-dependent pathways.[309] We hypothesized that if Gipr expression was decreased in our model and consequently decreased GIPR activation and downstream signaling, we would observe a decrease in *Tcf7* expression. Although not statistically significant, cKO HFD mice had increased in *Tcf7* expression compared to WT HFD mice (Figure 5.2).

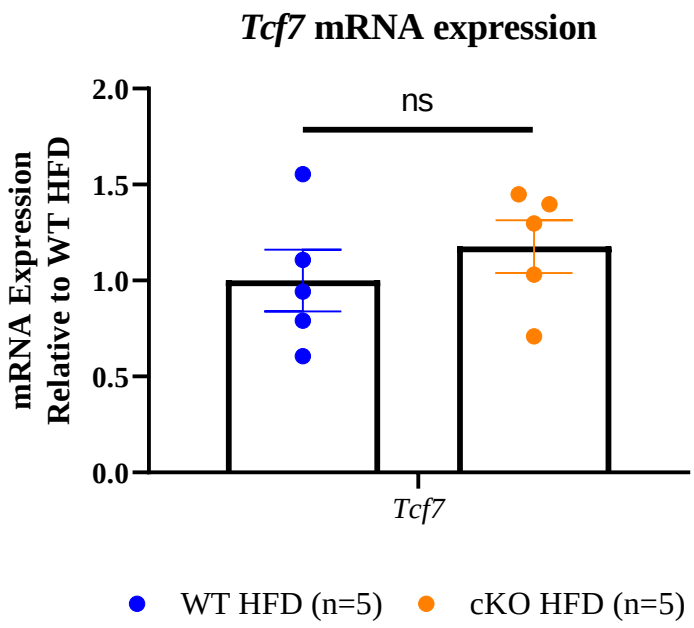

Figure 5.2 Islet mRNA expression of *Tcf7* in WT HFD and cKO HFD mice

mRNA expression of *Tcf7* in pancreatic islets was measured by RTqPCR. mRNA expression was normalized to *Ppa1* (housekeeping gene) and expressed relative to WT HFD mice. Each data point represents a mouse (n=5 mice/group). Results are presented as means ± SEM of 3 independent experiments. Statistical analysis was done using an unpaired Student's t-test between groups where: "**ns**" not significant.

5.3 Overall Summary and interpretation of results

The purpose of this project was to determine the role of PRLR outside of pregnancy. We used a transgenic mouse line with homozygous deletion of PRLR in β cells using the Cre-LoxP method. These mice were exposed to two pregnancies and subsequently, placed on a HFD for 12 weeks. First, we explored how the absence of PRLR in β cells affected metabolic physiology by measuring glucose tolerance, insulin sensitivity, and insulin secretion. Then, we determined how β cells may be compensating by measuring differences in insulin content, β cell mass, and genes involved in β cell function. Finally, we used a candidate gene approach to investigate the molecular mechanisms that could be responsible for the phenotypes observed.

Initially, we found that activation of Cre recombinase and two pregnancies did not affect glucose homeostasis between WT and cKO mice. However, when exposed to HFD, glucose tolerance was worse in cKO mice compared to WT mice. This difference in glucose tolerance was not due to differences in insulin sensitivity but a reduction in the first phase of insulin secretion *in vivo*. We found no statistically significant difference in the total amount of insulin secreted in response to glucose or KCl (which assesses glucose-independent pathways) *in vitro*. Our *in vitro* results suggest that there is no difference in the ability of β cells of WT and cKO mice to secrete insulin, but an *in vivo* factor is likely responsible for the difference observed in *in vivo* insulin secretion in response to an oral glucose challenge.

Unlike during pregnancy, where PRLR has been shown to increase β cell mass, our morphometric data revealed comparable results between WT and cKO mice. Our candidate gene approach revealed the downregulation of many β cell function genes: *Gck, Glut2, Pc, Ffar1,*

Gipr, and *Glp-1r*. The incretin hormone receptors GIPR and GlP-1R are of great interest, as they are responsible for most of the insulin secreted in response to meal ingestion and play an important role in the first phase of insulin secretion. Measurement of the incretin effect by comparing blood glucose levels and serum insulin during an OGTT and an IPGTT revealed that indeed cKO had a reduction in incretin effect. We identified the reduction in expressions of *Epac1* and *Epac2*, a downstream effector that increases intracellular Ca^{2+} to promote insulin granule exocytosis.[23,126] We also found that mRNA expression of the transcription factors: *E2f1*, *Nkx6.1*, *Pax6*, *Pparg*, and *Tcf7l2* were decreased in cKO mice compared to WT, all of which have been shown to regulate Gipr and/or Glp-1r expressions.[91,136,138,139,148] However, only E2F1 and PPARG are known to be downstream of PRLR.[212,289] Here we propose that mice with β cell-specific deletion of PRLR fail to increase the expression of *E2f1* and *Pparg* during HFD, which in turn decreases the expression of *Gipr* and *Glp-1r*, and diminishes the incretin effect.

5.4 Future directions

This work supports epidemiological studies on the protective role of PRLR outside of pregnancy. This protective role may be in part by PRLR regulating the incretin effect. Although GLP-1 is the most well-studied incretin hormone, discerning the contribution of GIPR and GLP-1R in pancreatic β cells of our model is necessary. Immediate future directions would be to perform *in vitro* GSIS in the presence of GIP and GLP-1 to verify that islets from cKO mice are less responsive to GIP and/or GLP-1. We will also need to measure serum GIP and GLP-1 levels during OGTT and IPGTT to ensure that incretin hormone secretion is not blunted in cKO mice.

Cre recombinase was temporally activated before two pregnancies in our model. The importance of PRLR during pregnancy has been well-studied in preventing GDM in rodents. It could be that the impaired glucose homeostasis due to the absence of PRLR during the two pregnancies increases susceptibility to glucose intolerance during HFD. These findings bear similarities to the situation in humans, as women diagnosed with GDM are more susceptible to developing T2D later on in life.[310] It would be interesting to activate Cre recombinase after two pregnancies but prior to HFD, as this more closely mimics humans where GDM is carefully managed during pregnancy and postpartum women adopt a Western Diet. It has also been shown that serum PRL was inversely associated T2D risk in both men and women.[48] Therefore, exposing both male mice and virgin female cKO mice to HFD would allow us to study sex differences in the role of PRLR in pancreatic β cells outside of pregnancy.

5.5 Significance

This work has revealed a role for PRLR in maintaining glucose homeostasis outside of pregnancy. Further studies are needed to determine how the absence of PRLR in β cells of multiparous mice exposed to HFD blunts the incretin effect. This is of physiological significance, as a blunted incretin effect is often the first clinical observation in the pathogenesis of T2D. If we can preserve the incretin effect, we could potentially delay the progression and onset of T2D.

References Cited

1. Saeedi, P. *et al.* Global and regional diabetes prevalence estimates for 2019 and projections for 2030 and 2045: Results from the International Diabetes Federation Diabetes Atlas, 9th edition. *Diabetes Res. Clin. Pract.* **157**, (2019).
2. Sievenpiper, J. L. *et al.* Nutrition Therapy. *Can. J. Diabetes* **42**, S64–S79 (2018).
3. Stumvoll, M. *et al.* Type 2 diabetes: principles of pathogenesis and therapy. *Lancet* **365**, 1333–1346 (2005).
4. Shapiro, A. M. J. *et al.* International Trial of the Edmonton Protocol for Islet Transplantation. *http://dx.doi.org/10.1056/NEJMoa061267* **355**, 1318–1330 (2009).
5. Feig, D. S. *et al.* 2018 Clinical Practice Guidelines Diabetes and Pregnancy Diabetes Canada Clinical Practice Guidelines Expert Committee Pre-Existing Diabetes Preconception and During Pregnancy. (2018) doi:10.1016/j.jcjd.2017.10.038.
6. Maxwell, K. G. *et al.* Applications of iPSC-derived beta cells from patients with diabetes. (2021) doi:10.1016/j.xcrm.2021.100238.
7. Odorico, J. *et al.* Report of the Key Opinion Leaders Meeting on Stem Cell-derived Beta Cells. *Transplantation* **102**, 1223 (2018).
8. Marchetti, P. *et al.* Pancreatic Beta Cell Identity in Humans and the Role of Type 2 Diabetes. *Front. Cell Dev. Biol.* **5**, 55 (2017).
9. Thorens, B. *et al.* Cloning and functional expression in bacteria of a novel glucose transporter present in liver, intestine, kidney, and β-pancreatic islet cells. *Cell* **55**, 281–290 (1988).
10. FM, A. *et al.* ATP-sensitive K+ channels: a link between B-cell metabolism and insulin secretion. *Biochem. Soc. Trans.* **18**, 109–111 (1990).

11. Fu, Z. *et al.* Regulation of Insulin Synthesis and Secretion and Pancreatic Beta-Cell Dysfunction in Diabetes. *Curr. Diabetes Rev.* (2012) doi:10.2174/15733998130104.

12. Nauck, M. A. *et al.* The incretin effect in healthy individuals and those with type 2 diabetes: physiology, pathophysiology, and response to therapeutic interventions. *Lancet Diabetes Endocrinol.* **4**, 525–536 (2016).

13. Campbell, J. E. *et al.* Pharmacology, Physiology, and Mechanisms of Incretin Hormone Action. *Cell Metab.* **17**, 819–837 (2013).

14. Holst, J. J. The incretin system in healthy humans: The role of GIP and GLP-1. *Metabolism.* **96**, 46–55 (2019).

15. Diakogiannaki, E. *et al.* Nutrient detection by incretin hormone secreting cells. *Physiol. Behav.* **106**, 387 (2012).

16. Barbour, L. A. *et al.* Cellular Mechanisms for Insulin Resistance in Normal Pregnancy and Gestational Diabetes. *Diabetes Care* **30**, S112–S119 (2007).

17. Golson, M. L. *et al.* High Fat Diet Regulation of β-Cell Proliferation and β-Cell Mass. *Open Endocrinol. J.* **4**, 66–77 (2010).

18. Grattan, D. R. *et al.* Pregnancy-Induced Adaptation in the Neuroendocrine Control of Prolactin Secretion. *J. Neuroendocrinol.* **20**, 497–507 (2008).

19. Ryan, E. A. *et al.* Role of Gestational Hormones in the Induction of Insulin Resistance. *J. Clin. Endocrinol. Metab.* **67**, 341–347 (1988).

20. Napso, T. *et al.* The Role of Placental Hormones in Mediating Maternal Adaptations to Support Pregnancy and Lactation. *Front. Physiol.* **9**, 1091 (2018).

21. Porat, S. *et al.* Control of pancreatic β cell regeneration by glucose metabolism. *Cell Metab.* **13**, 440–449 (2011).

22. Fatrai, S. *et al.* Akt Induces β-Cell Proliferation by Regulating Cyclin D1, Cyclin D2, and p21 Levels and Cyclin-Dependent Kinase-4 Activity. *Diabetes* **55**, 318–325 (2006).

23. Mayendraraj, A. *et al.* GLP-1 and GIP receptor signaling in beta cells - A review of receptor interactions and co-stimulation. *Peptides* **151**, (2022).

24. Song, W. J. *et al.* Exendin-4 Stimulation of Cyclin A2 in β-Cell Proliferation. *Diabetes* **57**, 2371–2381 (2008).

25. Scheuner, D. *et al.* Control of mRNA translation preserves endoplasmic reticulum function in beta cells and maintains glucose homeostasis. *Nat. Med. 2005 117* **11**, 757–764 (2005).

26. Xin, Y. *et al.* Pseudotime Ordering of Single Human β-Cells Reveals States of Insulin Production and Unfolded Protein Response. *Diabetes* **67**, 1783–1794 (2018).

27. Sharma, R. B. *et al.* Lipotoxicity in the Pancreatic Beta Cell: Not Just Survival and Function, but Proliferation as Well? *Curr. Diab. Rep.* **14**, 492 (2014).

28. Poitout, V. Lipotoxicity impairs incretin signalling. *Diabetologia* **56**, 231–233 (2013).

29. Bensellam, M. *et al.* The molecular mechanisms of pancreatic β-cell glucotoxicity: Recent findings and future research directions. *Mol. Cell. Endocrinol.* **364**, 1–27 (2012).

30. Moin, A. S. M. *et al.* Alterations in Beta Cell Identity in Type 1 and Type 2 Diabetes. *Curr. Diab. Rep.* **19**, (2019).

31. Guo, S. *et al.* Inactivation of specific β cell transcription factors in type 2 diabetes. *J. Clin. Invest.* **123**, 3305 (2013).

32. Aguayo-Mazzucato, C. Functional changes in beta cells during ageing and senescence. *Diabetologia* **63**, 2022 (2020).

33. Maedler, K. *et al.* Aging correlates with decreased β-cell proliferative capacity and

enhanced sensitivity to apoptosis: A potential role for fas and pancreatic duodenal homeobox-1. *Diabetes* **55**, 2455–2462 (2006).

34. Freeman, M. E. *et al.* Prolactin: Structure, Function, and Regulation of Secretion. *https://doi.org/10.1152/physrev.2000.80.4.1523* **80**, 1523–1631 (2000).

35. Foitzik, K. *et al.* Prolactin and Its Receptor Are Expressed in Murine Hair Follicle Epithelium, Show Hair Cycle-Dependent Expression, and Induce Catagen. *Am. J. Pathol.* **162**, 1611 (2003).

36. García-Caballero, T. *et al.* Cellular distribution of prolactin receptors in human digestive tissues. *J. Clin. Endocrinol. Metab.* **81**, 1861–1866 (1996).

37. Rivera, J. C. *et al.* Expression and cellular localization of prolactin and the prolactin receptor in mammalian retina. *Exp. Eye Res.* **86**, 314–321 (2008).

38. Huang, C. *et al.* Prolactin receptor is required for normal glucose homeostasis and modulation of β-cell mass during pregnancy. *Endocrinology* (2009) doi:10.1210/en.2008-1003.

39. Ling, C. *et al.* Identification of Functional Prolactin (PRL) Receptor Gene Expression: PRL Inhibits Lipoprotein Lipase Activity in Human White Adipose Tissue. *J. Clin. Endocrinol. Metab.* **88**, 1804–1808 (2003).

40. Rieck, S. *et al.* Expansion of β-cell mass in response to pregnancy. *Trends Endocrinol. Metab.* **21**, 151 (2010).

41. Banerjee, R. R. Piecing together the puzzle of pancreatic islet adaptation in pregnancy. *Annals of the New York Academy of Sciences* at https://doi.org/10.1111/nyas.13552 (2018).

42. Sorenson, R. L. *et al.* Prolactin Receptors Are Critical to the Adaptation of Islets to

Pregnancy. *Endocrinology* **150**, 1566–1569 (2009).

43. Sorenson, R. L. *et al.* Adaptation of islets of Langerhans to pregnancy: β-cell growth, enhanced insulin secretion and the role of lactogenic hormones. *Horm. Metab. Res.* **29**, 301–307 (1997).

44. Banerjee, R. R. *et al.* Gestational Diabetes Mellitus From Inactivation of Prolactin Receptor and MafB in Islet β-Cells. *Diabetes* **65**, 2331–2341 (2016).

45. Le, T. N. *et al.* Prolactin Receptor Gene Polymorphisms Are Associated with Gestational Diabetes. *https://home.liebertpub.com/gtmb* **17**, 567–571 (2013).

46. Shrivastava, V. *et al.* Beta cell adaptation to pregnancy requires prolactin action on both beta and non-beta cells. *Sci. Reports 2021 111* **11**, 1–14 (2021).

47. Li, J. *et al.* Circulating prolactin concentrations and risk of type 2 diabetes in US women. *Diabetologia* **61**, 2549 (2018).

48. Balbach, L. *et al.* Serum prolactin concentrations as risk factor of metabolic syndrome or type 2 diabetes? *BMC Endocr. Disord.* **13**, 12 (2013).

49. Wagner, R. *et al.* Age-dependent association of serum prolactin with glycaemia and insulin sensitivity in humans. *Acta Diabetol.* **51**, 71–78 (2014).

50. Chirico, V. *et al.* Prolactin in obese children: a bridge between inflammation and metabolic-endocrine dysfunction. *Clin. Endocrinol. (Oxf).* **79**, 537–544 (2013).

51. What is diabetes? - Diabetes Canada. https://www.diabetes.ca/about-diabetes/what-is-diabetes.

52. DiMeglio, L. A. *et al.* Type 1 diabetes. *Lancet (London, England)* **391**, 2449 (2018).

53. Sweeting, A. *et al.* A Clinical Update on Gestational Diabetes Mellitus. *Endocr. Rev.* **43**, 763–793 (2022).

54. Lain, K. Y. *et al.* Metabolic changes in pregnancy. *Clin. Obstet. Gynecol.* **50**, 938–948 (2007).

55. Costrini, N. V. *et al.* Relative effects of pregnancy, estradiol, and progesterone on plasma insulin and pancreatic islet insulin secretion. *J. Clin. Invest.* **50**, 992–999 (1971).

56. Møldrup, A. *et al.* Effects of sex and pregnancy hormones on growth hormone and prolactin receptor gene expression in insulin-producing cells. *Endocrinology* **133**, 1165–1172 (1993).

57. Homko, C. *et al.* Insulin Secretion during and after Pregnancy in Patients with Gestational Diabetes Mellitus. *J. Clin. Endocrinol. Metab.* **86**, 568–573 (2001).

58. Powe, C. E. *et al.* Augmented insulin secretory response in early pregnancy. *Diabetologia* **62**, 1445–1452 (2019).

59. Saravanan, P. *et al.* Gestational diabetes: opportunities for improving maternal and child health. *lancet. Diabetes Endocrinol.* **8**, 793–800 (2020).

60. Scholtens, D. M. *et al.* Hyperglycemia and adverse Pregnancy Outcome follow-up study (HAPO FUS): Maternal glycemia and childhood glucose metabolism. *Diabetes Care* **42**, 381–392 (2019).

61. Frayling, T. M. Genome–wide association studies provide new insights into type 2 diabetes aetiology. *Nat. Rev. Genet. 2007 89* **8**, 657–662 (2007).

62. Prentki, M. *et al.* Islet β cell failure in type 2 diabetes. *J. Clin. Invest.* **116**, 1802 (2006).

63. Al-Goblan, A. S. *et al.* Mechanism linking diabetes mellitus and obesity. *Diabetes, Metab. Syndr. Obes. Targets Ther.* **7**, 587 (2014).

64. Bjørbaek, C. *et al.* Leptin signaling in the central nervous system and the periphery. *Recent Prog. Horm. Res.* **59**, 305–331 (2004).

65. Ahrén, B. *et al.* Acylation stimulating protein stimulates insulin secretion. *Int. J. Obes. 2003 279* **27**, 1037–1043 (2003).

66. Cerf, M. E. Beta Cell Dysfunction and Insulin Resistance. *Front. Endocrinol. (Lausanne).* **4**, (2013).

67. Pinhas-Hamiel, O. *et al.* Acute and chronic complications of type 2 diabetes mellitus in children and adolescents. *Lancet* **369**, 1823–1831 (2007).

68. Petrie, J. R. *et al.* Implications of genome wide association studies for the understanding of type 2 diabetes pathophysiology. *Biochem. Pharmacol.* **81**, 471–477 (2011).

69. Voight, B. F. *et al.* Twelve type 2 diabetes susceptibility loci identified through large-scale association analysis. *Nat. Genet.* **42**, 579 (2010).

70. McCarthy, M. I. Genomics, Type 2 Diabetes, and Obesity. *N. Engl. J. Med.* **363**, 2339–2350 (2010).

71. Florez, J. C. Newly identified loci highlight beta cell dysfunction as a key cause of type 2 diabetes: Where are the insulin resistance genes? *Diabetologia* **51**, 1100–1110 (2008).

72. Punthakee, Z. *et al.* Definition, Classification and Diagnosis of Diabetes, Prediabetes and Metabolic Syndrome. *Can. J. diabetes* **42 Suppl 1**, S10–S15 (2018).

73. Turner, R. *et al.* Tight blood pressure control and risk of macrovascular and microvascular complications in type 2 diabetes: UKPDS 38. *BMJ Br. Med. J.* **317**, 703 (1998).

74. Bancej, C. *et al.* Trends and projections of obesity among Canadians. *Heal. Promot. Chronic Dis. Prev. Canada Res. Policy Pract.* **35**, 109 (2015).

75. Xavier, G. D. S. The Cells of the Islets of Langerhans. *J. Clin. Med.* **7**, 54 (2018).

76. Baron, M. *et al.* A Single-Cell Transcriptomic Map of the Human and Mouse Pancreas Reveals Inter- and Intra-cell Population Structure. *Cell Syst.* **3**, 346-360.e4 (2016).

77. Dai, C. *et al.* Islet-enriched gene expression and glucose-induced insulin secretion in human and mouse islets. *Diabetologia* **55**, 707–718 (2012).

78. Cabrera, O. *et al.* The unique cytoarchitecture of human pancreatic islets has implications for islet cell function. *Proc. Natl. Acad. Sci. U. S. A.* **103**, 2334–2339 (2006).

79. Moede, T. *et al.* Alpha cell regulation of beta cell function. *Diabetologia* **63**, 2064 (2020).

80. Arrojo e Drigo, R. *et al.* Structural basis for delta cell paracrine regulation in pancreatic islets. *Nat. Commun.* **10**, (2019).

81. Melloul, D. *et al.* Regulation of insulin gene transcription. *Diabetologia* **45**, 309–326 (2002).

82. Weiss, M. *et al.* Insulin Biosynthesis, Secretion, Structure, and Structure-Activity Relationships. *Endotext* (2014).

83. Van Lommel, L. *et al.* Probe-Independent and Direct Quantification of Insulin mRNA and Growth Hormone mRNA in Enriched Cell Preparations. *Diabetes* **55**, 3214–3220 (2006).

84. Harper, M. E. *et al.* Localization of the human insulin gene to the distal end of the short arm of chromosome 11. *Proc. Natl. Acad. Sci. U. S. A.* **78**, 4458 (1981).

85. Babaya, N. *et al.* A new model of insulin-deficient diabetes: Male NOD mice with a single copy of Ins1 and no Ins2. *Diabetologia* **49**, 1222–1228 (2006).

86. Mauvais-Jarvis, F. *et al.* The Role of Estrogens in Control of Energy Balance and Glucose Homeostasis. *Endocr. Rev.* **34**, 309 (2013).

87. Tramunt, B. *et al.* Sex differences in metabolic regulation and diabetes susceptibility. *Diabetologia* **63**, 453 (2020).

88. Ebrahim, N. *et al.* PDX1 is the cornerstone of pancreatic β-cell functions and identity. *Front. Mol. Biosci.* **9**, 1091757 (2022).

89. Kaneto, H. *et al.* PDX-1 and MafA play a crucial role in pancreatic beta-cell differentiation and maintenance of mature beta-cell function. *Endocr. J.* **55**, 235–252 (2008).

90. Fagerberg, L. *et al.* Analysis of the human tissue-specific expression by genome-wide integration of transcriptomics and antibody-based proteomics. *Mol. Cell. Proteomics* **13**, 397–406 (2014).

91. Taylor, B. L. *et al.* Nkx6.1 Is Essential for Maintaining the Functional State of Pancreatic Beta Cells. *Cell Rep.* **4**, 1262–1275 (2013).

92. Salinno, C. *et al.* β-Cell Maturation and Identity in Health and Disease. *Int. J. Mol. Sci.* **20**, (2019).

93. Poitout, V. *et al.* Regulation of the Insulin Gene by Glucose and Fatty Acids. *J. Nutr.* **136**, 873 (2006).

94. Hagman, D. K. *et al.* Palmitate inhibits insulin gene expression by altering PDX-1 nuclear localization and reducing MafA expression in isolated rat islets of Langerhans. *J. Biol. Chem.* **280**, 32413–32418 (2005).

95. Rutter, G. A. Insulin secretion: Feed-forward control of insulin biosynthesis. *Curr. Biol.* **9**, R443–R445 (1999).

96. Nielsen, J. H. *et al.* Regulation of beta-cell mass by hormones and growth factors. *Diabetes* **50**, S25-9 (2001).

97. Wong, W. P. S. *et al.* Extranuclear estrogen receptor-α stimulates NeuroD1 binding to the insulin promoter and favors insulin synthesis. *Proc. Natl. Acad. Sci. U. S. A.* (2010) doi:10.1073/pnas.0914501107.

98. Rorsman, P. *et al.* Insulin granule dynamics in pancreatic beta cells. *Diabetol. 2003 468*

46, 1029–1045 (2003).

99. Weir, G. C. *et al.* Reduced glucose-induced first-phase insulin release is a danger signal that predicts diabetes. *J. Clin. Invest.* **131**, (2021).

100. Gerich, J. E. Is Reduced First-Phase Insulin Release the Earliest Detectable Abnormality in Individuals Destined to Develop Type 2 Diabetes? *Diabetes* **51**, S117–S121 (2002).

101. Jansson, L. *et al.* Pancreatic islet blood flow and its measurement. *Ups. J. Med. Sci.* **121**, 81 (2016).

102. Suckale, J. *et al.* Pancreas islets in metabolic signaling--focus on the beta-cell. *Front. Biosci.* **13**, 7156–7171 (2008).

103. Johnson, J. H. *et al.* The high Km glucose transporter of islets of Langerhans is functionally similar to the low affinity transporter of liver and has an identical primary sequence. *J. Biol. Chem.* **265**, 6548–6551 (1990).

104. Xu, J. *et al.* The role of pyruvate carboxylase in insulin secretion and proliferation in rat pancreatic beta-cells. *Diabetologia* **51**, 2022 (2008).

105. Khan, A. *et al.* Quantifying the carboxylation of pyruvate in pancreatic islets. *J. Biol. Chem.* **271**, 2539–2542 (1996).

106. Liu, Y. Q. *et al.* β-Cell Adaptation to Insulin Resistance. *J. Biol. Chem.* **277**, 39163–39168 (2002).

107. Newsholme, P. *et al.* Amino acid metabolism, insulin secretion and diabetes. *Biochem. Soc. Trans.* **35**, 1180–1186 (2007).

108. Newsholme, P. *et al.* Nutritional Regulation of Insulin Secretion: Implications for Diabetes. *Clin. Biochem. Rev.* **33**, 35 (2012).

109. Berne, C. The metabolism of lipids in mouse pancreatic islets. The biosynthesis of

triacylglycerols and phospholipids. *Biochem. J.* **152**, 667 (1975).

110. Haber, E. P. *et al.* New Insights into Fatty Acid Modulation of Pancreatic β-Cell Function. *Int. Rev. Cytol.* **248**, 1–41 (2006).

111. Deeney, J. T. *et al.* Acute stimulation with long chain acyl-CoA enhances exocytosis in insulin-secreting cells (HIT T-15 and NMRI β-cells). *J. Biol. Chem.* **275**, 9363–9368 (2000).

112. Kristinsson, H. *et al.* FFAR1 Is Involved in Both the Acute and Chronic Effects of Palmitate on Insulin Secretion. *Endocrinology* **154**, 4078–4088 (2013).

113. Ghislain, J. *et al.* The role and future of FFA1 as a therapeutic target. *Handb. Exp. Pharmacol.* **236**, 159–180 (2017).

114. Rady, B. *et al.* A FFAR1 full agonist restores islet function in models of impaired glucose-stimulated insulin secretion and diabetic non-human primates. *Front. Endocrinol. (Lausanne).* **13**, 1061688 (2022).

115. Aspinwall, C. A. *et al.* Insulin-stimulated insulin secretion in single pancreatic beta cells. *J. Biol. Chem.* **274**, 6360–6365 (1999).

116. Huypens, P. *et al.* Glucagon receptors on human islet cells contribute to glucose competence of insulin release. *Diabetologia* **43**, 1012–1019 (2000).

117. Svendsen, B. *et al.* Paracrine regulation of somatostatin secretion by insulin and glucagon in mouse pancreatic islets. *Diabetologia* **64**, 142–151 (2021).

118. Sutter-Dub, M. T. Rapid non-genomic and genomic responses to progestogens, estrogens, and glucocorticoids in the endocrine pancreatic B cell, the adipocyte and other cell types. *Steroids* **67**, 77–93 (2002).

119. Ropero, A. B. *et al.* Non-genomic actions of 17beta-oestradiol in mouse pancreatic beta-

cells are mediated by a cGMP-dependent protein kinase. *J. Physiol.* **521 Pt 2**, 397–407 (1999).

120. Brelje, T. C. *et al.* Effect of homologous placental lactogens, prolactins, and growth hormones on islet B-cell division and insulin secretion in rat, mouse, and human islets: implication for placental lactogen regulation of islet function during pregnancy. *Endocrinology* **132**, 879–887 (1993).
121. Holst, J. J. From the Incretin Concept and the Discovery of GLP-1 to Today's Diabetes Therapy. *Front. Endocrinol. (Lausanne).* **10**, 260 (2019).
122. Caumo, A. *et al.* First-phase insulin secretion: Does it exist in real life? Considerations on shape and function. *Am. J. Physiol. - Endocrinol. Metab.* **287**, 371–385 (2004).
123. Ugleholdt, R. *et al.* Prohormone convertase 1/3 is essential for processing of the glucose-dependent insulinotropic polypeptide precursor. *J. Biol. Chem.* **281**, 11050–11057 (2006).
124. Campbell, S. A. *et al.* Evidence for the existence and potential roles of intra-islet glucagon-like peptide-1. *Islets* **13**, 32–50 (2021).
125. Vasu, S. *et al.* Role of Endogenous GLP-1 and GIP in Beta Cell Compensatory Responses to Insulin Resistance and Cellular Stress. *PLoS One* **9**, (2014).
126. Ämmälä, C. *et al.* Calcium-independent potentiation of insulin release by cyclic AMP in single β-cells. *Nat. 1993 3636427* **363**, 356–358 (1993).
127. Wang, X. *et al.* Glucagon-Like Peptide-1 Regulates the Beta Cell Transcription Factor, PDX-1, in Insulinoma Cells. *Endocrinology* **140**, 4904–4907 (1999).
128. Hanyaloglu, A. C. *et al.* Regulation of GPCRs by endocytic membrane trafficking and its potential implications. *Annu. Rev. Pharmacol. Toxicol.* **48**, 537–568 (2008).
129. Kuna, R. S. *et al.* Glucagon-like peptide-1 receptor-mediated endosomal cAMP generation

promotes glucose-stimulated insulin secretion in pancreatic β-cells. *Am. J. Physiol. - Endocrinol. Metab.* **305**, 161–170 (2013).

130. Sonoda, N. *et al.* β-Arrestin-1 mediates glucagon-like peptide-1 signaling to insulin secretion in cultured pancreatic β cells. *Proc. Natl. Acad. Sci. U. S. A.* **105**, 6614–6619 (2008).

131. Holz, G. G. Epac: A New cAMP-Binding Protein in Support of Glucagon-Like Peptide-1 Receptor–Mediated Signal Transduction in the Pancreatic β-Cell. *Diabetes* **53**, 5 (2004).

132. Kashima, Y. *et al.* Critical Role of cAMP-GEFII·Rim2 Complex in Incretin-potentiated Insulin Secretion. *J. Biol. Chem.* **276**, 46046–46053 (2001).

133. Natalicchio, A. *et al.* Long-Term Exposure of Pancreatic β-Cells to Palmitate Results in SREBP-1C-Dependent Decreases in GLP-1 Receptor Signaling via CREB and AKT and Insulin Secretory Response. *Endocrinology* **157**, 2243–2258 (2016).

134. Xu, G. *et al.* Downregulation of GLP-1 and GIP Receptor Expression by HyperglycemiaPossible Contribution to Impaired Incretin Effects in Diabetes. *Diabetes* **56**, 1551–1558 (2007).

135. Grant, S. F. A. *et al.* Variant of transcription factor 7-like 2 (TCF7L2) gene confers risk of type 2 diabetes. *Nat. Genet.* **38**, 320–323 (2006).

136. Shu, L. *et al.* Decreased TCF7L2 protein levels in type 2 diabetes mellitus correlate with downregulation of GIP- and GLP-1 receptors and impaired beta-cell function. *Hum. Mol. Genet.* **18**, 2388 (2009).

137. Wang, H. *et al.* MAFA controls genes implicated in insulin biosynthesis and secretion. *Diabetologia* **50**, 348–358 (2007).

138. Gosmain, Y. *et al.* Pax6 Is Crucial for β-Cell Function, Insulin Biosynthesis, and Glucose-

Induced Insulin Secretion. *Mol. Endocrinol.* **26**, 696–709 (2012).

139. Bourouh, C. *et al.* The transcription factor E2F1 controls the GLP-1 receptor pathway in pancreatic β cells. *Cell Rep.* **40**, (2022).

140. Tyagi, S. *et al.* The peroxisome proliferator-activated receptor: A family of nuclear receptors role in various diseases. *J. Adv. Pharm. Technol. Res.* **2**, 236 (2011).

141. Gupta, D. *et al.* The role of peroxisome proliferator-activated receptor γ in pancreatic β cell function and survival: therapeutic implications for the treatment of type 2 diabetes mellitus. *Diabetes. Obes. Metab.* **12**, 1036 (2010).

142. Ahmadian, M. *et al.* PPARγ signaling and metabolism: the good, the bad and the future. *Nat. Med.* **19**, 557–566 (2013).

143. Nanjan, M. J. *et al.* Thiazolidinediones as antidiabetic agents: A critical review. *Bioorg. Chem.* **77**, 548–567 (2018).

144. Gremlich, S. *et al.* Pancreatic Islet Adaptation to Fasting Is Dependent on Peroxisome Proliferator-Activated Receptor α Transcriptional Up-Regulation of Fatty Acid Oxidation. *Endocrinology* **146**, 375–382 (2005).

145. Santini, E. *et al.* Effect of PPAR-gamma activation and inhibition on glucose-stimulated insulin release in INS-1e cells. *Diabetes* **53 Suppl 3**, (2004).

146. Nakamichi, Y. *et al.* PPAR-γ overexpression suppresses glucose-induced proinsulin biosynthesis and insulin release synergistically with pioglitazone in MIN6 cells. *Biochem. Biophys. Res. Commun.* **306**, 832–836 (2003).

147. Maida, A. *et al.* Metformin regulates the incretin receptor axis via a pathway dependent on peroxisome proliferator-activated receptor-α in mice. *Diabetologia* **54**, 339–349 (2011).

148. Gupta, D. *et al.* Physiologic and Pharmacologic Modulation of Glucose-Dependent

Insulinotropic Polypeptide (GIP) Receptor Expression in β-Cells by Peroxisome Proliferator–Activated Receptor (PPAR)-γ SignalingPossible Mechanism for the GIP Resistance in Type 2 Diabetes. *Diabetes* **59**, 1445–1450 (2010).

149. Hardy, O. T. *et al.* What causes the insulin resistance underlying obesity? *Curr. Opin. Endocrinol. Diabetes. Obes.* **19**, 81 (2012).

150. McLaughlin, T. *et al.* Preferential Fat Deposition in Subcutaneous Versus Visceral Depots Is Associated with Insulin Sensitivity. *J. Clin. Endocrinol. Metab.* **96**, E1756 (2011).

151. Gabriely, I. *et al.* Removal of Visceral Fat Prevents Insulin Resistance and Glucose Intolerance of Aging. *Diabetes* **51**, 2951–2958 (2002).

152. Sonagra, A. D. *et al.* Normal Pregnancy- A State of Insulin Resistance. *J. Clin. Diagn. Res.* **8**, CC01 (2014).

153. Beamish, C. A. *et al.* An increase in immature β-cells lacking Glut2 precedes the expansion of β-cell mass in the pregnant mouse. *PLoS One* **12**, e0182256 (2017).

154. Van Assche, F. A. *et al.* A morphological study of the endocrine pancreas in human pregnancy. *Br. J. Obstet. Gynaecol.* **85**, 818–820 (1978).

155. Butler, A. E. *et al.* Adaptive changes in pancreatic beta cell fractional area and beta cell turnover in human pregnancy. *Diabetologia* **53**, 2167–2176 (2010).

156. Mosser, R. E. *et al.* High-fat diet-induced β-cell proliferation occurs prior to insulin resistance in C57Bl/6J male mice. *Am. J. Physiol. - Endocrinol. Metab.* **308**, E573 (2015).

157. Gupta, D. *et al.* Temporal characterization of β cell-adaptive and -maladaptive mechanisms during chronic high-fat feeding in C57BL/6NTac mice. *J. Biol. Chem.* **292**, 12449–12459 (2017).

158. Butler, A. E. *et al.* Beta-cell deficit and increased beta-cell apoptosis in humans with type

2 diabetes. *Diabetes* **52**, 102–110 (2003).

159. Hanley, S. C. *et al.* β-Cell Mass Dynamics and Islet Cell Plasticity in Human Type 2 Diabetes. *Endocrinology* **151**, 1462–1472 (2010).

160. Weir, G. C. *et al.* Five Stages of Evolving Beta-Cell Dysfunction During Progression to Diabetes. *Diabetes* **53**, S16–S21 (2004).

161. Rask-Madsen, C. *et al.* Tissue-specific insulin signaling, metabolic syndrome and cardiovascular disease. *Arterioscler. Thromb. Vasc. Biol.* **32**, 2052 (2012).

162. Kahn, C. R. Insulin resistance, insulin insensitivity, and insulin unresponsiveness: A necessary distinction. *Metab. - Clin. Exp.* **27**, 1893–1902 (1978).

163. Ferrannini, E. *et al.* Insulin resistance and hypersecretion in obesity. European Group for the Study of Insulin Resistance (EGIR). *J. Clin. Invest.* **100**, 1166 (1997).

164. Fonseca, S. G. *et al.* Endoplasmic reticulum stress and pancreatic beta cell death. *Trends Endocrinol. Metab.* **22**, 266 (2011).

165. Evans-Molina, C. *et al*. Lost in Translation: ER Stress and the Decline of β-cell Health in Diabetes Mellitus. *Diabetes. Obes. Metab.* **15**, 159 (2013).

166. Papa, F. R. Endoplasmic Reticulum Stress, Pancreatic β-Cell Degeneration, and Diabetes. *Cold Spring Harb. Perspect. Med.* **2**, (2012).

167. Kim, M. K. *et al.* Endoplasmic Reticulum Stress and Insulin Biosynthesis: A Review. *Exp. Diabetes Res.* **2012**, (2012).

168. Adams, C. J. *et al.* Structure and Molecular Mechanism of ER Stress Signaling by the Unfolded Protein Response Signal Activator IRE1. *Front. Mol. Biosci.* **0**, 11 (2019).

169. Sano, R. *et al.* ER stress-induced cell death mechanisms. *Biochim. Biophys. Acta* **1833**, 3460–3470 (2013).

170. Cory, S. *et al.* The Bcl2 family: regulators of the cellular life-or-death switch. *Nat. Rev. Cancer 2002 29* **2**, 647–656 (2002).

171. Tait, S. W. G. *et al.* Mitochondria and cell death: outer membrane permeabilization and beyond. *Nat. Rev. Mol. Cell Biol. 2010 119* **11**, 621–632 (2010).

172. Gao, C. *et al.* Significance of Increased Apoptosis and Bax Expression in Human Small Intestinal Adenocarcinoma. *J. Histochem. Cytochem.* **57**, 1139 (2009).

173. Oyadomari, S. *et al.* Roles of CHOP/GADD153 in endoplasmic reticulum stress. *Cell Death Differ. 2004 114* **11**, 381–389 (2003).

174. Jonas, J. C. *et al.* Glucose regulation of islet stress responses and β-cell failure in type 2 diabetes. *Diabetes, Obes. Metab.* **11**, 65–81 (2009).

175. Jetton, T. L. *et al.* Enhanced β-cell mass without increased proliferation following chronic mild glucose infusion. *Am. J. Physiol. - Endocrinol. Metab.* **294**, 679–687 (2008).

176. Pascoe, J. *et al.* Free Fatty Acids Block Glucose-Induced β-Cell Proliferation in Mice by Inducing Cell Cycle Inhibitors p16 and p18. *Diabetes* **61**, 632–641 (2012).

177. Jonas, J. C. *et al.* Chronic hyperglycemia triggers loss of pancreatic β cell differentiation in an animal model of diabetes. *J. Biol. Chem.* **274**, 14112–14121 (1999).

178. Klein, S. *et al.* Why Does Obesity Cause Diabetes? *Cell Metab.* **34**, 11 (2022).

179. Yaney, G. C. *et al.* Fatty acid metabolism and insulin secretion in pancreatic beta cells. *Diabetologia* **46**, 1297–1312 (2003).

180. Boden, G. *et al.* Acute lowering of plasma fatty acids lowers basal insulin secretion in diabetic and nondiabetic subjects. *Diabetes* **47**, 1609–1612 (1998).

181. Vivas, Y. *et al.* Early peroxisome proliferator-activated receptor gamma regulated genes involved in expansion of pancreatic beta cell mass. *BMC Med. Genomics* **4**, 86 (2011).

182. Hogh, K. L. N. *et al.* Overexpression of peroxisome proliferator-activated receptor α in pancreatic β-cells improves glucose tolerance in diet-induced obese mice. *Exp. Physiol.* **98**, 564–575 (2013).

183. Maedler, K. *et al.* Monounsaturated Fatty Acids Prevent the Deleterious Effects of Palmitate and High Glucose on Human Pancreatic β-Cell Turnover and Function. *Diabetes* **52**, 726–733 (2003).

184. Maedler, K. *et al.* Distinct Effects of Saturated and Monounsaturated Fatty Acids on β-Cell Turnover and Function. *Diabetes* **50**, 69–76 (2001).

185. Zhou, Y. P. *et al.* Long term exposure to fatty acids and ketones inhibits B-cell functions in human pancreatic islets of Langerhans. *J. Clin. Endocrinol. Metab.* **80**, 1584–1590 (1995).

186. Bollheimer, L. C. *et al.* Chronic exposure to free fatty acid reduces pancreatic beta cell insulin content by increasing basal insulin secretion that is not compensated for by a corresponding increase in proinsulin biosynthesis translation. *J. Clin. Invest.* **101**, 1094 (1998).

187. Boden, G. *et al.* Effects of a 48-h Fat Infusion on Insulin Secretion and Glucose Utilization. *Diabetes* **44**, 1239–1242 (1995).

188. Kashyap, S. *et al.* A Sustained Increase in Plasma Free Fatty Acids Impairs Insulin Secretion in Nondiabetic Subjects Genetically Predisposed to Develop Type 2 Diabetes. *Diabetes* **52**, 2461–2474 (2003).

189. Astiarraga, B. *et al.* Effects of acute NEFA manipulation on incretin-induced insulin secretion in participants with and without type 2 diabetes. *Diabetologia* **61**, 1829–1837 (2018).

190. Kang, Z. F. *et al.* Pharmacological reduction of NEFA restores the efficacy of incretin-based therapies through GLP-1 receptor signalling in the beta cell in mouse models of diabetes. *Diabetologia* **56**, 423 (2013).

191. Hodson, D. J. *et al.* Lipotoxicity disrupts incretin-regulated human β cellconnectivity. *J. Clin. Invest.* **123**, 4182 (2013).

192. Wang, Y. J. *et al.* Single-Cell Transcriptomics of the Human Endocrine Pancreas. *Diabetes* **65**, 3028 (2016).

193. Dalbøge, L. S. *et al.* Characterisation of Age-Dependent Beta Cell Dynamics in the Male db/db Mice. *PLoS One* **8**, 82813 (2013).

194. Tschen, S. I. *et al.* Age-Dependent Decline in β-Cell Proliferation Restricts the Capacity of β-Cell Regeneration in Mice. *Diabetes* **58**, 1312–1320 (2009).

195. Li, N. *et al.* Aging and stress induced β cell senescence and its implication in diabetes development. *Aging (Albany NY)* **11**, 9947 (2019).

196. Aguayo-Mazzucato, C. *et al.* β-cell aging markers have heterogeneous distribution and are induced by insulin resistance. *Cell Metab.* **25**, 898 (2017).

197. Aguayo-Mazzucato, C. *et al.* Acceleration of β-cell aging determines diabetes and senolysis improves disease outcomes. *Cell Metab.* **30**, 129 (2019).

198. Miller, W. L. *et al.* Structure and Evolution of the Growth Hormone Gene Family. *Endocr. Rev.* **4**, 97–130 (1983).

199. Ben-Jonathan, N. *et al.* What Can We Learn from Rodents about Prolactin in Humans? *Endocr. Rev.* **29**, 1 (2008).

200. Nagano, M. *et al.* Tissue distribution and regulation of rat prolactin receptor gene expression. Quantitative analysis by polymerase chain reaction. *J. Biol. Chem.* (1994)

doi:10.1016/s0021-9258(17)36838-2.

201. Hughes, E. *et al.* Participation of Akt, Menin, and p21 in Pregnancy-Induced β-Cell Proliferation. *Endocrinology* **152**, 847–855 (2011).

202. Devi, Y. S. *et al.* Regulation of Transcription Factors and Repression of Sp1 by Prolactin Signaling Through the Short Isoform of Its Cognate Receptor. *Endocrinology* **150**, 3327 (2009).

203. Binart, N. *et al.* Impact of prolactin receptor isoforms on reproduction. *Trends Endocrinol. Metab.* **21**, 362–368 (2010).

204. Scaglia, L. *et al.* Apoptosis contributes to the involution of β cell mass in the post partum rat pancreas. *Endocrinology* (1995) doi:10.1210/endo.136.12.7588296.

205. Weinhaus, A. J. *et al.* Glucokinase, hexokinase, glucose transporter 2, and glucose metabolism in islets during pregnancy and prolactin-treated islets in vitro: mechanisms for long term up-regulation of islets. *Endocrinology* **137**, 1640–1649 (1996).

206. Vasavada, R. C. *et al.* Targeted expression of placental lactogen in the beta cells of transgenic mice results in beta cell proliferation, islet mass augmentation, and hypoglycemia. *J. Biol. Chem.* **275**, 15399–15406 (2000).

207. Freemark, M. *et al.* Targeted deletion of the PRL receptor: effects on islet development, insulin production, and glucose tolerance. *Endocrinology* **143**, 1378–1385 (2002).

208. Ormandy, C. J. *et al.* Null mutation of the prolactin receptor gene produces multiple reproductive defects in the mouse. *Genes Dev.* **11**, 167–178 (1997).

209. Goyvaerts, L. *et al.* Prolactin Receptors and Placental Lactogen Drive Male Mouse Pancreatic Islets to Pregnancy-Related mRNA Changes. *PLoS One* **10**, e0121868 (2015).

210. Brooks, C. L. Molecular Mechanisms of Prolactin and Its Receptor. *Endocr. Rev.* **33**, 504

(2012).

211. Galsgaard, E. D. *et al.* Regulation of Prolactin Receptor (PRLR) Gene Expression in Insulin-producing Cells. *J. Biol. Chem.* **274**, 18686–18692 (1999).

212. Zhao, X. *et al.* Involvement of the STAT5-cyclin D/CDK4-pRb pathway in β-cell proliferation stimulated by prolactin during pregnancy. *Am. J. Physiol. - Endocrinol. Metab.* **316**, E135–E144 (2019).

213. Camaya, I. *et al.* Targeting the PI3K/Akt signaling pathway in pancreatic β-cells to enhance their survival and function: An emerging therapeutic strategy for type 1 diabetes. *J. Diabetes* **14**, 247 (2022).

214. Chamberlain, C. E. *et al.* Menin determines K-RAS proliferative outputs in endocrine cells. *J. Clin. Invest.* **124**, 4093 (2014).

215. Ikushima, Y. M. *et al.* MEK/ERK Signaling in β-Cells Bifunctionally Regulates β-Cell Mass and Glucose-Stimulated Insulin Secretion Response to Maintain Glucose Homeostasis. *Diabetes* **70**, 1519–1535 (2021).

216. Ruiz-Herrera, X. *et al.* Prolactin Promotes Adipose Tissue Fitness and Insulin Sensitivity in Obese Males. *Endocrinology* **158**, 56–68 (2017).

217. Ben-Jonathan, N. *et al.* Focus on prolactin as a metabolic hormone. *Trends Endocrinol. Metab.* **17**, 110–116 (2006).

218. Jackerott, M. *et al.* STAT5 Activity in Pancreatic β-Cells Influences the Severity of Diabetes in Animal Models of Type 1 and 2 Diabetes. *Diabetes* **55**, 2705–2712 (2006).

219. Makkar, G. *et al.* Lrrc55 is a novel prosurvival factor in pancreatic islets. *Am. J. Physiol. - Endocrinol. Metab.* **317**, E794–E804 (2019).

220. Pepin, M. E. *et al.* Prolactin receptor signaling regulates a pregnancy-specific

transcriptional program in mouse islets. *Endocrinology* (2019) doi:10.1210/en.2018-00991.

221. Landgraf, R. *et al.* Prolactin: A diabetogenic hormone. *Diabetol. 1977 132* **13**, 99–104 (1977).

222. Schernthaner, G. *et al.* Severe hyperprolactinaemia is associated with decreased insulin binding in vitro and insulin resistance in vivo. *Diabetologia* **28**, 138–142 (1985).

223. Tuzcu, A. *et al.* Evaluation of insulin sensitivity in hyperprolactinemic subjects by euglycemic hyperinsulinemic clamp technique. *Pituitary* **12**, 330–334 (2009).

224. Tuzcu, A. *et al.* Insulin sensitivity and hyperprolactinemia. *J. Endocrinol. Invest.* **26**, 341–346 (2003).

225. Guyda, H. J. *et al.* Serum Prolactin Levels in Humans from Birth to Adult Life. *Pediatr. Res. 1973 75* **7**, 534–540 (1973).

226. Heianza, Y. *et al.* Effect of Postmenopausal Status and Age at Menopause on Type 2 Diabetes and Prediabetes in Japanese Individuals: Toranomon Hospital Health Management Center Study 17 (TOPICS 17). *Diabetes Care* **36**, 4007 (2013).

227. Butte, N. F. Carbohydrate and lipid metabolism in pregnancy: normal compared with gestational diabetes mellitus. *Am. J. Clin. Nutr.* **71**, (2000).

228. Kelly, P. A. *et al.* Different forms of the prolactin receptor insights into the mechanism of prolactin action. *Trends Endocrinol. Metab.* **3**, 54–59 (1992).

229. Seif, F. *et al.* The role of JAK-STAT signaling pathway and its regulators in the fate of T helper cells. *Cell Commun. Signal. 2017 151* **15**, 1–13 (2017).

230. Parsons, J. A. *et al.* Adaptation of islets of Langerhans to pregnancy: increased islet cell proliferation and insulin secretion correlates with the onset of placental lactogen secretion.

Endocrinology **130**, 1459–1466 (1992).

231. Usman, T. O. *et al.* Beta-cell compensation and gestational diabetes. *J. Biol. Chem.* **299**, 105405 (2023).

232. Macotela, Y. *et al.* Time for a New Perspective on Prolactin in Metabolism. *Trends in Endocrinology and Metabolism* at https://doi.org/10.1016/j.tem.2020.01.004 (2020).

233. Papoutsis, Di. *et al.* A High-Fat Western Diet Attenuates Intestinal Changes in Mice with DSS-Induced Low-Grade Inflammation. *J. Nutr.* **152**, 758–769 (2022).

234. Cano, P. *et al.* Effect of a high-fat diet on 24-h pattern of circulating levels of prolactin, luteinizing hormone, testosterone, corticosterone, thyroid-stimulating hormone and glucose, and pineal melatonin content, in rats. *Endocrine* **33**, 118–125 (2008).

235. Speakman, J. *et al.* Animal models of obesity. *Obes. Rev.* **8**, 55–61 (2007).

236. Sato, A. *et al.* Antiobesity Effect of Eicosapentaenoic Acid in High-Fat/High-Sucrose Diet–Induced ObesityImportance of Hepatic Lipogenesis. *Diabetes* **59**, 2495–2504 (2010).

237. Kowalski, G. M. *et al.* Resolution of glucose intolerance in long-term high-fat, high-sucrose-fed mice. *J. Endocrinol.* **233**, 269–279 (2017).

238. Sears, B. *et al.* The role of fatty acids in insulin resistance. *Lipids Heal. Dis. 2015 141* **14**, 1–9 (2015).

239. Rorsman, P. *et al.* The cell physiology of biphasic insulin secretion. *News Physiol. Sci.* **15**, 72–77 (2000).

240. Komatsu, M. *et al.* Glucose-stimulated insulin secretion: A newer perspective. *J. Diabetes Investig.* **4**, 511 (2013).

241. Kim, H. *et al.* Mouse Cre-LoxP system: general principles to determine tissue-specific

roles of target genes. *Lab. Anim. Res.* **34**, 147 (2018).

242. Corbin, K. L. *et al.* A Practical Guide to Rodent Islet Isolation and Assessment Revisited. *Biol. Proced. Online 2021 231* **23**, 1–21 (2021).

243. Dula, S. B. *et al.* Evidence that low-grade systemic inflammation can induce islet dysfunction as measured by impaired calcium handling. *Cell Calcium* **48**, 133–142 (2010).

244. Huang, C. Wild-type offspring of heterozygous prolactin receptor-null female mice have maladaptive β-cell responses during pregnancy. *J. Physiol.* (2013) doi:10.1113/jphysiol.2012.244830.

245. Benedé-Ubieto, R. *et al.* Guidelines and Considerations for Metabolic Tolerance Tests in Mice. *Diabetes, Metab. Syndr. Obes. Targets Ther.* **13**, 439 (2020).

246. Fajardo, R. J. *et al.* A Review of Rodent Models of Type 2 Diabetic Skeletal Fragility. *J. Bone Miner. Res.* **29**, 1025–1040 (2014).

247. Clee, S. M. *et al.* The Genetic Landscape of Type 2 Diabetes in Mice. *Endocr. Rev.* **28**, 48–83 (2007).

248. Nagy, C. *et al.* Study of In Vivo Glucose Metabolism in High-fat Diet-fed Mice Using Oral Glucose Tolerance Test (OGTT) and Insulin Tolerance Test (ITT). *J. Vis. Exp.* **2018**, 56672 (2018).

249. Yeckel, C. W. *et al.* Validation of Insulin Sensitivity Indices from Oral Glucose Tolerance Test Parameters in Obese Children and Adolescents. *J. Clin. Endocrinol. Metab.* **89**, 1096–1101 (2004).

250. Soares, M. J. The prolactin and growth hormone families: Pregnancy-specific hormones/cytokines at the maternal-fetal interface. *Reprod. Biol. Endocrinol.* **2**, 51 (2004).

251. Alvarsson, M. *et al.* K-value and low insulin secretion in a non-obese white population: Predicted glucose tolerance after 25 years. *Diabetologia* **48**, 2262–2268 (2005).

252. Baeyens, L. *et al.* β-Cell Adaptation in Pregnancy. *Diabetes. Obes. Metab.* **18**, 63 (2016).

253. Able, A. A. *et al.* STAT5-Interacting Proteins: A Synopsis of Proteins that Regulate STAT5 Activity. *Biology (Basel).* **6**, (2017).

254. Auffret, J. *et al.* Defective prolactin signaling impairs pancreatic β-cell development during the perinatal period. *Am. J. Physiol. - Endocrinol. Metab.* **305**, E1309 (2013).

255. Speakman, J. R. Use of high-fat diets to study rodent obesity as a model of human obesity. *Int. J. Obes. 2019 438* **43**, 1491–1492 (2019).

256. Takahashi, M. *et al.* Effect of the Fat/Carbohydrate Ratio in the Diet on Obesity and Oral Glucose Tolerance in C57BL/6J Mice. *J. Nutr. Sci. Vitaminol. (Tokyo).* **45**, 583–593 (1999).

257. Lee, J. Y. *et al.* The transcription factors Stat5a/b are not required for islet development but modulate pancreatic β-cell physiology upon aging. *Biochim. Biophys. Acta* **1773**, 1455 (2007).

258. Prentki, M. *et al.* Nutrient-Induced Metabolic Stress, Adaptation, Detoxification, and Toxicity in the Pancreatic β-Cell. *Diabetes* **69**, 279–290 (2020).

259. Moffett, R. C. *et al.* Functional GIP receptors play a major role in islet compensatory response to high fat feeding in mice. *Biochim. Biophys. Acta - Gen. Subj.* **1850**, 1206–1214 (2015).

260. Burchfield, J. G. *et al.* High dietary fat and sucrose results in an extensive and time-dependent deterioration in health of multiple physiological systems in mice. *J. Biol. Chem.* **293**, 5731–5745 (2018).

261. Lee, J. Y. *et al.* RIP-Cre Revisited, Evidence for Impairments of Pancreatic β-Cell Function. *J. Biol. Chem.* **281**, 2649–2653 (2006).

262. Brereton, M. F. *et al.* Reversible changes in pancreatic islet structure and function produced by elevated blood glucose. *Nat. Commun.* **5**, (2014).

263. Cinti, F. *et al.* Evidence of β-Cell Dedifferentiation in Human Type 2 Diabetes. *J. Clin. Endocrinol. Metab.* **101**, 1044–1054 (2016).

264. Henquin, J. C. *et al.* Insulin, glucagon and somatostatin stores in the pancreas of subjects with type-2 diabetes and their lean and obese non-diabetic controls. *Sci. Reports 2017 71* **7**, 1–9 (2017).

265. Cataldo, L. R. *et al.* The MafA-target gene PPP1R1A regulates GLP1R-mediated amplification of glucose-stimulated insulin secretion in β-cells. *Metabolism.* **118**, 154734 (2021).

266. Yoshida, H. *et al.* A time-dependent phase shift in the mammalian unfolded protein response. *Dev. Cell* **4**, 265–271 (2003).

267. Hu, H. *et al.* The C/EBP homologous protein (CHOP) transcription factor functions in endoplasmic reticulum stress-induced apoptosis and microbial infection. *Front. Immunol.* **10**, 423124 (2019).

268. Porter, A. G. *et al.* Emerging roles of caspase-3 in apoptosis. *Cell Death Differ. 1999 62* **6**, 99–104 (1999).

269. Kee, N. *et al.* The utility of Ki-67 and BrdU as proliferative markers of adult neurogenesis. *J. Neurosci. Methods* **115**, 97–105 (2002).

270. Jo, J. *et al.* Size Distribution of Mouse Langerhans Islets. *Biophys. J.* **93**, 2655 (2007).

271. Kondegowda, N. G. *et al.* Lactogens protect rodent and human beta cells against

glucolipotoxicity-induced cell death through Janus kinase-2 (JAK2)/signal transducer and activator of transcription-5 (STAT5) signalling. *Diabetologia* **55**, 1721–1732 (2012).

272. Terra, L. F. *et al.* Recombinant human prolactin promotes human beta cell survival via inhibition of extrinsic and intrinsic apoptosis pathways. *Diabetologia* **54**, 1388–1397 (2011).

273. González, P. *et al.* Expression of Pancreatic Endocrine Markers by Prolactin-Treated Rat Bone Marrow Mesenchymal Stem Cells. *Transplant. Proc.* **42**, 566–569 (2010).

274. Thorpe, J. A. *et al.* IRE1α controls cyclin A1 expression and promotes cell proliferation through XBP-1. *Cell Stress Chaperones* **15**, 497 (2010).

275. Stamateris, R. E. *et al.* Adaptive β-cell proliferation increases early in high-fat feeding in mice, concurrent with metabolic changes, with induction of islet cyclin D2 expression. *Am. J. Physiol. - Endocrinol. Metab.* **305**, E149 (2013).

276. Bonner-Weir, S. *et al.* β-Cell Growth and Regeneration: Replication Is Only Part of the Story. *Diabetes* **59**, 2340 (2010).

277. Saisho, Y. *et al.* β-Cell mass and turnover in humans: Effects of obesity and aging. *Diabetes Care* **36**, 111–117 (2013).

278. Matschinsky, F. M. *et al.* Glucokinase as Glucose Sensor and Metabolic Signal Generator in Pancreatic β-Cells and Hepatocytes. *Diabetes* **39**, 647–652 (1990).

279. Liu, Y. Q. *et al.* beta-Cell adaptation to insulin resistance. Increased pyruvate carboxylase and malate-pyruvate shuttle activity in islets of nondiabetic Zucker fatty rats. *J. Biol. Chem.* **277**, 39163–39168 (2002).

280. Liu, Y. Q. *et al.* Enhanced rat β-cell proliferation in 60% pancreatectomized islets by increased glucose metabolic flux through pyruvate carboxylase pathway. *Am. J. Physiol. -*

Endocrinol. Metab. **288**, (2005).

281. Farfari, S. *et al.* Glucose-regulated anaplerosis and cataplerosis in pancreatic beta-cells: possible implication of a pyruvate/citrate shuttle in insulin secretion. *Diabetes* **49**, 718–726 (2000).

282. Laybutt, D. R. *et al.* Critical Reduction in β-Cell Mass Results in Two Distinct Outcomes over Time. *J. Biol. Chem.* **278**, 2997–3005 (2003).

283. Bartoov-Shifman, R. *et al.* Regulation of the gene encoding GPR40, a fatty acid receptor expressed selectively in pancreatic β Cells. *J. Biol. Chem.* **282**, 23561–23571 (2007).

284. Bensellam, M. *et al.* Mechanisms of β-cell dedifferentiation in diabetes: recent findings and future research directions. *J. Endocrinol.* **236**, R109–R143 (2018).

285. Muller, D. R. P. *et al.* Effects of GLP-1 agonists and SGLT2 inhibitors during pregnancy and lactation on offspring outcomes: a systematic review of the evidence. *Front. Endocrinol. (Lausanne).* **14**, 1215356 (2023).

286. Shirakawa, J. *et al.* E2F1 transcription factor mediates a link between fat and islets to promote β cell proliferation in response to acute insulin resistance. *Cell Rep.* **41**, 111436 (2022).

287. Chen, Y. *et al.* High-fat diet induces early-onset diabetes in heterozygous Pax6 mutant mice. *Diabetes. Metab. Res. Rev.* **30**, 467–475 (2014).

288. Huang, T. *et al.* Interaction of Diet/Lifestyle Intervention and TCF7L2 Genotype on Glycemic Control and Adiposity among Overweight or Obese Adults: Big Data from Seven Randomized Controlled Trials Worldwide. *Heal. Data Sci.* **2021**, (2021).

289. Nanbu-Wakao, R. *et al.* Prolactin enhances CCAAT enhancer-binding protein-beta (C/EBP beta) and peroxisome proliferator-activated receptor gamma (PPAR gamma)

messenger RNA expression and stimulates adipogenic conversion of NIH-3T3 cells. *Mol. Endocrinol.* **14**, 307–316 (2000).

290. Kawasaki, F. *et al.* Structural and functional analysis of pancreatic islets preserved by pioglitazone in db/db mice. *Am. J. Physiol. - Endocrinol. Metab.* **288**, 510–518 (2005).

291. Matsui, J. *et al.* Pioglitazone Reduces Islet Triglyceride Content and Restores Impaired Glucose-Stimulated Insulin Secretion in Heterozygous Peroxisome Proliferator–Activated Receptor-γ–Deficient Mice on a High-Fat Diet. *Diabetes* **53**, 2844–2854 (2004).

292. Ishida, H. *et al.* Pioglitazone Improves Insulin Secretory Capacity and Prevents the Loss of β-Cell Mass in Obese Diabetic db/db Mice: Possible Protection of β Cells from Oxidative Stress. *Metabolism.* **53**, 488–494 (2004).

293. Rawn, S. M. *et al.* Pregnancy Hyperglycemia in Prolactin Receptor Mutant, but Not Prolactin Mutant, Mice and Feeding-Responsive Regulation of Placental Lactogen Genes Implies Placental Control of Maternal Glucose Homeostasis. *Biol. Reprod.* **93**, 1–12 (2015).

294. Magnuson, M. A. *et al.* Pancreas-specific Cre driver lines and considerations for their prudent use. *Cell Metab.* **18**, 9 (2013).

295. Liu, Y. *et al.* Tamoxifen-Independent Recombination in the RIP-CreER Mouse. *PLoS One* **5**, e13533 (2010).

296. Lin, X. *et al.* Dysregulation of insulin receptor substrate 2 in β cells and brain causes obesity and diabetes. *J. Clin. Invest.* **114**, 908 (2004).

297. Wicksteed, B. *et al.* Conditional Gene Targeting in Mouse Pancreatic β-Cells: Analysis of Ectopic Cre Transgene Expression in the Brain. *Diabetes* **59**, 3090 (2010).

298. Kubota, N. *et al.* Insulin receptor substrate 2 plays a crucial role in β cells and the

hypothalamus. *J. Clin. Invest.* **114**, 917 (2004).

299. Choudhury, A. I. *et al.* The role of insulin receptor substrate 2 in hypothalamic and β cell function. *J. Clin. Invest.* **115**, 940 (2005).

300. Gannon, M. *et al.* Mosaic Cre-Mediated Recombination in Pancreas Using the pdx-1 Enhancer/Promoter. (2000) doi:10.1002/(SICI)1526-968X(200002)26:2.

301. Vooijs, M. *et al.* A highly efficient ligand-regulated Cre recombinase mouse line shows that LoxP recombination is position dependent. *EMBO Rep.* **2**, 292–297 (2001).

302. Reinert, R. B. *et al.* Tamoxifen-Induced Cre-loxP Recombination Is Prolonged in Pancreatic Islets of Adult Mice. *PLoS One* **7**, e33529 (2012).

303. Dorrell, C. *et al.* Human islets contain four distinct subtypes of β cells. *Nat. Commun. 2016 71* **7**, 1–9 (2016).

304. Loonstra, A. *et al.* Growth inhibition and DNA damage induced by Cre recombinase in mammalian cells. *Proc. Natl. Acad. Sci. U. S. A.* **98**, 9209–9214 (2001).

305. Roos, W. P. *et al.* DNA damage-induced cell death: From specific DNA lesions to the DNA damage response and apoptosis. *Cancer Lett.* **332**, 237–248 (2013).

306. Azqueta, A. *et al.* The essential comet assay: A comprehensive guide to measuring DNA damage and repair. *Arch. Toxicol.* **87**, 949–968 (2013).

307. Gremlich, S. *et al.* Dexamethasone Induces Posttranslational Degradation of GLUT2 and Inhibition of Insulin Secretion in Isolated Pancreatic β Cells: COMPARISON WITH THE EFFECTS OF FATTY ACIDS. *J. Biol. Chem.* **272**, 3216–3222 (1997).

308. Ruijter, J. M. *et al.* Removal of artifact bias from qPCR results using DNA melting curve analysis. *FASEB J.* **33**, 14542–14555 (2019).

309. Campbell, J. E. *et al.* TCF1 links GIPR signaling to the control of beta cell function and

survival. *Nat. Med. 2015 221* **22**, 84–90 (2015).

310. Diaz-Santana, M. V. *et al.* Persistence of Risk for Type 2 Diabetes After Gestational Diabetes Mellitus. *Diabetes Care* **45**, 864 (2022).

Supplementary Tables and Figures

Gene	Sense/Anti-Sense	Sequence 5' →3'

Bax	Sense	GGAGATGAACTGGATAGCAATATGG
	Anti-Sense	GTTTGCTAGCAAAGTAGAAGAGGGC
Bcl-2	Sense	GGGGTCATGTGTGTGGAGAG
	Anti-Sense	TCCACAAAGGCATCCCAGC
Chop	Sense	TCTTGAGCCTAACACGTCGAT
	Anti-Sense	CCAGGTTCTCTCTCCTCAGGT
E2f1	Sense	GGTGGGGCTGATATTTGAACTG
	Anti-Sense	GCCTCCGTTTCACCTCCAAC
Epac1	Sense	CTGTCTCTGCCCTGTTCCTG
	Anti-Sense	CTTCTGCTCCTTGAGGTGGG
Epac2	Sense	CCTGCCTGGATAAAAGGCCG
	Anti-Sense	TAACTCCTTTCAGCCGCGTG
Ffar1	Sense	GGGCATCAACATACCCGTGA
	Anti-Sense	GAGAAACTGAGACGGGCAGG
Gck	Sense	GAAAGCTGCTGCGGAACAC
	Anti-Sense	GCCAGGATCTGCTCTACCTTT
Gipr	Sense	TGGCCAGAGTTTCCATCACC
	Anti-Sense	CTCAGAGTCTGTCTCCGCCC
Glp-1r	Sense	TTCACTTCCTTCCAGGGCTTG
	Anti-Sense	CTGCTGGTGGGACACTTGAG
Glut2	Sense	ATCGCTCCAACCACACTCAG
	Anti-Sense	GCTGAGGCCAGCAATCTGAC
Ins1	Sense	GGCCAAACAGCAAAGTCCA
	Anti-Sense	CACTAAGGGCTGGGGGTTACT
Ins2	Sense	CACCCAGGCTTTTGTCAAGC
	Anti-Sense	GCTCCAGTTGTGCCACTTGT
Ire1α	Sense	CAACCCTACCTACACGGTGG
	Anti-Sense	AGGATGGTTGCCCTCAGAGA
Lrrc55	Sense	TTGCTGAAGTGGCTGCGGAA
	Anti-Sense	GTCAGAGTCAGGTGGCAGGC
Mafa	Sense	AGCGCTTCTCCGACGACCAG
	Anti-Sense	GGCCCGCCAACTTCTCGTAT
Neurod1	Sense	CAGCATCAATGGCAACTTCT
	Anti-Sense	GAAGATTGATCCGTGGCTTT
Nkx6.1	Sense	CTGGACAGCAAATCTTCGCC
	Anti-Sense	TCTGGAACCAGACCTTGACCT
Pax6	Sense	AGAAGTGTGGGAACCAGCG
	Anti-Sense	TGGTTAAAGTCTTCTGCCTGTGA
Pc	Sense	CTGTTCCCTGTCAGTGGAGG
	Anti-Sense	GGTAGATGTTAGCTCCGCCC
Pdx1	Sense	GCTCCCTTTCCCGTGGATG
	Anti-Sense	GTGTAAGCACCTCCTGCCC
Pparg	Sense	ACGTTCTGACAGGACTGTGT
	Anti-Sense	TGTGTCAACCATGGTAATTTCAGT
***Prlr*-L**	Sense	TGAGGACGAGCGGCTAATG
	Anti-Sense	GGTGTGTGGGTTTAACACCTTGA

***Prlr*-S**	Sense	GGCTCTGATAGAGCTCCCTG
	Anti-Sense	AGAAGCGTTCTTTAGCTTGAGG
Ppa1	Sense	CACTGCCGACAGATGTGGAT
	Anti-Sense	AACAGCTCGTGTTCCAGAGG
Tcf7	Sense	TACATGGAGAAGCCGAGGGA
	Anti-Sense	GCCTTCAGGCCGTCCTCT
Tcf7l2	Sense	CCATATTACCCGCTGTCGCC
	Anti-Sense	ACAGGCTGACCTTGCTGTG
***Xbp1*-S**	Sense	GCTTGGGAATGGACACGCT
	Anti-Sense	CACCTGCTGCGGACTCA
***Xbp1*-U**	Sense	CTGAGTCCGCAGCAGGTG
	Anti-Sense	GGCAACAGTGTCAGAGTCCA

Supplemental Table 1. Sense and Anti-Sense Primers used for RTqPCR

Sense and anti-sense primer sequences (5' → 3') for mRNA expression measured using RTqPCR.

Target	**Primary antibody Source**	**Primary antibody Dilution**	**Secondary antibody Target**	**Secondary antibody Source**	**Secondary antibody Dilution**
pSTAT5	Rabbit (CS #4322)	[1:50]	Rabbit	Goat	[1:500]
Insulin	Guinea Pig	[1:25]	Guinea Pig	Goat	[1:500]

	(Dako IR002)				
Cleaved caspase 3 Insulin	Rabbit (Ab23023) Guinea Pig (Dako IR002)	[1:100] [1:25]	Rabbit Guinea Pig	Goat Goat	[1:500] [1:500]
Ki67 Insulin	Rabbit (Ab11580) Guinea Pig (Dako IR002)	[1:200] [1:25]	Rabbit Guinea Pig	Goat Goat	[1:500] [1:500]
Pdx1 Insulin	Rabbit (CS #5679) Guinea Pig (Dako IR002)	[1:300] [1:25]	Rabbit Guinea Pig	Goat Goat	[1:500] [1:500]

Supplemental Table 2. Immunofluorescence antibodies used

Sources of primary and secondary antibodies used for immunofluorescence.

Prlr-L

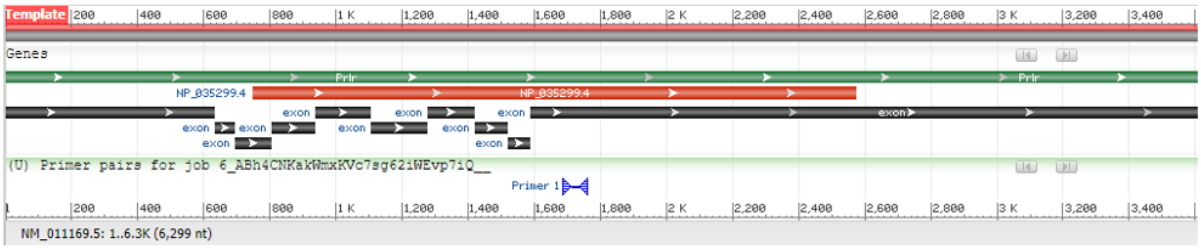

Prlr-S

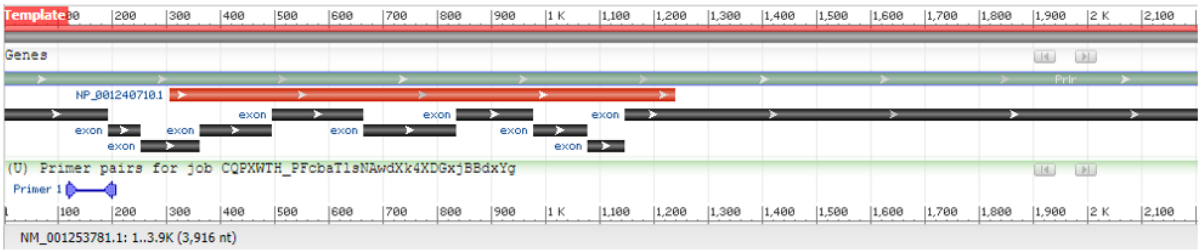

Supplemental Figure 1. Location of qPCR primers for *Prlr*-L (top) and P*rlr*-S (bottom)

Location of qPCR primers (blue) for *Prlr*-L (long) located on exon 10 and P*rlr*-S (short) spanning exon 1 and exon 2. Images were taken from Primer-BLAST (National Center for Biotechnology Information).

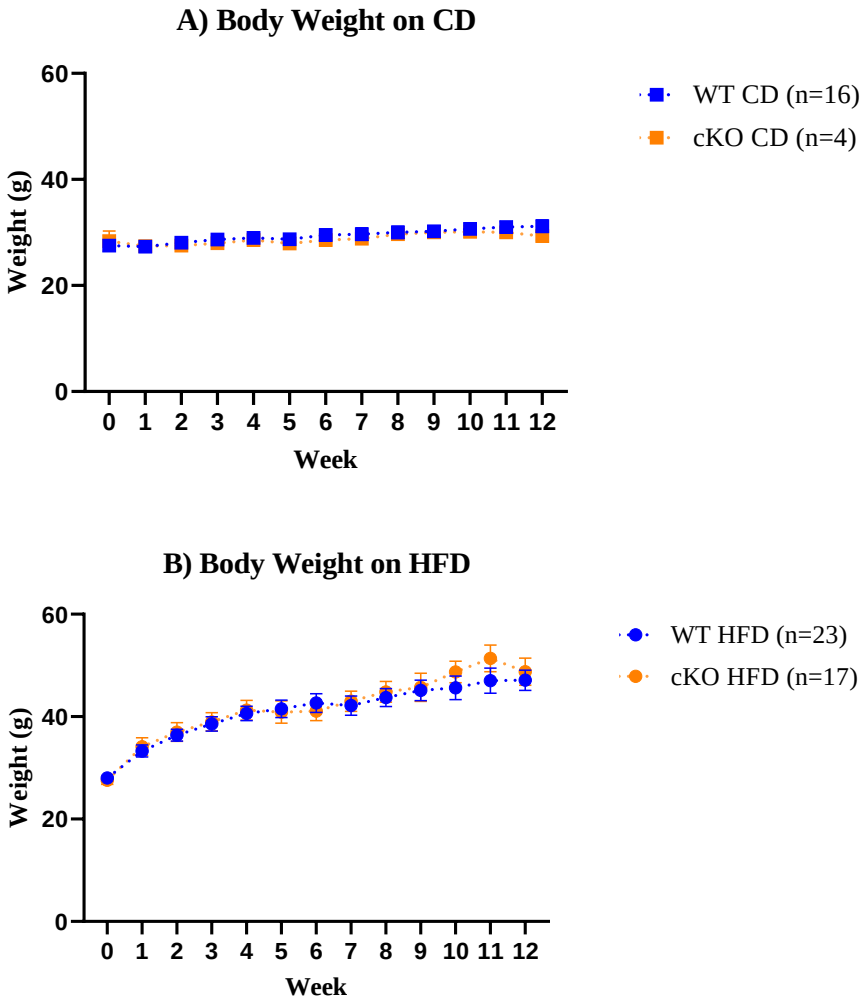

Supplemental Figure 2. Body weight of WT and cKO mice on either 12 weeks of A) CD or B) HFD

Multiparous mice were either placed on CD or HFD for 12 weeks. Results are expressed as mean ± SEM. Two-way ANOVA was performed to determine statistical significance. Carol Huang assisted with data collection.

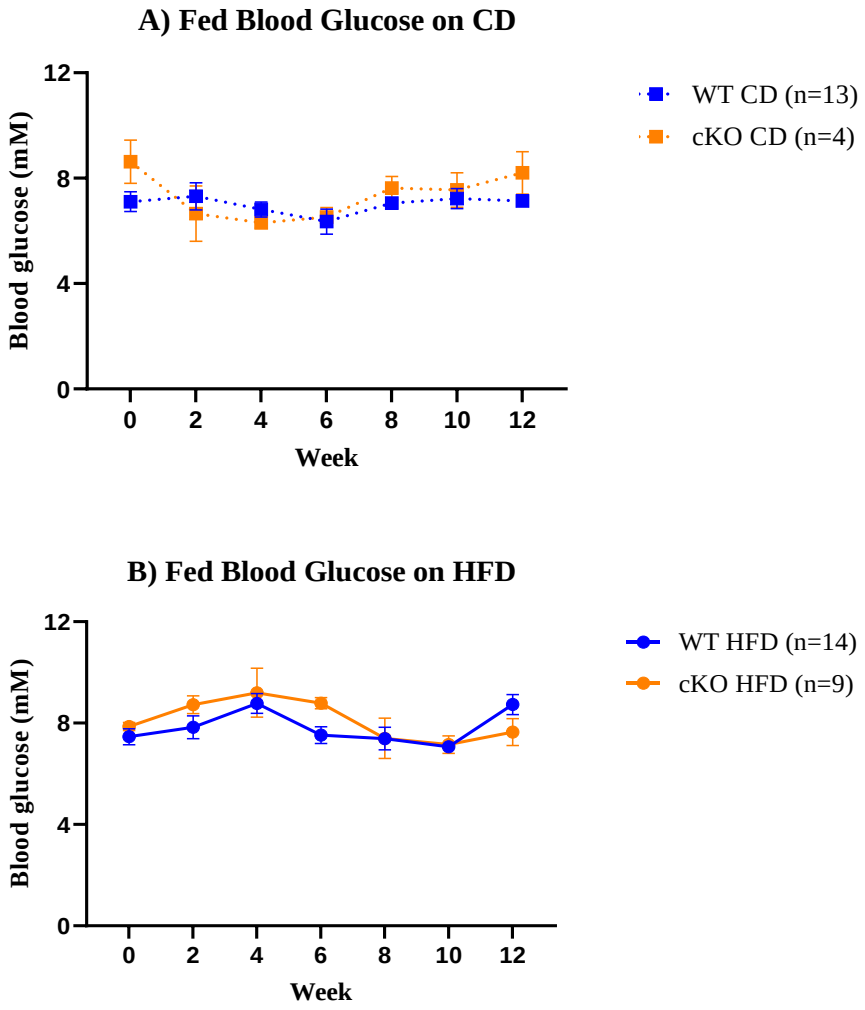

Supplemental Figure 3. Fed blood glucose of WT and cKO mice on either A) CD or B) HFD

Bi-weekly fed blood glucose measurements in multiparous mice during 12 weeks of HFD or CD. Blood glucose measurements were taken bi-weekly between 08:00-09:00. Results are expressed as mean ± SEM. Two-way ANOVA was performed to determine statistical significance. Carol Huang assisted with data collection.

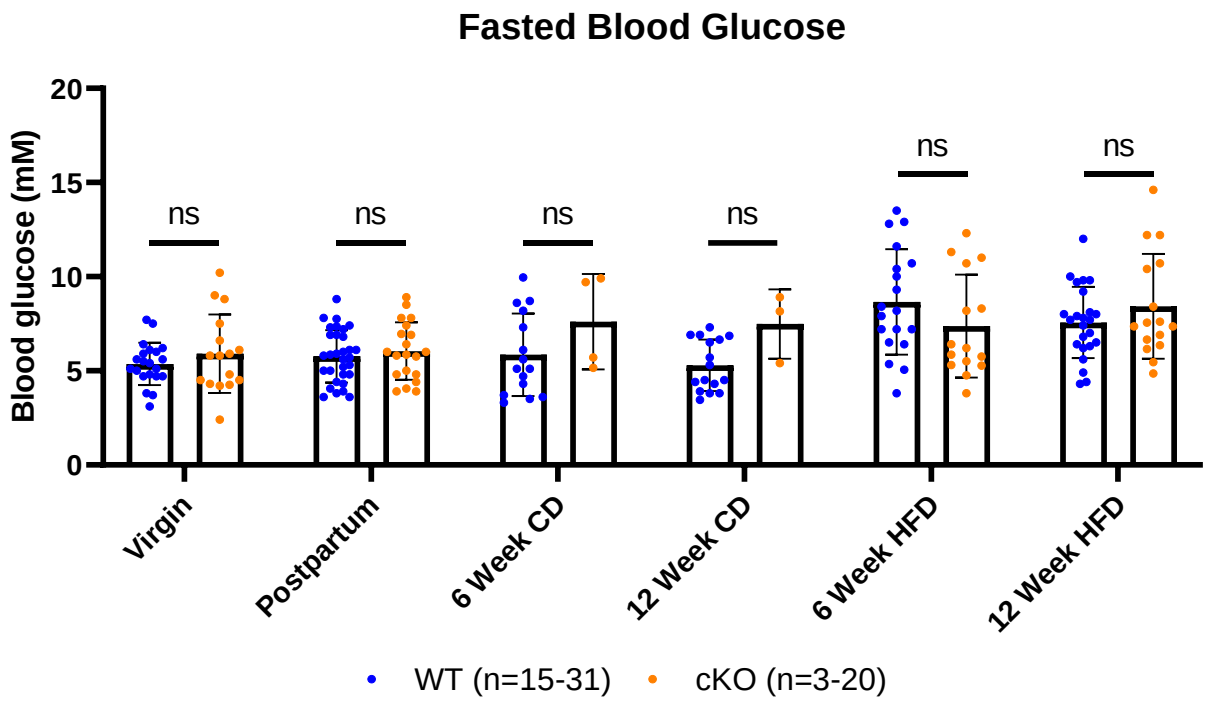

Supplemental Figure 4. Fasted blood glucose (FBG) between WT and cKO mice at timepoints: Virgin, Postpartum, Week 6 CD, Week 12 CD, Week 6 HFD, and Week 12 HFD

Fasted blood glucose (FBG) in WT and cKO mice at time points: Virgin, Postpartum, Week 6 CD, Week 12 CD, Week 6 HFD, and Week 12 HFD. FBG were measured at the start of glucose tolerance tests OGTT and IPGTT. Blood glucose measurements were taken after a 14-16 hour fast at 08:00-09:00. Results are expressed as mean $\pm$ SEM. ANOVA was performed, and statistical significance was determined using Tukey's post hoc test where ns = not significant. Carol Huang assisted with data collection.

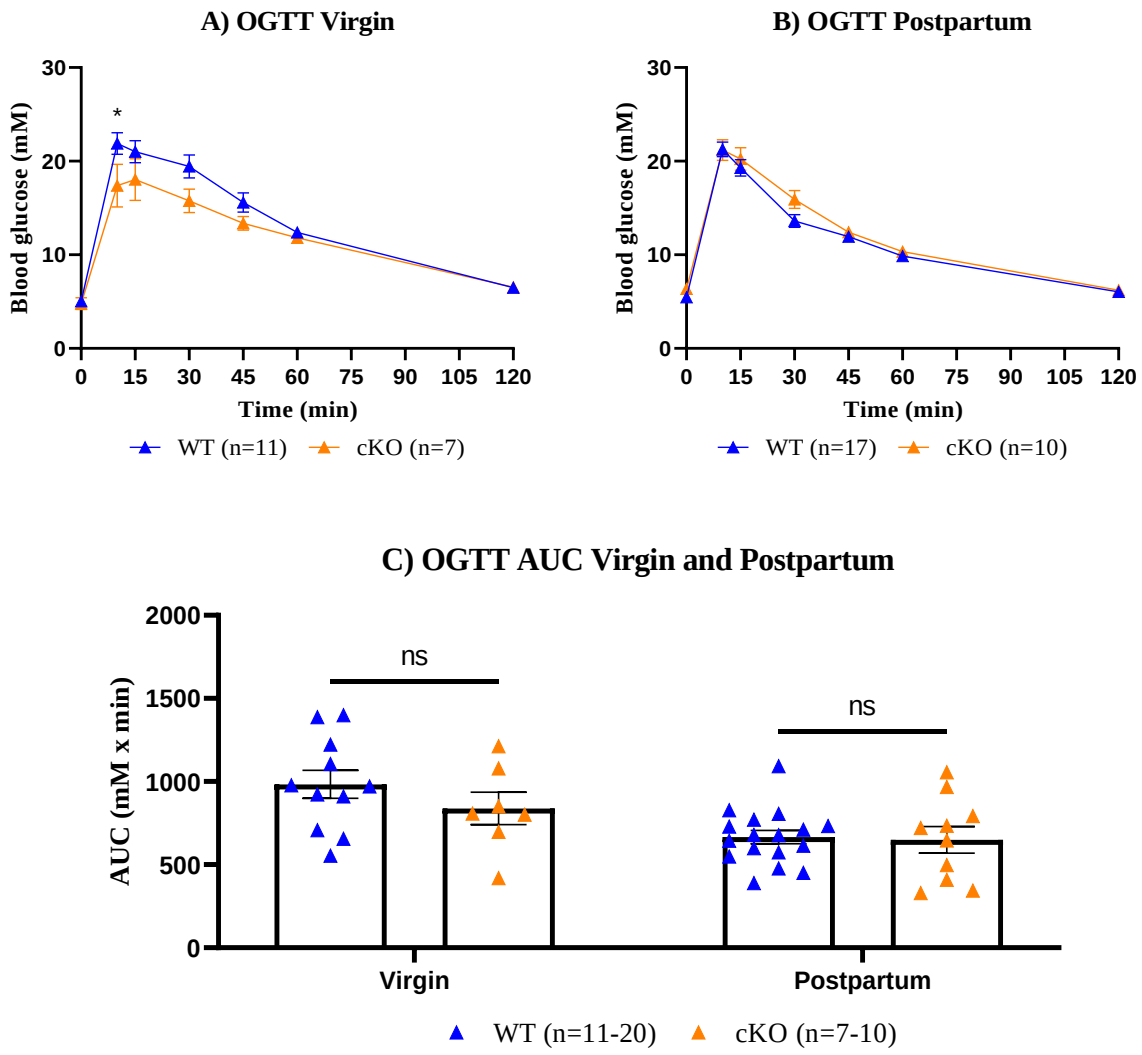

Supplemental Figure 5. OGTT in A) Virgin, B) Postpartum mice, and C) AUC

Blood glucose levels during OGTT at timepoints A) Virgin, B) Postpartum, and C) AUC. After an overnight fast, glucose solution by oral gavage (2g glucose/kg body weight) was administered and blood glucose was measured at 0, 10, 15, 30, 45, 60, 120 minutes. Results are means ± SEM (n=7-20). Two-way ANOVA was performed, and significance determined using Tukey's post hoc test where: "*" $p<0.05$, WT vs. cKO and ns = not significant. Carol Huang assisted with oral gavage and data collection.

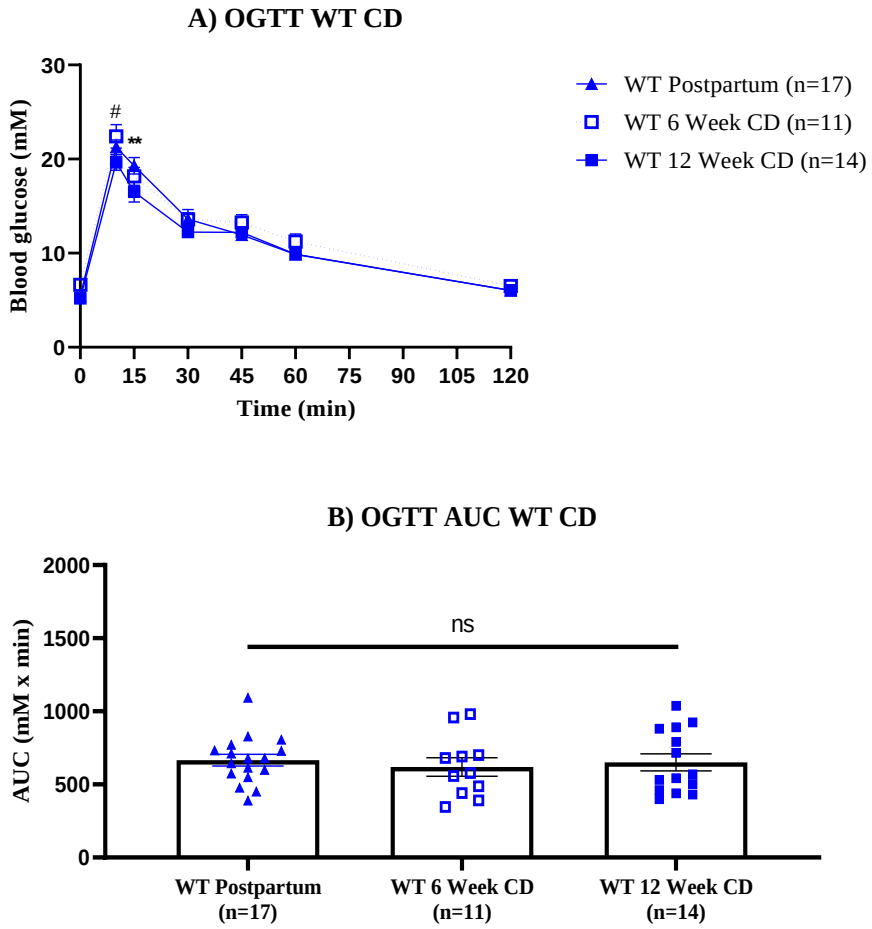

Supplemental Figure 6. A) OGTT in WT mice Postpartum, 6- and 12-Week of CD and B) AUC

(A) Blood glucose levels in WT mice during OGTT at timepoints: Postpartum, 6- and 12-Week of CD. After an overnight fast, glucose solution by oral gavage (2g glucose/kg body weight) was administered and blood glucose was measured at 0, 10, 15, 30, 45, 60, 120 minutes. (B) AUC was calculated using trapezoidal method where time point 0 minutes as baseline. Results are means ± SEM (n=11-17). Two-way ANOVA was performed, and significance determined using Tukey's post hoc test where: "#" $p<0.05$ Week 6 CD vs. Week 12 CD, "**" $p<0.005$ Postpartum vs. Week 12 CD, and ns = not significant. Carol Huang assisted with oral gavage and data collection.

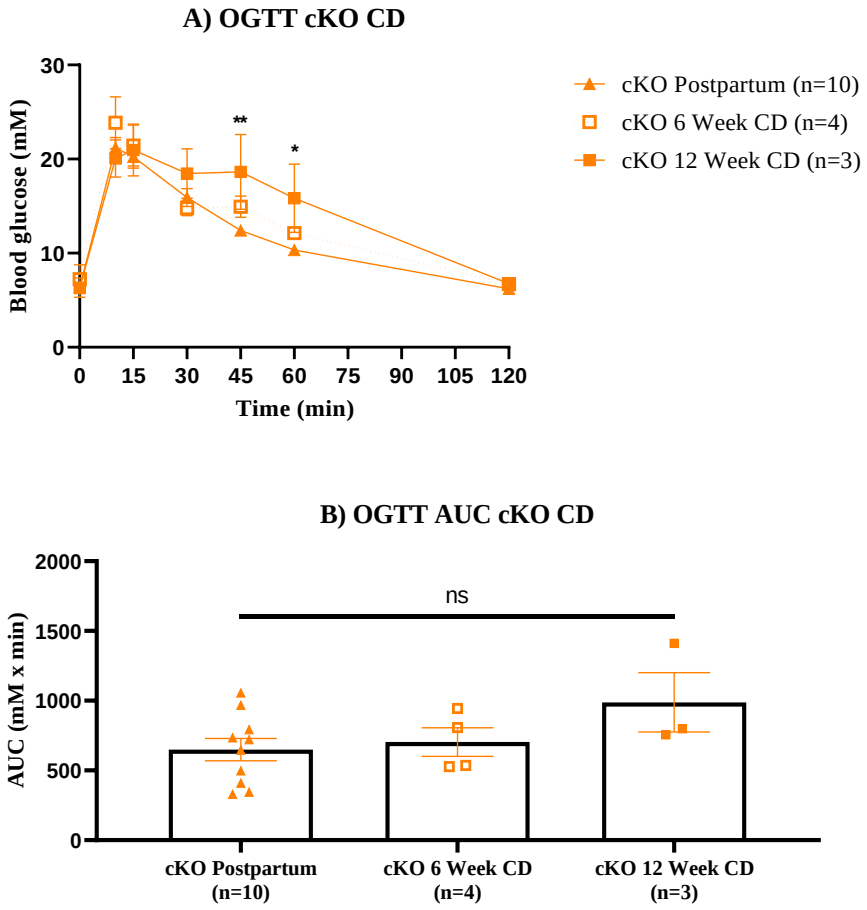

Supplemental Figure 7. A) OGTT in cKO mice Postpartum, 6- and 12-Week of CD and B) AUC

(A) Blood glucose levels in cKO mice during OGTT at timepoints: Postpartum, 6- and 12-Week of CD. After an overnight fast, glucose solution by oral gavage (2g glucose/kg) was administered and blood glucose was measured at 0, 10, 15, 30, 45, 60, 120 minutes. (B) AUC was calculated using trapezoidal method where time point 0 minutes as baseline. Results are means ± SEM (n=4-10). Two-way ANOVA was performed, and significance determined using Tukey's post hoc test where: "*" $p<0.05$, "**" $p<0.005$ Postpartum vs. Week 12 CD, and ns = not significant. Carol Huang assisted with oral gavage and data collection.

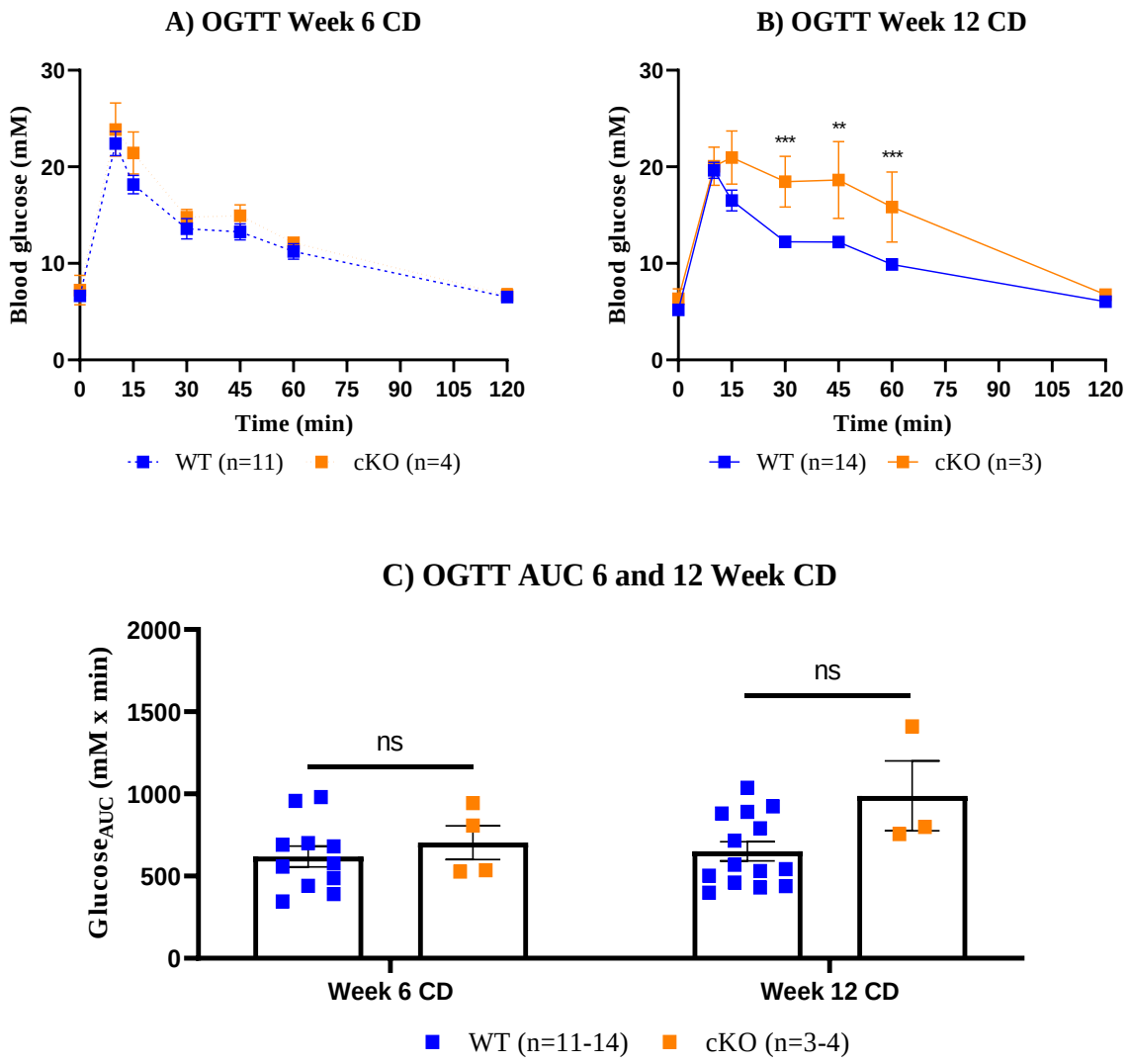

Supplemental Figure 8. OGTT in A) 6 Week CD, B) 12-Week CD, and C) AUC

Blood glucose levels during OGTT at timepoints A) 6 Week CD, B) 12 Week CD, and C) AUC. After an overnight fast, glucose solution by oral gavage (2g glucose/kg) was administered and blood glucose was measured at 0, 10, 15, 30, 45, 60, 120 minutes. Results are means ± SEM (n=3-14). Two-way ANOVA was performed, and statistical significance was determined using Tukey's post hoc test where ** $p<0.005$, *** $p<0.0005$ WT vs. cKO, and ns = not significant. Carol Huang assisted with oral gavage and data collection.

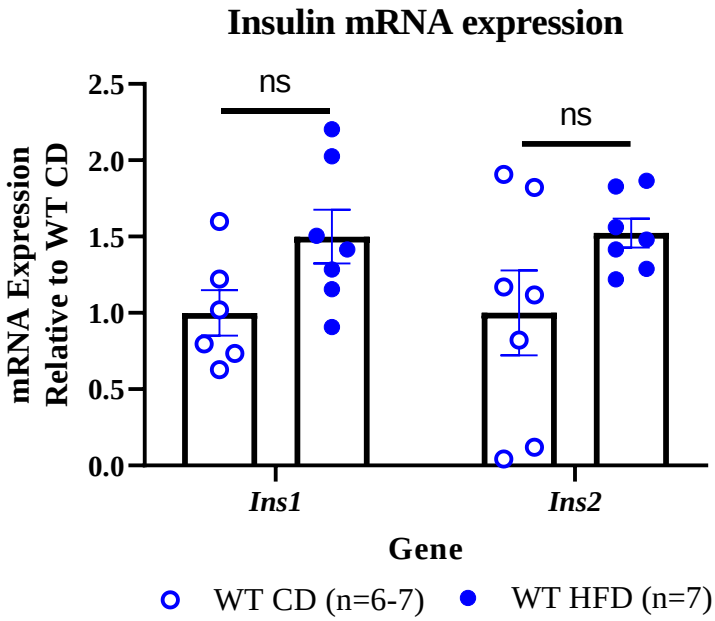

Supplemental Figure 9. Islet *Ins1* and *Ins2* mRNA expression in WT mice after 12 weeks of CD or HFD

mRNA expression of *Ins1* and *Ins2* was measured by RTqPCR. mRNA expression was normalized to *Ppa1* (housekeeping gene) and expressed relative to WT CD mice. Each data point represents a mouse (n=6-7 mice/group). Results are presented as means ± SEM of 3 independent experiments. Statistical analysis was done using an unpaired Student's t-test between groups where: "ns" not significant.

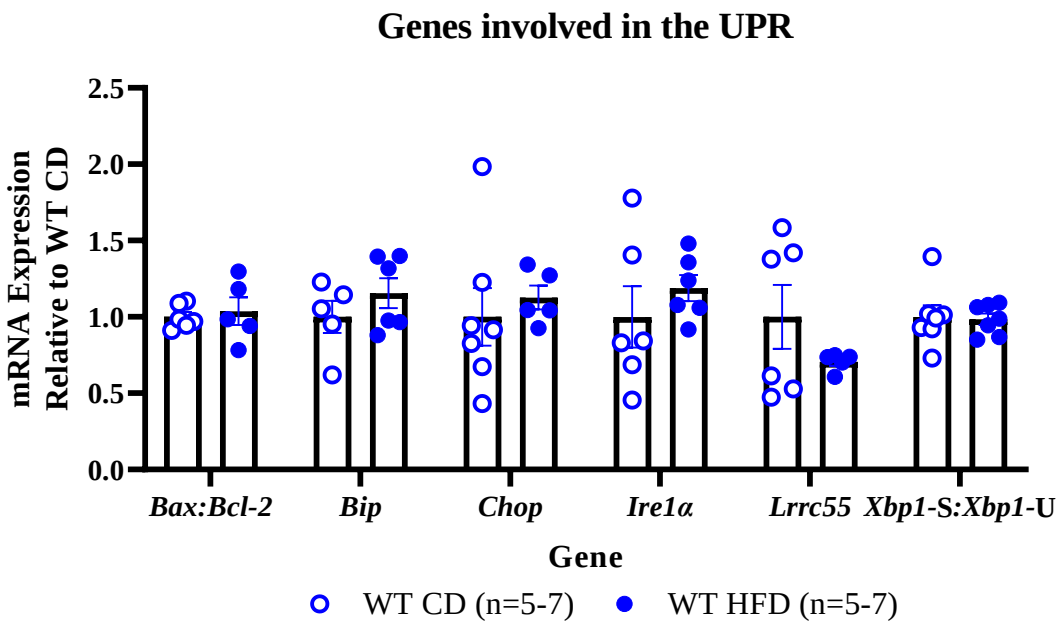

Supplemental Figure 10. Islet mRNA expression of genes involved in UPR in WT HFD vs. WT CD mice after 12 weeks of diet

mRNA expressions of *Bax*:*Bcl-2*, *Bip*, *Chop*, *Ire1α*, *Lrrc55*, and *Xbp1*-S:*Xbp1*-U were measured by RTqPCR. mRNA expression was normalized to *Ppa1* (housekeeping gene) and expressed relative to WT CD mice. Each data point represents a mouse (n=5-7 mice/group). Results are presented as means ± SEM of 3 independent experiments. Statistical analysis was done using an unpaired Student's t-test between groups.

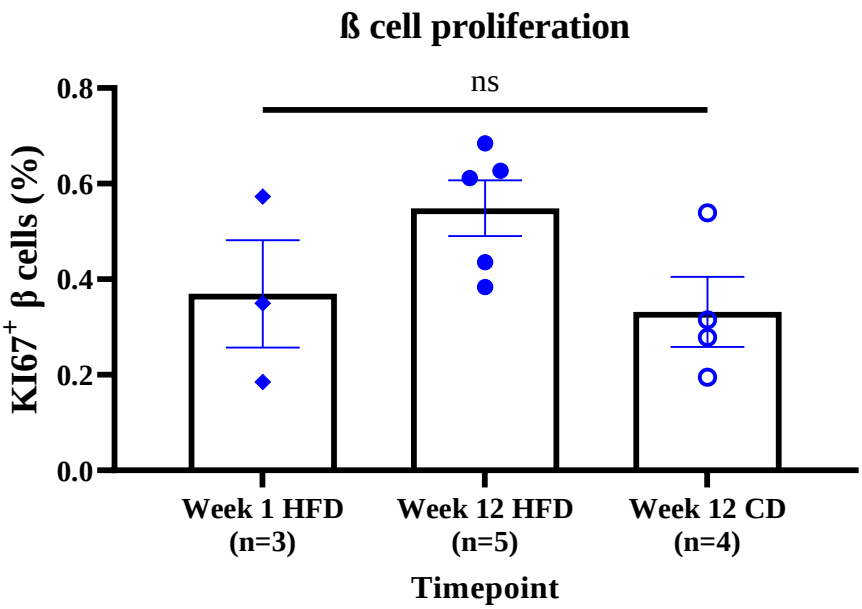

Supplemental Figure 11: β cell proliferation in WT mice after 1 week of HFD, 12 weeks of HFD, and 12 weeks of CD

After 1 or 12 weeks of HFD and 12 weeks of CD, pancreases from WT mice were labeled with insulin and KI67. β cell proliferation was determined by the percentage of nuclei that were KI67-positive with cytoplasmic insulin-positivity relative to the total insulin-positive cells counted. At least 1000 β cells were counted per mouse. Each data point represents a mouse (n = 3-5 mice/group). Two-way ANOVA was conducted, and significance was determined using Tukey's post hoc test where: "ns" = not significant. Raneet Khalon, Sristi Dey, and Valerie Ho assisted with immunofluorescence, imaging, and quantification.

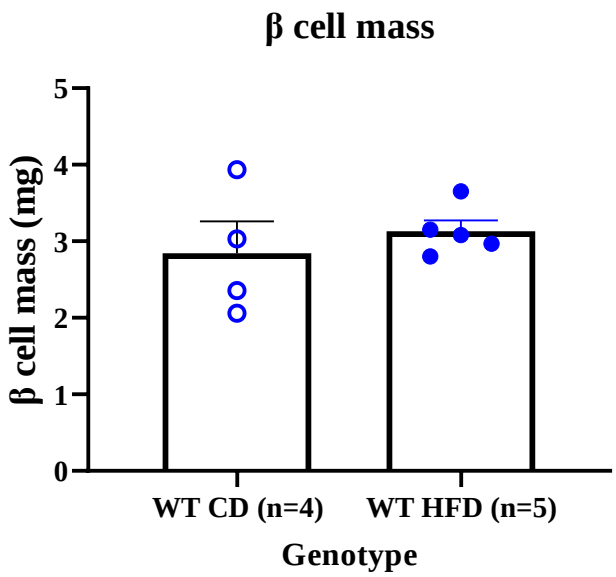

Supplemental Figure 12: β cell mass after 12 weeks of HFD or CD in WT mice

β cell mass after 12 weeks of HFD or CD in WT mice was measured. β cell mass was determined by multiplying pancreas weight by the insulin-positive area and dividing it by the total pancreas area. At least three sections were examined, with 6000 β cells per mouse across 4 sections 200 μm apart. Each data point represents a mouse (n = 4-5 mice/group). Statistical analysis was done using an unpaired Student's t-test. Raneet Khalon, Sristi Dey, and Valerie Ho assisted with immunofluorescence, imaging, and quantification.

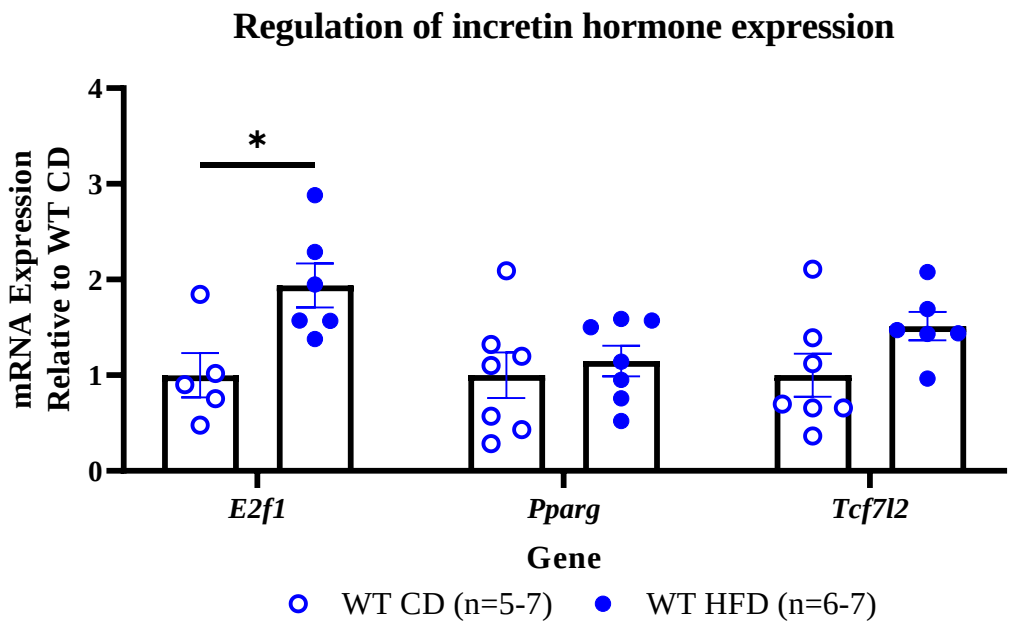

Supplemental Figure 13: Islet mRNA expression of transcription factors that regulate incretin hormone receptor expression in WT mice after 12 weeks of CD or HFD

mRNA expressions of *E2f1*, *Pparg*, and *Tcf7l2* were measured by RTqPCR. mRNA expression was normalized to *Ppa1* (housekeeping gene) and expressed relative to WT CD mice. Each data point represents a mouse (n=5-7 mice/group). Results are presented as means ± SEM of 3 independent experiments. Statistical analysis was done using an unpaired Student's t-test between groups where: "*" $p<0.05$.